AD 765322

NAVAL SHIP RESEARCH AND DEVELOPMENT CENTER
Bethesda, Maryland 20034

PROPELLER PERTURBATION PROBLEMS

by

Terry Brockett

SHIP PERFORMANCE DEPARTMENT
RESEARCH AND DEVELOPMENT REPORT

20070122102

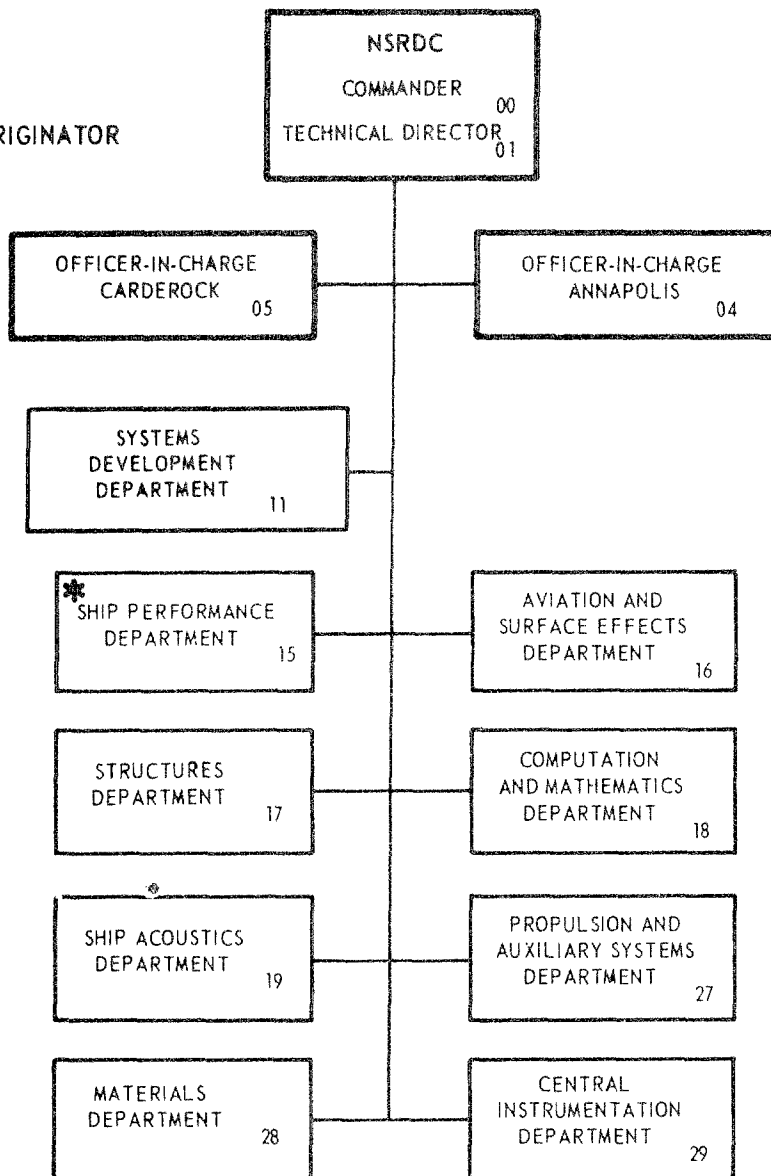OCTOBER 1972   Report 3880

The Naval Ship Research and Development Center is a U. S. Navy center for laboratory effort directed at achieving improved sea and air vehicles. It was formed in March 1967 by merging the David Taylor Model Basin at Carderock, Maryland with the Marine Engineering Laboratory at Annapolis, Maryland.

Naval Ship Research and Development Center

Bethesda, Md. 20034

MAJOR NSRDC ORGANIZATIONAL COMPONENTS

* REPORT ORIGINATOR

```
                    NSRDC
                  COMMANDER
                            00
               TECHNICAL DIRECTOR
                            01
```

| OFFICER-IN-CHARGE CARDEROCK 05 | | OFFICER-IN-CHARGE ANNAPOLIS 04 |

```
SYSTEMS
DEVELOPMENT
DEPARTMENT   11
```

* SHIP PERFORMANCE DEPARTMENT 15	AVIATION AND SURFACE EFFECTS DEPARTMENT 16
STRUCTURES DEPARTMENT 17	COMPUTATION AND MATHEMATICS DEPARTMENT 18
SHIP ACOUSTICS DEPARTMENT 19	PROPULSION AND AUXILIARY SYSTEMS DEPARTMENT 27
MATERIALS DEPARTMENT 28	CENTRAL INSTRUMENTATION DEPARTMENT 29

DEPARTMENT OF THE NAVY

NAVAL SHIP RESEARCH AND DEVELOPMENT CENTER

BETHESDA, MD. 20034

PROPELLER PERTURBATION PROBLEMS

by

Terry Brockett

OCTOBER 1972

Report 3880

TABLE OF CONTENTS

LIST OF FIGURES

$a(z)$	Radius of circle which is transformed to profile in the inner flow (singular-perturbation problem)
$a_n(z)$	Complex coefficients in inverse mapping function - f
$\underline{B}$	Vector potential for velocity
$C_T = \dfrac{THRUST}{(1/2)\,\rho U^2\,\pi R^2}$	Thrust coefficient
E	Profile shape function
$\underline{e}_i$	Unit base vector, subscript gives direction
f	Inverse mapping function
f_1	Radius of lines of constant circulation in shed vortex sheet
f_2	Axial position of lines of constant circulation
$g(\epsilon)$	Gage function in intermediate region
$\underline{i},\underline{j},\underline{k}$	Unit base vectors in the Cartesian reference frame
$\underline{N}$	Vector normal to surface, pointing into the flow field
$\underline{n}$	Unit vector normal to surface, pointing into the flow field
p	Pressure
$P(z)$	Pitch of blade-reference surface
$P_i(z)$	Pitch of shed vortex sheet at lifting line
$\underline{q}$	Velocity vector
$\underline{q}_o$	Velocity vector far upstream
R	Propeller radius
$\underline{r} = (x, y, z)$	Position vector of field point
$\underline{s}$	Position vector on blade surface
T	Thrust of propeller
$\underline{t}_i$	Tangent vector to surface, subscript denotes direction
U	Magnitude of velocity component along propeller axis
$u_i^{(n)}$	Component of induced velocity, subscript gives direction, superscript gives order of term in expansion
$V_n(z)$	Equivalent free-stream velocity for n^{th} term problem in inner flow (singular-perturbation problem)
$W(\widetilde{\omega})$	Propeller warp, angular position of blade-reference line
x	Cartesian component of position vector along axis of rotation, pointing downstream
$\bar{x} = x/\epsilon$	Inner variable
$\bar{\bar{x}} = x/g$	Intermediate variable

y	Cartesian component of position vector
$\bar{y} = y/\epsilon$	Inner variable
$\bar{\bar{y}} = y/g$	Intermediate variable
Z	Number of blades
z	Cartesian component of position vector pointing along upward vertical
$\alpha_0(z)$	Angle of zero lift of two-dimensional section
$\alpha_n(z)$	Angle of attack of nth term inner problem
$\beta = tan^{-1} \dfrac{U}{\Omega z}$	Pitch of incoming flow at lifting line
$\Gamma = \oint \underline{q} \cdot d\underline{r}$	Circulation enclosed by contour
$\Gamma_B = \phi^+ - \phi^-$	Jump in potential across blade surface; local circulation
$\gamma(\xi_1, \tilde{\omega})$	Chordwise component of velocity difference across the blade
$\delta_n(\epsilon)$	Gage function in outer flow
ϵ	Thickness- or camber-to-chord ratio, small parameter in regular-perturbation problem
$\bar{\epsilon}$	Chord-to-diameter ratio, small parameter in singular-perturbation problem
$\underline{\zeta} = f_1 \underline{e}_{\tilde{\omega}} + f_2 \underline{e}_\theta$	Position vector of lines of constant circulation in shed vortex sheet
$\theta = tan^{-1} \dfrac{-y}{z}$	Angular coordinate in cylindrical reference frame
$\theta_b = \dfrac{2\pi b}{Z}$	Angular coordinate of propeller blade-reference line
$\underline{\Lambda}$	Vorticity vector
$\mu_N(\epsilon)$	Gage function for matching to order N
$\mu = \sqrt{\sigma_1^2 + \sigma_2^2}$	Radius in profile plane, inner flow
$\nu_n(\epsilon)$	Gage function in inner flow
ξ_i	Profile coordinates, subscript denotes direction
ρ	Fluid density
σ	Component of velocity difference across blade
$\sigma_i = \xi_i/\epsilon$	Inner variable for ξ_i
Φ	Scalar potential for velocity, expressed in inner variables
ϕ	Scalar potential for velocity, expressed in outer variables
$\varphi_B(z)$	Pitch angle of profile section, measured at constant z
$\varphi_P(\tilde{\omega})$	Pitch angle of blade-reference surface, measured on cylinder of radius $\tilde{\omega}$
$\psi = \phi^+ + \phi^-$	Average value of ϕ across a surface

$\underline{\Omega} = -\Omega\underline{i}$ Rotational velocity of propeller, Ω in radians per unit time, $\Omega > 0$ for right-hand rotation

$\tilde{\omega}$ Radial coordinate in cylindrical reference frame

$\omega = tan^{-1}\dfrac{\sigma_2}{\sigma_1}$ Angular coordinate in profile plane, inner problem

$\beta(\tilde{\omega})$ Propeller rake, axial displacement of blade-reference line from propeller plane

ABSTRACT

For steady motion of a propeller operating in an inviscid fluid having an unbounded irrotational flow field, an expression for the velocity potential (in excess of the body motion) is derived in terms of the boundary values. From this expression perturbation solutions are determined—one for small thickness—or camber-to-chord ratio and one for small chord-to-diameter ratio.

The first problem (lifting-surface theory) is a regular-perturbation problem, and the second (lifting-line theory) is a singular-perturbation problem which requires construction of matched asymptotic expansions. Two terms of each series are found. Numerical techniques are not discussed. The outer solution for the lifting line is the same as that published in the literature. The formal lifting-surface analysis differs from other developments in several ways. The most important of these is that for propellers with variable pitch, warp, and rake, the normal to the blade has a radial component which requires consideration of the radial velocity in determining the blade shape. For the case considered the sign of the contributions in the inner radii differ from the outer radii values; thus, this additional term might cause little effect on thrust but could be important for cavitation performance. A design procedure is discussed which involves only quantities appropriate for the lifting-surface analysis.

ADMINISTRATIVE INFORMATION

ACKNOWLEDGMENT

INTRODUCTION

A—OBJECTIVE

Calculations pertaining to lifting bodies are based on linearized versions of the mathematical model used to describe the flow field about such objects. The traditional names for the two approximations used are lifting-surface and lifting-line. Each of these is associated with a different small parameter. These parameters are discussed in Section B.

Until recently, developments in the linearized theory have usually been presented on an intuitive basis, rather than on a formal mathematical basis. In wing theory, the formal linearization procedures have not altered the lower-order theory significantly; however, they have permitted higher-order effects to be calculated. Perhaps the best example of the formalization of the previous intuitive procedure

1

is the lifting-line theory presented by Friedrichs[1] and Van Dyke.[2] In particular, Van Dyke showed that the integral equation could be simplified to a quadrature and that higher-order terms could be found. The contribution of Friedrichs and Van Dyke will be discussed further in later paragraphs and are mentioned here as an example of the formalization.

To date, a similar formal development appropriate for propeller geometry has not been presented. Accordingly, the objective of the present work is to develop the formal linearized solutions for propeller lifting-surface theory and lifting-line theory.

B—REGULAR AND SINGULAR-PERTURBATION PROBLEMS

A hubless propeller has three characteristic lengths: the diameter, a representative chordlength, and a representative thickness or camber. For lifting-surface theory, the ratio of thickness and/or camber to either chordlength or diameter is the small parameter, and the exact formulation is implicity expanded in a perturbation series. Such a series is herein called a regular-perturbation series, since useful information can be obtained without further analysis. However, the resulting formulation is not uniformly valid since it fails at the leading edge. The lifting-surface equations are derived in Chapter 3.

Instead of the thickness and camber ratio being considered small, the chord-to-diameter ratio can be taken as the perturbation parameter. This leads to lifting-line theory which is the subject of Chapter 4.

Unfortunately a vanishing chordlength leads to a singular-perturbation problem as opposed to the regular-perturbation problem in lifting-surface theory. It is often sufficient to distinguish between them by defining the regular problem as that for which the order of the governing equations and the number of boundary conditions remain fixed as the parameter goes to zero. This definition is adopted here, although an additional requirement is violated. The additional requirement is that the resulting formulation must be uniformly valid throughout the flow field. As already mentioned, the point of view adopted here is that useful information can be obtained from the regular-perturbation series without consideration of the singular region.[*]

---

[1]Friedrichs, K.O., "Special Topics in Fluid Dynamics," New York University (1953); also published by Gordon and Breach, New York (1966). (A complete listing of references is given on page(s) 115).

[2]Van Dyke, M., "Lifting Line Theory as a Singular Perturbation Problem," Archiwum Mechaniki Stosowanej, Vol. 3, No. 16, pp. 601-614 (1964).

[*]A singular region can be anticipated since the formulation requires a derivative of the shape function. Although the shape relative to the reference surface is uniformly small, the derivative of the thickness function is infinite at the leading edge and small away from it.

For a singular-perturbation problem, the order of the governing equation is decreased, and/or one or more of the boundary conditions has to be discarded. In problems involving a lifting body of small chordlength, the limiting process as the chordlength goes to zero replaces the body by a lifting line, and, hence, the body boundary conditions cannot be applied. (The order of the equations remains unchanged.) To regain the details of the flow near the body, this region must be magnified by stretching the coordinates. The flow field near the body is calculated in these stretched variables and must be matched to the flow determined for the lifting line. The mathematical techniques involved in the analysis are explained by Van Dyke,[3] Kaplun,[4] and Cole.[5]

The first application of singular-perturbation concepts to wings of finite span was made by Prandtl.[6] Later, Friedrichs[1] formalized the concept of inner and outer regions and derived Prandtl's integral equation for circulation. Van Dyke[2] obtained higher-order terms in the perturbation series and showed that the circulation was obtained as a quadrature rather than from an integral equation. A singular-perturbation solution has also been obtained for a swept wing by Thurber[7] and for a nonplanar wing by Rotta.[8] The formal perturbation series assume zero thickness. Van Dyke[2] compared his calculations with results from exact theory for the total lift of elliptic wings and found good agreement for aspect ratios as low as about 2.7. He was able to identify terms in the solution which gave streamline curvature and which slightly modified the angle of attack.

For marine propellers the chord-to-diameter ratio is about unity, and the thickness-to-chord ratio is about one-tenth. One intuitively expects then that the lifting-surface formulation will be more accurate than the lifting-line theory for the same number of terms.

C–DESIGN AND PERFORMANCE PROBLEMS

In the present work a distinction is made between the design problem and the performance-evaluation problem. This distinction does not apply to the mathematical formulation but to the application

[3]Van Dyke, M., "Perturbation Methods in Fluid Mechanics," Academic Press, Inc., New York (1964).

[4]Kaplun, S., "Fluid Mechanics and Singular Perturbations," Edited by P.A. Lagerstrom, et al., Academic Press, Inc., New York (1967).

[5]Cole, J.D., "Perturbation Methods in Applied Mathematics," Blaisdell (1968).

[6]Prandtl, L., "Application of Modern Hydrodynamics to Aeronautics," National Advisory Committee for Aeronautics Report 116 (1921).

[7]Thurber, J.K., "An Asymptotic Method for Determining the Lift Distribution of a Swept-Back Wing of Finite Span," Communications on Pure and Applied Mathematics, Vol. 18, pp. 733-756 (1965).

[8]Rotta, N.R., "The Non-Planar, Moderate Aspect Ratio, Subsonic Winds," Ph.D. Thesis, New York University, University Microfilms 69-4576 (1968).

of theoretical results since certain quantities are assumed known in one problem while they would be unknown in the other.

In the typical design problem, one specifies the blade loading, the diameter, number of blades, blade outline and hub details. One seeks the blade-section thickness, camber and pitch angle for operation in a given flow field. Variations often occur in the specifications; in early design procedures, the camber-line shape was specified, and the radial magnitude needed to obtain a specified thrust was sought. In some modern design techniques, the spanwise and chordwise shape of the loading function as well as the thrust is specified, and the camberline shape is to be calculated. In both of these design problems, the thickness distribution is specified from strength and cavitation considerations. When the thickness distribution and loading function are specified, the design calculations become quadratures in the lifting-surface problem. This point is elaborated in Chapter 3. Recently techniques for determining the thickness distribution from a specified pressure distribution have been developed by Hille.[9] This would allow a design problem for which the total pressure distribution was specified and for which the thrust and geometry would be calculated. However, the combination of strength considerations and the simplicity of the design based on quadratures will probably insure continued usage of thickness specification.

In contrast to the possible variations for the design problem, the performance-evaluation problem is straightforward to describe. The geometry is specified and from it one seeks to calculate some desired quantities when the propeller operates in a given upstream flow field. A formal solution of this problem is obtained as a quadrature in the lifting-line theory of Chapter 4. Unfortunately, an insufficient number of terms in the series is determined to permit accurate calculations, so investigators in this area currently attempt a solution of the integral equation from the lifting-surface analysis.

D—HISTORICAL DEVELOPMENT OF PROPELLER THEORY AND STATE OF THE ART

Propeller theory is based on the principles applied to conventional wings, except that the propeller geometry adds a significant complication. As discussed in Section B, Prandtl[6] laid the foundation for lifting-line analysis of wings. In the same paper he included an approximate solution for propellers with small chord-to-diameter ratios. Several years later, Goldstein[10] obtained a more accurate solution for a propeller lifting-line with a specific circulation distribution; however, it was not until more than two decades later that Moriya[11] presented a derivation of the induced velocities at a lifting-line of an arbitrary

---

[9]Hille, R., "Bestimmung der Dickenlinie von Propellerflügelprofilen bei vorgegebener Druckverteilung," Report 262 of the Institut für Schiffbau der Universität Hamburg, West Germany (1970).

[10]Goldstein, S., "On the Vortex Theory of Screw Propellers," Procedure Royal Society of London, Series A, Vol. 123, pp. 440-465 (1929).

[11]Moriya, T., "On the Integration of Biot-Savart's Law in Propeller Theory," (in Japanese), Journal of the Society for Aeronautical Science, Japan, Vol. 9, No. 89, of 1015-1020 (1942); English translation in Selected Scientific and Technical Papers by Tomijiro Moriya, Moriya Memorial Committee, University of Tokyo, Japan, pp. 74-80 (1959).

propeller. This derivation was written in Japanese and went unnoticed for many years. Previous to Moriya's work, Kawada[12] had derived the potential for an infinitely long vortex filament which Lerbs[13] used to develop charts useful in design. Since the work of Lerbs, only minor refinements have taken place in lifting-line theory. A derivation of the lifting-line equations and explanation of the numerical techniques used in their evaluation are given by Morgan and Wrench.[14]

Even while development of the lifting-line theory was in progress, it was recognized that marine propellers were too broad for direct application of the lifting-line results. Efforts were devoted to finding correction factors which would allow use of the lifting-line results by modifying the propeller design so that they would actually deliver the required thrust. The calculation of such correction factors was quite tedious, and a considerable amount of simplification was incorporated. Ludwieg and Ginzel[15] derived an approximate correction factor for wide-bladed propellers which was extensively used before high-speed computers made possible more accurate calculations for the individual design. Strscheletzky[16] presented a basis and some numerical results[17] for a general lifting-surface theory; however, it was not until the use of computers became popular in the early 1960's that lifting-surface calculations became practical. Typical of

[12]Kawada, S., "Induced Velocity by Helical Vortices," Journal of Aeronautical Sciences, Vol. 3, pp. 86-87 (1936).

[13]Lerbs, H.W., "Moderately Loaded Propellers with a Finite Number of Blades and an Arbitrary Distribution of Circulation," Society of Naval Architects and Marine Engineers Transactions, Vol. 60, pp. 73-123 (1952).

[14]Morgan, W.B. and J.W. Wrench, "Some Computational Aspects of Propeller Design," Methods of Computational Physicis, No. 4, pp. 301-331, Academic Press, Inc., New York (1965).

[15]Ludwieg, H. and I. Ginzel, "Zur Theorie der Breitblattschraube," Aerodynamische Versuchsanstalt, Göttingen, Report 44/A/08 (1944); see Ginzel, G.I., "Theory of the Broad-Bladed Propeller," Aeronautical Research Council, Current Papers 208 (1955).

[16]Strscheletzky, M., "Hydrodynamische Grundlagen zur Berechnung der Schiffsschrauben," Verlag G. Braun, Karlsruhe, West Germany (1950).

[17]Strscheletzky, M., "Berechnungskurven für dreiflügelige Schiffsschrauben," Verlag G. Braun, Karlsruhe, West Germany (1955).

the lifting-surface investigations are the analyses presented by Yamazaki[18-24] Sparenberg,[25] Kerwin,[26,27] Kerwin and Leopold,[28,29] Pien,[30] Pien and Strom-Tejsen,[31] Hanaoka,[32] and Murray.[33] Reviews of many

[18]Yamazaki, R., "A Study on Screw Propellers," Memoirs of the Faculty of Engineering, Kyushu University, Japan, Vol. 19, No. 1, pp. 1-75 (1960).

[19]Yamazaki, R., "On the Theory of Screw Propellers," Fourth Symposium on Naval Hydrodynamics (1962).

[20]Yamazaki, R., "On the Theory of Screw Propellers," Memoirs of the Faculty of Engineering, Kyushu University, Japan, Vol. 23, No. 2, pp. 97-112 (1963); corrected version of 1962 paper.

[21]Yamazaki, R., "On the Theory of Screw Propellers in Non-Uniform Flows," Memoirs of the Faculty of Engineering, Kyushu University, Japan, Vol. 25, No. 2, pp. 107-174 (1966).

[22]Yamazaki, R., "On the Propulsion of Ships in Still Water (Introduction)," Memoirs of the Faculty of Engineering, Kyushu University, Japan, Vol. 27, No. 4, pp. 187-220 (1968).

[23]Yamazaki, R., "Theory of Unsteady Propeller Forces," Seventh Symposium on Naval Hydrodynamics, Rome (1968).

[24]Yamazaki, R., "On the Theory of Unsteady Propeller Forces," Memoirs of the Faculty of Engineering, Kyushu University, Japan, Vol. 28, No. 3, pp. 157-206 (1969).

[25]Sparenberg, J.A., "Application of Lifting Surface Theory to Ship Screws," International Shipbuilding Progress, Vol. 7, No. 67, pp. 99-106 (1960).

[26]Kerwin, J.E., "The Solution of Propeller Lifting Surface Problems by Vortex Lattice Methods," Massachusetts Institute of Technology, Naval Architecture Department Report (June 1961).

[27]Kerwin, J.E., "Linearized Theory for Propellers in Steady Flow," Massachusetts Institute of Technology, Naval Architecture Department Report (1963).

[28]Kerwin, J.E. and R. Leopold, "Propeller Incidence Correction Due to Blade Thickness," Journal of Ship Research, Vol. 7, No. 2, pp. 1-6 (1963).

[29]Kerwin, J.E. and R. Leopold, "A Design Theory for Subcavitating Propellers," Society of Naval Architects and Marine Engineers Transactions, Vol. 72, pp. 294-335 (1964).

[30]Pien, P.C., "The Calculation of Marine Propellers Based on Lifting Surface Theory," Journal of Ship Research, Vol. 5, No. 2, pp. 1-14 (1961).

[31]Pien, P.C. and J. Strom-Tejsen, "A General Theory for Marine Propellers," Seventh Symposium on Naval Hydrodynamics, Rome (1968).

[32]Hanaoka, T., "Hydrodynamics of an Oscillating Screw Propeller," Fourth Symposium on Naval Hydrodynamics (1962).

[33]Murray, M.T., "Propeller Design and Analysis by Lifting Surface Theory," International Shipbuilding Progress, Vol. 14, No. 160, pp. 433-451 (1967).

of these investigations can be found in the paper by Wu[34] and the books of Isay.[35,36] Cox[37] has surveyed the state of the art for subcavitating propeller design and concludes that for propellers described as lightly[*] to moderately[*] loaded, experimental results for propeller performance agree with the requirements set in the design procedure. (Since the design procedures are based on inviscid flow, viscous corrections must be made. Presently this is done on an empirical basis.) Cox points out that research is still needed in steady-flow design theory to extend the theory to heavily loaded propellers. The present work contributes to the heavily loaded design problem since the lifting-surface theory of Chapter 3 is carried out to second order.

While these design theories were being developed, the problem of predicting the performance was also being investigated. Kerwin[38] calculated the performance of a series of propellers over an operating range, using approximate curved-flow corrections derived for use in design. Differences of 10 percent, compared with experimental results, were found, although occasionally excellent agreement was obtained.

Analyses of the lifting-surface formulations to predict performance from the geometry have been attempted since Kerwin's investigation. To date most of these investigations have not compared predictions with experimental results. Yamazaki[19,20] made some comparisons with experiments, and he concluded good agreement when the pitch-to-diameter ratio was small. Murray[33] calculated the performance of propellers he had previously designed and found discrepancies between the calculations. For one propeller the predicted and design value of the thrust differed by 8 percent. Isay and Armonat[39] calculated

---

[34]Wu, T.Y., "Some Recent Developments in Propeller Theory," Schiffstechnik, Vol. 12, No. 60, pp. 1-11 (1965).

[35]Isay, W.H., "Propellertheorie, Hydrodynamische Probleme," Springer-Verlay, Berlin (1964).

[36]Isay, W.H., "Moderne Probleme der Propellertheorie," Springer-Verlag, Berlin (1970).

[37]Cox, G.G., "State-of-the-Art for Subcavitating Propeller Design Methods," Appendix II of the Report of the Propeller Committee, 12th International Towing Tank Conference, Rome (1969).

[38]Kerwin, J.E., "Machine Computation of Marine Propeller Characteristics," International Shipbuilding Progress, Vol. 6, No. 60, pp. 343-354 (1959).

[39]Isay, W.H. and R. Armonat, "Zur Berechnung der Potentialtheoretischen Druckverteilung am Flügelblatt eines Propellers," Schiffstechnik, Vol. 13, No. 67, pp. 75-89 (1966).

[*]Lerbs[13] defines loading ranges based on the importance of the trailing-vortex position in the calculations of induced velocities at the lifting line.

blade-pressure distribution but made no comparisons with experiments. Sugai[40] made extensive calculations of blade pressure distributions, thrust coefficient, and comparative camberline studies but did not compare his results with experiments.

None of the performance evaluation studies mentioned previously included thickness effects. All were linearized formulations, although Yamazaki[18-21] formulated a theory which did not explicitly require linearization but did require zero thickness. Later papers by Yamazaki[22-24] included thickness effects but were based on linearized formulations. He also gave equations governing the position of the shed vortex sheet. In each case described, evaluation of the numerical formulation usually required further approximation. The linearization and approximations point out the complexity of the problem resulting from the geometry of the propeller and its shed vortex sheet.

Other problems in propeller theory which are being investigated concern unsteady effects and viscous effects. Study of these two aspects of propeller theory is still in its infancy, and relatively few papers have been presented. Most of the literature on unsteady effects can be found in Yamazaki,[21-24] Pien and Strom-Tejsen,[31] and Tsakonas and Jacobs.[41] Several references concerning boundary layers applicable to propeller blades can be found in Armonat.[42] Since these two areas are not covered in the present work, no further details of these investigations will be given.

E—STATEMENT OF THE PROBLEM

It is appropriate at this point to define the problem to be considered; the flow field of a hubless propeller with Z identical, equally spaced, blades operating in an unbounded, inviscid, incompressible fluid. The rectilinear and angular velocity are coaxial and constant. The exact lifting-surface theory is first formulated without further restrictions; however, the singular-perturbation problem is further restricted in geometry. Experience with wings, Van Dyke,[2] Thurber,[7] and Rotta,[8] indicates that more terms can be calculated for the simplest geometry, i.e., without sweep and dihedral. Accordingly, the blade should be neither raked nor warped (these terms are defined in Chapter 1). The reason for this restriction is explained in Chapter 4.

The usual assumptions (Lerbs)[13] about the significant interaction effects of importance to the position of the shed vortex sheet are not made in the lifting-surface analysis. The position of the vortex sheets can be taken into account as the perturbation solutions evolve. An approximation is made in the lifting-line analysis which corresponds to moderately loaded theory.

---

[40]Sugai, K., "Hydrodynamics of Screw Propellers Based on a New Lifting Surface Theory," Selected Papers from the Journal of the Society of Naval Architects of Japan, Vol. 4, Tokyo, pp. 96-106 (1970).

[41]Tsakonas, S. and W.R. Jacobs, "Propeller Loading Distributions," Journal of Ship Research, Vol. 13, No. 4, pp. 237-257 (1969).

[42]Armonat, R., "Untersuchung der Druckverteilung eines Propellers unter Berücksichtigung grenzschichtbedingter Massstabseffekte," Schiffstechnik, Vol. 16, No. 81, pp. 41-54 (1969).

F—DESCRIPTION OF CONTENTS

Because the geometry plays such an essential role in propeller theory, the first chapter is devoted to an examination of the geometrical specification of a propeller blade. The normal to a blade is determined, and certain differentials are examined. The findings are used in later chapters.

Since no derivation of the exact potential function associated with the finite dimensions of the propeller could be found in the published literature, an expression has been formulated in terms of boundary values in Chapter 2. By a straightforward linearization, the regular-perturbation problem has been obtained in Chapter 3. The applications to both design and performance calculations is discussed. The perturbation solution is carried out to second order. Although the performance calculations result in an integral equation in the regular-perturbation problem, in Chapter 4 the performance problem is considered from the viewpoint of singular perturbations, and a quadrature results. Two terms in the series have also been calculated in this analysis.

In Appendix A, an integral expression for the potential of a lifting-line has been derived from the Biot-Savart Law. (Although this expression can be integrated in terms of known functions, the nested infinite series which result are not thought to be practical for computation.) In Appendix B the intermediate expansion of the outer potential is obtained. This expansion is used in Chapter 4.

CHAPTER 1
PROPELLER GEOMETRY

The details of propeller theory are considerably more complicated than wing theory because of the geometry. In this chapter, the analytical specification of the blade shape is developed, and certain expressions needed later in the analysis are obtained. First the coordinate systems are described, and the relations between them are derived. In addition, the normal to the blade is found. In another section, the blade sections are discussed, and the small parameters (thickness- and camber-to-chord ratio or chord-diameter ratio) are explicitly considered in the expressions for the derivatives appearing in the normal. In the last section, the gradients of functions expressed in these coordinate systems are obtained.

A—COORDINATE SYSTEMS AND BLADE GEOMETRY

To describe the flow field quantitatively, two right-handed coordinate systems are used, both attached to the moving propeller. The first of these is a Cartesian reference frame (x,y,z) with z pointing away from the axis of rotation along a reference line in the blade and with x pointing along the axis of rotation with positive displacement measured downstream from the propeller. The second system is cylindrical polar coordinates $(\tilde{\omega},\theta,x)$. Radial distances are measured from the axis of rotation in a (y,z) plane, and Θ is measured from the z axis in the clockwise direction looking along the positive x axis; see Figure 1.
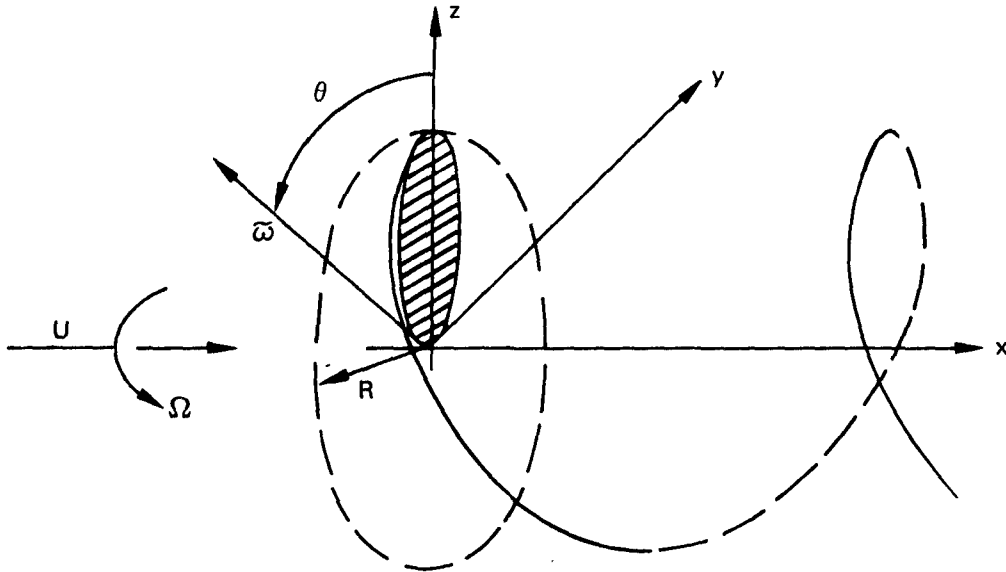

Figure 1 — Coordinate Reference Frames
for Stationary Blade

Unit base vectors in the (x,y,z) system are the usual $(\underline{i},\underline{j},\underline{k})$ and base vectors in the $(\tilde{\omega},\theta,x)$ system are denoted by $(\underline{e}_{\tilde{\omega}}, \underline{e}_{\theta}, \underline{i})$, respectively, where

10

$$\underline{e}\widetilde{\omega} = -\sin\,\theta\,\underline{j} + \cos\,\theta\,\underline{k}$$

and   (1-1)

$$\underline{e}_\theta = -\cos\,\theta\,\underline{j} - \sin\,\theta\,\underline{k}$$

In general, blade-section offsets for propellers are measured from a reference line lying on a cylinder of constant radius. This viewpoint is adopted for some of the analyses (Chapters 2 and 3) but for another portion of the work (Chapter 4) a slightly different viewpoint is necessary. This second viewpoint is that the geometry is defined for sections cut by a plane at constant z on the reference blade (the reference blade is the one which lies as close as possible to the z-axis). Although a set of unit orthogonal reference vectors is assigned for each viewpoint, neither system is an orthogonal curvilinear coordinate system, except for a special case in the second system. (The orthogonal coordinate system with the cylindrical surface would be cylindrical polar coordinates.)

For the sections defined on a right circular cylinder, the blade-section reference line on the surface of the cylinder is called the geometric pitch line. It makes an angle $\varphi_p(\widetilde{\omega})$ with the y,z plane. The geometric pitch line usually lies along the nose-tail line, which is a line on the cylindrical surface joining the leading point and the trailing point of the blade section cut by the cylinder. Another important line is the blade-reference line (also called stacking line) which is defined as the line through an approximate datum point at each radius. The datum point is usually on the nose-tail line and generally will be the midchord point. The blade is raked when the blade-reference line is given by $x = \mathcal{R}(\widetilde{\omega})$; $\theta = \theta_b = \dfrac{2\pi b}{Z}$ $(b = 0, 1,... Z - 1)$. When the reference line is given by $\theta = \theta_b + W(\widetilde{\omega})$, $x = 0$, the blade is said to be warped. A combination of warp and rake is called skew; usually the displacement is along a helix which passes through a straight line in the plane $x = 0$. On the cylindrical surface $\widetilde{\omega} = constant$, a coordinate system $(\xi_1, \xi_2, \widetilde{\omega})$ is constructed with ξ_1 on the surface of the cylinder and measured from the blade-reference line along the constant pitch of the nose-tail line. Positive ξ_1 values point in the downstream direction. The variable ξ_2 is normal to the ξ_1 axis and points in the upstream direction. Unit orthogonal reference vectors $(\underline{e}_1, \underline{e}_2, \underline{e}\widetilde{\omega})$ are in the $(\xi_1, \xi_2, \widetilde{\omega})$ direction, respectively, but the coordinate system is only locally orthogonal, i.e., these are not the unitary base vectors described by Wills.[43] The system is left handed to permit specification of the blade-section geometry in the conventional two-dimensional orientation (positive camber in the positive ξ_2 direction). A schematic of the blade-coordinate system is shown in Figure 2. Although the blade-section reference line is shown as the nose-tail line, it is not necessary in the following development and will not always be used that way.

---

[43]Wills, A.P., "Vector Analysis with an Introduction to Tensor Analysis," Dover Publications, Inc., New York (1958).

In terms of the blade-reference system, the cylindrical polar coordinates are

$$\widetilde{\omega} = \widetilde{\omega}$$

$$\theta = \theta_b + W(\widetilde{\omega}) + \frac{\xi_1 \, \cos \, \varphi_p \, (\widetilde{\omega}) + \xi_2 \, \sin \, \varphi_p \, (\widetilde{\omega})}{\widetilde{\omega}}$$

$$x = \Re(\widetilde{\omega}) + \xi_1 \, \sin \, \varphi_p \, (\widetilde{\omega}) - \xi_2 \, \cos \, \varphi_p \, (\widetilde{\omega})$$

(1-2)
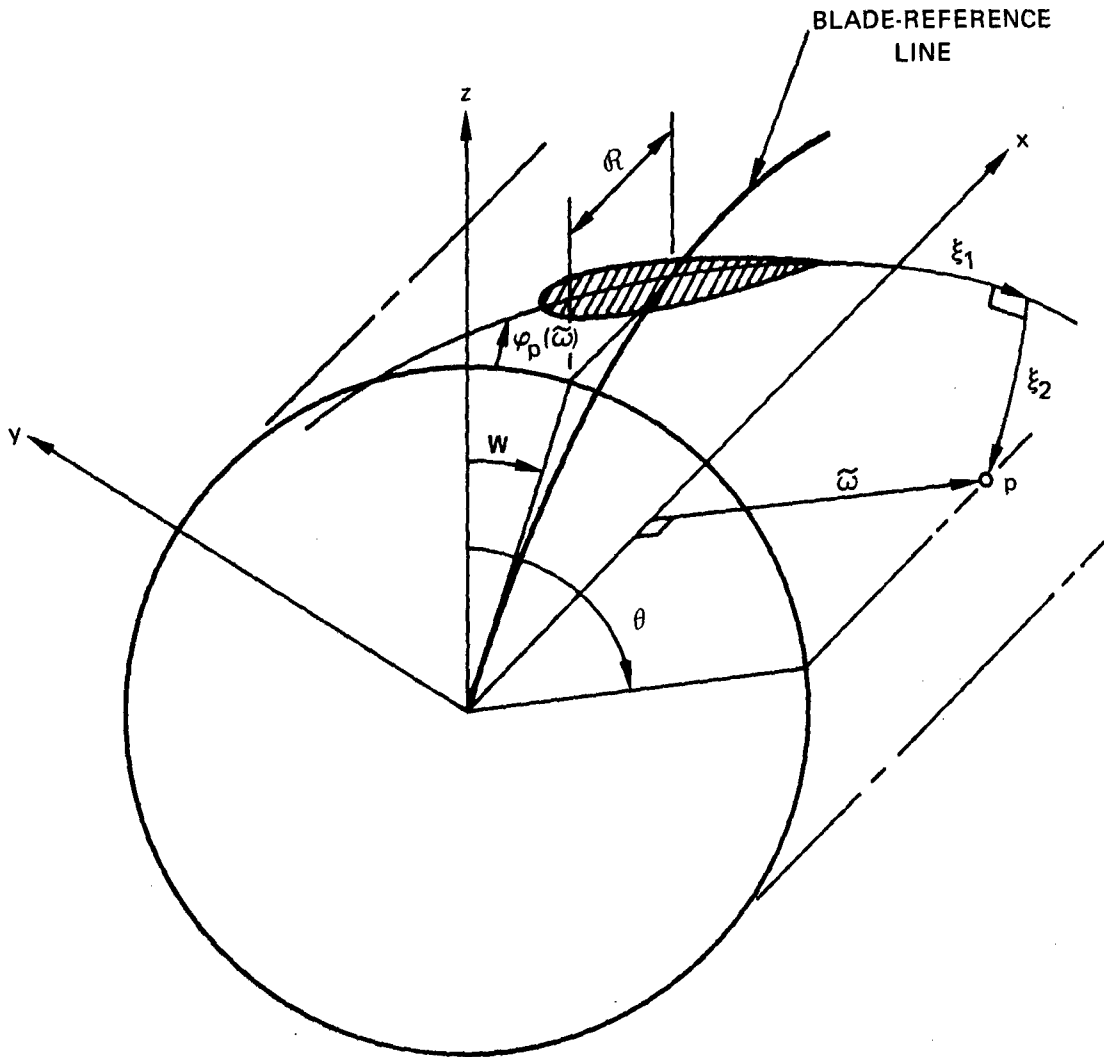

Figure 2 — Blade Coordinate System

Hence the Cartesian expressions are

$$x = \Re(\widetilde{\omega}) + \xi_1 \sin \varphi_p (\widetilde{\omega}) - \xi_2 \cos \varphi_p (\widetilde{\omega})$$

$$y = - \widetilde{\omega} \sin \left(\theta_b + W(\widetilde{\omega}) + \frac{\xi_1 \cos \varphi_p + \xi_2 \sin \varphi_p}{\widetilde{\omega}} \right) \qquad (1\text{-}3)$$

$$z = \widetilde{\omega} \cos \left(\theta_b + W(\widetilde{\omega}) + \frac{\xi_1 \cos \varphi_p + \xi_2 \sin \varphi_p}{\widetilde{\omega}} \right)$$

One can express the position vector in these variables by substituting into the expression

$$\underline{r} = x \, \underline{i} + y \, \underline{j} + z \, \underline{k}$$

and the unit base vectors in the ξ_1 and ξ_2 direction can be found:

$$\underline{e}_1 = \frac{\partial \underline{r}}{\partial \xi_1} = \sin \varphi_p \underline{i} - \cos \theta \cos \varphi_p \underline{j} - \sin \theta \cos \varphi_p \underline{k}$$

$$= \sin \varphi_p \underline{i} + \cos \varphi_p \, \underline{e}_\theta \qquad (1\text{-}4)$$

$$\underline{e}_2 = \frac{\partial \underline{r}}{\partial \xi_2} = - \cos \varphi_p \underline{i} - \cos \theta \sin \varphi_p \underline{j} - \sin \theta \sin \varphi_p \underline{k}$$

$$= - \cos \varphi_p \underline{i} + \sin \varphi_p \, \underline{e}_\theta$$

where θ is given in Equation (1-2).

The unit base vector in the $\widetilde{\omega}$ direction is the unit cylindrical polar vector in the $\widetilde{\omega}$ direction. It is given by Equation (1-1):

$$\underline{e}_{\widetilde{\omega}} = - \underline{j} \sin \theta + \underline{k} \cos \theta$$

(The partial of $\underline{r}$ with respect to $\widetilde{\omega}$ will not give this value since the $\underline{e}_1$, $\underline{e}_2$ base vectors are functions of $\widetilde{\omega}$.)

By construction $\underline{e}_1 \times \underline{e}_2 = - \underline{e}_{\widetilde{\omega}}$

The inverse of Equations (1-3) is

$$\left. \begin{aligned} \xi_1 &= \cos \varphi_p \sqrt{y^2 + z^2} \left(\tan^{-1} \left(\frac{-y}{z} \right) - \theta_b - W \right) + (x - \Re) \sin \varphi_p \\ \xi_2 &= \sin \varphi_p \sqrt{y^2 + z^2} \left(\tan^{-1} \left(\frac{-y}{z} \right) - \theta_b - W \right) - (x - \Re) \cos \varphi_p \end{aligned} \right\} \qquad (1\text{-}5)$$

$$\widetilde{\omega} = \sqrt{y^2 + z^2}$$

Blade sections are given by

$$\xi_2 = E(\xi_1, \widetilde{\omega}) \qquad (1\text{-}6)$$

13

for

$$c_2(\widetilde{\omega}) \leq \xi_1 \leq c_1(\widetilde{\omega})$$

$$o \leq \widetilde{\omega} \leq R$$

where $c_2(\widetilde{\omega})$ is the distance to the leading edge,

$\quad c_1(\widetilde{\omega})$ is the distance to the trailing edge, and

$\quad R$ is the propeller radius.

E is the sum of a single-valued (camber) and a double-valued (thickness) function which combine to describe the offsets from the ξ_1 axis on the cylinder of radius $\widetilde{\omega}$. The function E is considered in detail later in this chapter. Figure 3 shows the profile geometry.
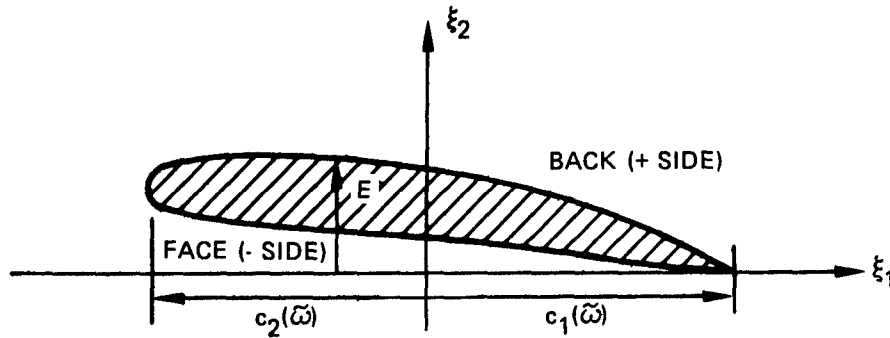
Figure 3 — Profile Geometry

A point on the surface of a blade is given as a function of two variables $(\xi_1, \widetilde{\omega})$ by

$$\underline{s} = (R + \xi_1 \sin \varphi_p - E \cos \varphi_p)\,\underline{i}$$

$$- \widetilde{\omega} \sin\left(\theta_b + W + \frac{\xi_1 \cos \varphi_p + E \sin \varphi_p}{\widetilde{\omega}}\right)\underline{j} \qquad (1\text{-}7)$$

$$+ \widetilde{\omega} \cos\left(\theta_b + W + \frac{\xi_1 \cos \varphi_p + E \sin \varphi_p}{\widetilde{\omega}}\right)\underline{k}$$

Two tangent vectors on the blade surface are given by

$$\underline{t}_1 = \frac{\partial \underline{s}}{\partial \xi_1}$$

<div align="right">(1-8)</div>

$$\underline{t}_2 = \frac{\partial \underline{s}}{\partial \widetilde{\omega}}$$

see. e.g., Wills[43] and a vector normal to the surface (but not a unit normal) is given by

$$\underline{N} = \pm \underline{t}_1 \times \underline{t}_2$$

<div align="right">(1-9)</div>

where the sign is positive on the suction or back side and negative on the pressure or face side.

The components of these vectors in the $(\underline{i},\underline{j},\underline{k})$ system are lengthy but when expressed in the $(\underline{e}_1,\underline{e}_2,\underline{e}_{\widetilde{\omega}})$ system they are shorter. In particular, the normal is

$$
\underline{N} = \pm \left[\underline{e}_2 - \frac{\partial E}{\partial \xi_1} \underline{e}_1 + \left\{ \left(\xi_1 + E \frac{\partial E}{\partial \xi_1} \right) \frac{d\varphi_p}{d\widetilde{\omega}} - \frac{\partial E}{\partial \widetilde{\omega}} \right. \right.
$$
$$
+ \frac{d\Re}{d\widetilde{\omega}} \left(\cos\varphi_p + \frac{\partial E}{\partial \xi_1} \sin\varphi_p \right)
$$

<div align="right">(1-10)</div>

$$
\left. \left. + \left(-\widetilde{\omega} \frac{dW}{d\widetilde{\omega}} + \frac{\xi_1 \cos\varphi_p + E \sin\varphi_p}{\widetilde{\omega}} \right) \left(\sin\varphi_p - \frac{\partial E}{\partial \xi_1} \cos\varphi_p \right) \right\} \underline{e}_{\widetilde{\omega}} \right]
$$

For $E = 0$, the resulting expression for the normal is

$$
\underline{N} \equiv \underline{N}_0
$$
$$
= \pm \left[\underline{e}_2 + \underline{e}_{\widetilde{\omega}} \left\{ \xi_1 \left(\frac{d\varphi_p}{d\widetilde{\omega}} + \frac{\sin\varphi_p \cos\varphi_p}{\widetilde{\omega}} \right) \right. \right.
$$

<div align="right">(1-11)</div>

$$
\left. \left. + \frac{d\Re}{d\widetilde{\omega}} \cos\varphi_p - \widetilde{\omega} \frac{dW'}{d\widetilde{\omega}} \sin\varphi_p \right\} \right]
$$

which is the normal to the helical surface of pitch angle $\varphi_p(\widetilde{\omega})$ through the blade-reference line. Components in the $(\underline{i},\underline{j},\underline{k})$ directions can be found when Equations (1-4) and (1-1) are substituted into these expressions.

Previous investigators have assumed that the only significant contribution to $\underline{N}_0$ was $\underline{e}_2$. Note that even for blades without rake or warp, an $\underline{e}_{\widetilde{\omega}}$ component exists. This remaining term can be simplified by expressing $\varphi_p(\widetilde{\omega})$ in terms of the pitch, $P(\widetilde{\omega})$. The pitch is the distance of axial advancement in one complete revolution of a screw of pitch angle $\varphi_p(\widetilde{\omega})$:

<div align="center">15</div>

$$tan\ \varphi_p(\widetilde{\omega}) = \frac{P(\widetilde{\omega})}{2\pi\widetilde{\omega}}$$

Using this relationship, one finds

$$\frac{d\varphi_p}{d\widetilde{\omega}} + \frac{sin\ \varphi_p\ cos\ \varphi_p}{\widetilde{\omega}} = \frac{dP}{d\widetilde{\omega}} \frac{\widetilde{\omega}}{2\pi\ (\widetilde{\omega}^2 + P^2/4\pi^2)}$$

$$= \frac{dP}{d\widetilde{\omega}} \frac{cos^2\ \varphi_p}{2\pi\widetilde{\omega}}$$

(1-12)

Thus for helical surfaces of constant pitch, this component of the normal is zero. Since few modern propellers have constant pitch, this term must be retained.

For the second system of blade specification the sections are cut out by a plane at a given z value. As will be explained in Chapter 4, neither rake nor warp is considered with this viewpoint. Hence the blade-reference lines are the θ_b values and for the reference blade along the z axes, the nose tail line is on a plane and forms an angle $\varphi_B(z)$ with the y-direction. The coordinate system is similar to the previous one, except that ξ_1, ξ_2 are measured in an x,y plane at a constant z value.

The Cartesian components are

$$\left. \begin{array}{l} x = \xi_1\ sin\ \varphi_B - \xi_2\ cos\ \varphi_B \\ y = -(\xi_1\ cos\ \varphi_B + \xi_2\ sin\ \varphi_B) \\ z = z \end{array} \right\}$$

(1-13)

Similar to the previous discussion, the unit vectors are

$$\left. \begin{array}{l} \underline{e}_1 = \frac{\partial \underline{r}}{\partial \xi_1} = sin\ \varphi_B \underline{i} - cos\ \varphi_B \underline{j} \\ \\ \underline{e}_2 = \frac{\partial \underline{r}}{\partial \xi_2} = - cos\ \varphi_B \underline{i} - sin\ \varphi_B \underline{j} \end{array} \right\}$$

(1-14)

and the third vector is the $\underline{k}$ vector such that $\underline{k} = -\underline{e}_1 \times \underline{e}_2$ and here also $\underline{k} \neq \frac{\partial \underline{r}}{\partial z}$.

The blade surface is here assumed to be given by

$$\xi_2 = E(\xi_1, z)$$

(1-15)

where E is a sum of a double- and a single-valued function describing the thickness and camber distributions, respectively.

As before, a point on the surface is found by substituting this expression in the Cartesian components given by Equation (1-13), and two tangent vectors to the surface are found by differentiation. The cross product of these two tangent vectors gives a normal vector,

$$\underline{N} = \pm \left[\underline{e}_2 - \frac{\partial E}{\partial \xi_1} \underline{e}_1 + \left(\xi_1 \frac{d\varphi_B}{dz} - \frac{\partial E}{\partial z} + E \frac{\partial E}{\partial \xi_1} \frac{d\varphi_B}{dz} \right) \underline{k} \right]$$

(1-16)

This is similar to the expression for the normal where the section shape was measured on the surface of a cylinder; however, the terms for the component normal to the template plane show marked differences.

B—SECTION GEOMETRY

In this section, the specific form of the shape function is examined. In general this shape function can be written

$$\xi_2 = E(\xi_1, \xi_3)$$

where ξ_3 is either the cylindrical radius or the z variable.

The blade shape is made up of a single-valued and a double-valued function. The single-valued function is the camberline, and the double-valued function is the thickness. These functions can be considered separately.

First the thickness can be represented by

$$\xi_2 = \pm E_T(\xi_1, \xi_3)$$

where

$$E_T = \sqrt{(c_1 - \xi_1)(\xi_1 - c_2)} \sum_{n=0}^{N} a_n \left(\frac{\xi_1}{c_1 - c_2} \right)^n$$

(1-17)

$c_1 = c_1(\xi_3)$ and $c_2 = c_2(\xi_3)$ are shown in Figure 3, and in general $a_n = a_n(\xi_3)$. At the leading edge $\xi_1 = c_2$, and at the trailing edge $\xi_1 = c_1$.

Often the same form is maintained spanwise and then $a_n(\xi_3) = \tau(\xi_3) a_n$, where $\tau(\xi_3)$ is the thickness to chord ratio and the a_n are now constants.

For the regular perturbation problem,

$$\tau(\xi_3) = \epsilon T(\xi_3)$$

(1-18)

that is, the thickness is small relative to the chord. By assumption all derivatives remain of first order although by inspection this breaks down at the leading and trailing edge, where at the leading edge

$$\frac{\partial E_T}{\partial \xi_1} \sim \frac{a_0}{\sqrt{\xi_1 - c_2}}$$

(1-19)

17

Even though this singularity is not compatible with the $O(\epsilon)$ assumptions in the derivation, solutions obtained by ignoring this discrepancy have been useful. Several techniques for improvement (Friedrichs[1] and Van Dyke[3]) are known but they usually break down after a few terms.

In the singular-perturbation problem, the chord length is the small quantity, and in this case it is convenient to put

$$c_1 = \bar{\epsilon} h_1 (\xi_3)$$
$$c_2 = \bar{\epsilon} h_2 (\xi_3) \tag{1-20}$$

where $\bar{\epsilon}$ can be considered the ratio of maximum chordlength to diameter. In this case, the equation for thickness becomes

$$E_T = \bar{\epsilon} \sqrt{\left(h_1 - \frac{\xi_1}{\bar{\epsilon}}\right)\left(\frac{\xi_1}{\bar{\epsilon}} - h_2\right)} \cdot \sum_{n=0}^{N} a_n \left\{ \frac{\xi_1}{\bar{\epsilon}(h_1 - h_2)} \right\}^n \tag{1-21}$$

The normal vector involves derivatives of this function with respect to both ξ_1 and ξ_3. First, the derivative with respect to ξ_1 is

$$\frac{\partial E_T}{\partial \xi_1} = \frac{1/2(h_1 + h_2) - \frac{\xi_1}{\bar{\epsilon}}}{\sqrt{\left(h_1 - \frac{\xi_1}{\bar{\epsilon}}\right)\left(\frac{\xi_1}{\bar{\epsilon}} - h_2\right)}} \sum_{n=0}^{N} a_n \left\{ \frac{\xi_1}{\bar{\epsilon}(h_1 - h_2)} \right\}^n$$

$$+ \frac{\sqrt{\left(h_1 - \frac{\xi_1}{\bar{\epsilon}}\right)\left(\frac{\xi_1}{\bar{\epsilon}} - h_2\right)}}{h_1 - h_2} \sum_{n=1}^{N} n a_n \left[\frac{\xi_1}{\bar{\epsilon}(h_1 - h_2)} \right]^{n-1} \tag{1-22}$$

In Chapter 4, the form of this expression in inner or stretched variables is needed. Let the variable be $\sigma_1 = \xi_1/\bar{\epsilon}$, then converting this to the stretched coordinate, one finds

$$\frac{\partial E_T}{\partial \xi_1}(\sigma_1, \xi_3) = \frac{1/2(h_1 + h_2) - \sigma_1}{\sqrt{(h_1 - \sigma_1)(\sigma_1 - h_2)}} \sum_{n=0}^{N} a_n \left(\frac{\sigma_1}{h_1 - h_2}\right)^n$$

$$+ \frac{\sqrt{(h_1 - \sigma_1)(\sigma_1 - h_2)}}{(h_1 - h_2)} \sum_{n=1}^{N} n a_n \left(\frac{\sigma_1}{h_1 - h_2}\right)^{n-1} \tag{1-23}$$

This is entirely a zero-order term with respect to the chordlength parameter.

18

Second, the derivative of the thickness function with respect to the ξ_3 variable is

$$\frac{\partial E_T}{\partial \xi_3} = 1/2 \, \frac{-(c_1 c_2)' + \xi_1 (c_1 + c_2)'}{\sqrt{(c_1 - \xi_1)(\xi_1 - c_2)}} \, \sum_{n=0}^{N} a_n \left(\frac{\xi_1}{c_1 - c_2}\right)^n$$

$$+ \sqrt{(c_1 - \xi_1)(\xi_1 - c_2)} \, \sum_{n=0}^{N} a'_n \left(\frac{\xi_1}{c_1 - c_2}\right)^n \qquad (1\text{-}24)$$

$$- \sqrt{(c_1 - \xi_1)(\xi_1 - c_2)} \, \frac{(c_1 - c_2)'}{(c_1 - c_2)^2} \, \xi_1 \sum_{n=1}^{N} n a_n \left(\frac{\xi_1}{c_1 - c_2}\right)^{n-1}$$

where the prime denotes derivative with respect to ξ_3. When this is converted to the inner variable, it becomes

$$\frac{\partial E_T}{\partial \xi_3}(\sigma_1, \xi_3) = \frac{\bar{\epsilon}}{2} \, \frac{(h_1 h_2)' + \sigma_1 (h_1 + h_2)'}{\sqrt{(h_1 - \sigma_1)(\sigma_1 - h_2)}} \, \sum_{n=0}^{N} a_n \left(\frac{\sigma_1}{h_1 - h_2}\right)^n$$

$$+ \bar{\epsilon} \sqrt{(h_1 - \sigma_1)(\sigma_1 - h_2)} \, \sum_{n=0}^{N} a'_n \left(\frac{\sigma_1}{h_1 - h_2}\right)^n \qquad (1\text{-}25)$$

$$- \bar{\epsilon} \sqrt{(h_1 - \sigma_1)(\sigma_1 - h_2)} \, \frac{(h_1 - h_2)'}{(h_1 - h_2)^2} \sigma_1 \sum_{n=1}^{N} n a_n \left(\frac{\sigma_1}{h_1 - h_2}\right)^{n-1}$$

Hence, this expression remains of order $\bar{\epsilon}$

For the camberline function, the appropriate expression is

$$\xi_2 = E_c \, (\xi_1, \xi_3)$$

where

$$E_c(\xi_1, \xi_2) = \frac{(c_1 - \xi_1)(\xi_1 - c_2)}{(c_1 - c_2)} \, \sum_{n=0}^{N} b_n \left(\frac{\xi_1}{c_1 - c_2}\right)^n + \xi_1 k \qquad (1\text{-}26)$$

In some current design procedures, the shape of the camberline is computed at each radius, and in general the coefficients in the summation are not a constant times the same function of ξ_3. The derivatives of this function follow the same patterns as the thickness function. For the regular-perturbation problem, they are

both the same order and for the singular-perturbation problem, the ξ_1 derivative is of zero-order and the ξ_3 derivative is of order $\bar{\epsilon}$. For most camberline shapes, the ξ_1 derivative is bounded.

C—DIFFERENTIALS EXPRESSED IN PROFILE COORDINATES

In some portions of later chapters, it is necessary to calculate the gradient of a function which is given in the profile coordinate system. For the hypothetical functions $J_1 = J_1 (\xi_1, \xi_2, \tilde{\omega})$ and $J_2 = J_2 (\xi_1, \xi_2, z)$, the gradient can be determined by straightforward application of the chain rule. Consider the function J_1 first.

$$\nabla J_1 = \frac{\partial J_1}{\partial x} \underline{i} + \frac{\partial J_1}{\partial y} \underline{j} + \frac{\partial J_1}{\partial z} \underline{k} \tag{1-27}$$

where

$$\frac{\partial J_1}{\partial x} = \frac{\partial J_1}{\partial \xi_1} \frac{\partial \xi_1}{\partial x} + \frac{\partial J_1}{\partial \xi_2} \frac{\partial \xi_2}{\partial x}$$

$$= \sin \varphi_p \frac{\partial J_1}{\partial \xi_1} - \cos \varphi_p \frac{\partial J_1}{\partial \xi_2} \tag{1-28}$$

and the expressions for $\dfrac{\partial J_1}{\partial y}$ and $\dfrac{\partial J_1}{\partial z}$ are obtained similarly but are more complicated. After arrangement of terms, the expression becomes

$$\nabla J_1 = \frac{\partial J_1}{\partial \xi_1} \underline{e}_1 + \frac{\partial J_1}{\partial \xi_2} \underline{e}_2 + \underline{e} \tilde{\omega} \left[\frac{\partial J_1}{\partial \tilde{\omega}} + \frac{\partial J_1}{\partial \xi_1} \left(\cos \varphi_p (\theta - \theta_b - W) \right. \right.$$

$$\left. - \xi_2 \frac{d\varphi_p}{d\tilde{\omega}} - \frac{dW}{d\tilde{\omega}} \tilde{\omega} \cos \varphi_p - \frac{d\Re}{d\tilde{\omega}} \sin \varphi_p \right) + \frac{\partial J_1}{\partial \xi_2} \left(\sin \varphi_p (\theta - \theta_b - W) \right. \tag{1-29}$$

$$\left. \left. + \xi_1 \frac{d\varphi_p}{d\tilde{\omega}} - \frac{dW}{d\tilde{\omega}} \tilde{\omega} \sin \varphi_p + \frac{d\Re}{d\tilde{\omega}} \cos \varphi_p \right) \right]$$

where $(\theta - \theta_b - W)$ is given in terms of $(\xi_1, \xi_2, \tilde{\omega})$ in Equation (1-2).

For the (ξ_1, ξ_2, z) variables, a similar transformation gives

$$\nabla J_2 = \frac{\partial J_2}{\partial \xi_1} \underline{e}_1 + \frac{\partial J_2}{\partial \xi_2} \underline{e}_2 + \left[\frac{\partial J_2}{\partial z} + \frac{d\varphi_B}{dz} \cdot \left(\xi_1 \frac{\partial J_2}{\partial \xi_2} - \xi_2 \frac{\partial J_2}{\partial \xi_1} \right) \right] \underline{k} \qquad (1\text{-}30)$$

This expression is used in Chapter 4 as well as one for the Laplace equation expressed in the profile coordinates (ξ_1, ξ_2, z). From repeated application of the chain rule, one finds

$$\frac{\partial^2 J_2}{\partial x^2} + \frac{\partial^2 J_2}{\partial y^2} = \frac{\partial^2 J_2}{\partial \xi_1^2} + \frac{\partial^2 J_2}{\partial \xi_2^2}$$

$$\frac{\partial^2 J_2}{\partial z^2} = \left(\frac{d\varphi_B}{dz}\right)^2 \left(\xi_2^2 \frac{\partial^2 J_2}{\partial \xi_1^2} + \xi_1^2 \frac{\partial^2 J_2}{\partial \xi_2^2} - \xi_2 \frac{\partial J_2}{\partial \xi_2} - \xi_1 \frac{\partial J_2}{\partial \xi_1} \right)$$

$$- 2 \xi_1 \xi_2 \left(\frac{d\varphi_B}{dz}\right)^2 \frac{\partial^2 J_2}{\partial \xi_1 \partial \xi_2} + \frac{d^2 \varphi_B}{dz^2} \left[\xi_1 \frac{\partial J_2}{\partial \xi_2} - \xi_2 \frac{\partial J_2}{\partial \xi_1} \right]$$

$$+ 2 \frac{d\varphi_B}{dz} \left(\xi_1 \frac{\partial^2 J_2}{\partial \xi_2 \partial z} - \xi_2 \frac{\partial^2 J_2}{\partial \xi_1 \partial z} \right) + \frac{\partial^2 J_2}{\partial z^2}$$

Obviously, the Laplace equation involves the sum of the previous two equations. It has been broken up to call attention to a feature of the expression for $\partial^2 J_2/\partial z^2$. This feature is that any scale change applied to both ξ_1 and ξ_2 cancels. This property is utilized in Chapter 4.

21

CHAPTER 2
GENERAL FORMULATION

A—DESCRIPTION OF FLOW FIELD*

A Z-bladed propeller of finite radius R is assumed to be rotating with constant angular velocity Ω and to be advancing at a uniform rate U into an unbounded, inviscid, incompressible fluid; however, one for which the Kutta condition is satisfied at the trailing edge. The propeller produces a thrust which requires that the average pressure on one side of the blade, called either the back or suction side, is lower than on the other, called either the face or pressure side. The Kutta condition requires that no flow cross the trailing edge. The general flow pattern then is that fluid is pushed from the high-pressure side to the low-pressure side around only the leading edge and the tips. The tip flow deflects the streamlines in the vicinity of the tips toward the axis of rotation on the low-pressure side and away from the axis on the high-pressure side. This flow behavior, together with the requirement of continuity in the pressure field, results in a discontinuity in direction, but not magnitude, of the fluid velocity leaving the blades at the trailing edge. This layer of fluid slip is called a vortex sheet.

The flow model thus consists of the lifting surface and the vortex sheet advancing and rotating into still fluid.

B—GOVERNING EQUATIONS AND BOUNDARY CONDITIONS

The unsteady flow field described in Section A can be made steady by considering the flow relative to the coordinate systems rotating with the blade. In a rotating-coordinate system, the equations of motion, e.g., Kochin, Kibel' and Roze[44] Equation 2.7.8, are

$$\underline{q} \cdot grad\ \underline{q} + \frac{1}{\rho} grad\ p = -2\underline{\Omega} \ \mathbf{X}\ \underline{q} - \underline{\Omega} \ \mathbf{X}\ (\underline{\Omega} \ \mathbf{X}\ \underline{r}) \tag{2-1}$$

$$div\ \underline{q} = 0 \tag{2-2}$$

where $\underline{q}(\underline{r})$ is the velocity vector,

p is the pressure,

ρ is the density,

$\underline{\Omega} = -\Omega\underline{i}$ is the angular velocity of the propeller for the assumed right-hand rotation shown in Figure 1,

$\underline{r}$ is the position vector of a point in the flow field.

---

*This discussion is patterned after that given by Prandtl[6] for planar wings.

[44]Kochin, N.E., et al., "Theoretical Hydromechanics," (Translation of Fifth Russian Edition), Interscience Publications, Inc., New York (1964).

The flow field in the inertial reference frame is irrotational everywhere except on the boundaries. In the rotating coordinate system the vorticity is given by

$$curl\ \underline{q} = -\ 2\underline{\Omega} = 2\,\Omega\underline{i} \qquad (2\text{-}3)$$

The boundary conditions are that the upstream velocity is specified; there is no flow through the blade; the vortex sheet moves with the fluid, i.e., the normal velocity at the sheet is zero; and the velocity at the trailing edge is finite (Kutta condition). If S_{B^-} represents the pressure side of the blades, S_{B^+} the suction side, S_{V^+} the continuation of S_{B^+} onto the vortex sheet, S_{V^-} the other side of the vortex sheet, and $T(z)$ the trailing edge, then the boundary conditions become

$$\underline{q} \to \underline{q}_0 = U\underline{i} + \Omega\widetilde{\omega}\underline{e}_\theta \ as \ x \to -\infty \qquad (2\text{-}4)$$

$$\underline{q} \cdot \underline{n} = 0 \ for \ \underline{r} \in S_b \qquad (2\text{-}5)$$

$$\underline{q} < +\infty \ for \ \underline{r} \in T \qquad (2\text{-}6)$$

where U is the advance velocity in the inertial reference frame

$\underline{n}$ is the normal pointing into the fluid

$S_b = S_{V^+} \cup S_{B^+} \cup S_{B^-} \cup S_{V^-}$ and

b denotes one of the Z blades, $b = 0,1, \dots Z - 1$

If the velocity is taken as[*]

$$\underline{q} = \nabla\phi + \nabla \times \underline{B} \qquad (2\text{-}7)$$

where $\underline{B}$ is the vector potential, and ϕ is the scalar potential, then Equation (2-3) gives

$$\nabla \times (\nabla \times \underline{B}) = 2\,\Omega\underline{i}$$

and Equation (2-2) gives

$$\nabla^2\phi = 0$$

If the boundary condition at upstream infinity is associated with $\underline{B}$, an expression for $\underline{B}$ can be immediately stated:

$$\underline{B} = \widetilde{\omega}(\Omega x - \theta U)\underline{e}_{\widetilde{\omega}} \qquad (2\text{-}8)$$

where U must be a constant[**] for this expression to satisfy Equations (2-3) and (2-4), and $\nabla \times \underline{B} = \underline{q}_0$.

---

[*]The symbolic vector notation is used for the differential operators in curvilinear coordinates.

[**]The velocity component U is commonly taken as a function of radius to approximate nonuniform inflow. One would expect such shear flows to be axially variable also. Shear flows imply vorticity, and careful consideration should be given to the propagation of vorticity from upstream infinity to the propeller and on downstream.

The remaining unknown is now only the scalar function ϕ, and the problem can be reformulated in terms of it. The boundary conditions are:

$$\nabla \phi \to 0 \quad as \quad x \to -\infty, \quad \widetilde{\omega} \to \infty \qquad (2\text{-}9)$$

$$\nabla \phi \cdot \underline{n} = -\underline{q}_0 \cdot \underline{n} \quad for \quad \underline{r} \in S_b \qquad (2\text{-}10)$$

$$|\nabla \phi| < +\infty \quad for \quad \underline{r} \in T \qquad (2\text{-}11)$$

In addition the pressure is continuous across the vortex sheet.

The three simultaneous equations of motion described by Equation (2-1) have been replaced by a single equation for the scalar potential ϕ which depends only on the kinematics of the flow. The dynamics of the flow enter only in the determination of pressure which can be obtained by integrating Equation (2-1). The integration is performed by using the expansion formula

$$\underline{q} \cdot grad \; \underline{q} = 1/2 \nabla (\underline{q} \cdot \underline{q}) - \underline{q} \; X \; curl \; \underline{q}$$
$$= 1/2 \nabla (\underline{q} \cdot \underline{q}) - 2 \underline{\Omega} \; X \; \underline{q} \qquad (2\text{-}12)$$

and by noting that for $\underline{\Omega} = -\Omega \underline{i}$

$$\underline{\Omega} \; X \; (\underline{\Omega} \; X \; \underline{r}) = -\Omega^2 \; \widetilde{\omega} \underline{e}_{\widetilde{\omega}}$$
$$= \frac{-\Omega^2}{2} \nabla \widetilde{\omega}^2 \qquad (2\text{-}13)$$

Hence, Equation (2-1) can be written as

$$\nabla (\frac{1}{2} \underline{q} \cdot \underline{q} + \frac{p}{\rho} - \frac{1}{2} \Omega^2 \; \widetilde{\omega}^2) = 0$$

Since the expression is zero for all spatial derivatives, it must be constant. Thus

$$\frac{1}{2} \underline{q} \cdot \underline{q} + \frac{p}{\rho} - \frac{1}{2} \Omega^2 \; \widetilde{\omega}^2 = \frac{K}{2}$$

where K is a constant everywhere in the fluid.
Hence the pressure is

$$p = \frac{\rho}{2} \left\{ K + \Omega^2 \; \widetilde{\omega}^2 - \underline{q} \cdot \underline{q} \right\} \qquad (2\text{-}14)$$

The condition that the pressure be continuous across the votex sheet can be expressed as

$$(\underline{q} \cdot \underline{q})_{\underline{r} \in S_{V+}} = (\underline{q} \cdot \underline{q})_{\underline{r} \in S_{V-}}$$

or

$$(2\underline{q}_0 + \nabla\phi) \cdot \nabla\phi\big|_{\underline{r} \,\epsilon\, S_{V^-}}^{\underline{r} \,\epsilon\, S_{V^+}} = 0 \qquad (2\text{-}15)$$

In the next section an expression for ϕ is found which satisfies the boundary conditions in Equations (2-9) through (2-11) and Equation (2-15).

C—SOLUTION IN TERMS OF BOUNDARY VALUES

The solution of Poisson's or Laplace's equation in a three-dimensional volume can be expressed using Green's second identity; see, e.g., Tychonov and Samarski:[45]

$$\iiint_v \left(\phi \nabla^2 \frac{1}{|\underline{r}'|} - \frac{1}{|\underline{r}'|} \nabla^2 \phi\right) d\tau = \oiint_\Sigma \left(\phi\underline{n} \cdot \nabla \frac{1}{|\underline{r}'|} - \frac{1}{|\underline{r}'|} \underline{n} \cdot \nabla\phi\right) dS \qquad (2\text{-}16)$$

where v is the total fluid volume,

Σ is the surface which bounds the volume, including the surface at $|\underline{r}| \to \infty$,

$\underline{r}'$ is the position vector, measured from a fixed point in the fluid,

$\underline{n}$ is the unit normal, pointing from the bounding surface into the fluid.

If ϕ satisfies Laplace's equation, the volume integral is zero everywhere in the fluid, except at the point $\underline{r}' = 0$. This point can be excluded from the volume by enclosing it in a sphere.[*] Taking the limit of the surface integral over the sphere[*] as the radius goes to zero, one finds the following standard formula

$$\phi(\underline{r}) = \frac{1}{4\pi} \oiint_\Sigma \left\{\phi\,\underline{n} \cdot \nabla \frac{1}{|\underline{r}\text{-}\underline{s}|} - \frac{1}{|\underline{r}\text{-}\underline{s}|} \underline{n} \cdot \nabla\phi\right\} dS \qquad (2\text{-}17)$$

where $\underline{r}$ is an arbitrary point in the fluid, and

$\underline{s}$ is a point on the boundary.

---

[45]Tychonov, A.N. and A.A. Samarski, "Partial Differential Equations of Mathematical Physics," Vol. 1, Holden-Day, Inc., San Francisco, Calif (1964).

[*]Tychonov and Samarski,[45] for example, show that other shapes excluding the singularity are also satisfactory as long as the maximum dimension of the excluded region goes to zero.

It is necessary to know the value of ϕ on the boundary as well as in the flow field. That is, one seeks

$$\lim_{\underline{r} \to \underline{r}_o} \phi(\underline{r}) = \lim_{\eta \to o} \phi(\underline{r}_o + \eta\underline{e}) \equiv \phi^{\pm}(\underline{r}_o)$$

where $\underline{r}$ is a point in the flow field

$\underline{r}_o$ is a point on the surface

$\underline{e}$ is an arbitrary vector pointing into the fluid from $\underline{r}_o$ and the

$\pm$ sign is used when $\underline{r}_o$ is on the $\pm$ surface

Two situations occur: one when $\underline{r}_o$ is a point on the boundary of a solid of finite thickness, and one when $\underline{r}_o$ is a point on a boundary, both sides of which are in the flow field, across which ϕ is discontinuous. In the second case, the limit $\underline{r} \to \underline{r}_o$ produces singularities in both sides of the surface.

For the first case, for which $\underline{r}_o$ is on a single-sided surface, one finds[*]

$$\phi^{\pm}(\underline{r}_o) = \frac{1}{2\pi} \iint_{\Sigma} \left\{ \phi\underline{n} \cdot \frac{\underline{r}_o \cdot \underline{s}}{|\underline{r}_o \cdot \underline{s}|^3} - \frac{1}{|\underline{r}_o \cdot \underline{s}|} \underline{n} \cdot \nabla\phi \right\} ds \tag{2-18a}$$

and for the second case, for which $\underline{r}_o$ is on a double-sided surface, one finds

$$\phi^+(\underline{r}_o) + \phi^-(\underline{r}_o) = \frac{1}{2\pi} \iint_{\Sigma} \left\{ \phi\underline{n} \cdot \frac{\underline{r}_o \cdot \underline{s}}{|\underline{r}_o \cdot \underline{s}|^3} - \frac{1}{|\underline{r}_o \cdot \underline{s}|} \underline{n} \cdot \nabla\phi \right\} ds \tag{2-18b}$$

where the improper surface integral is obtained by evaluating the integral over the bounding surface, excluding the region surrounding the point $\underline{r}_o$, and then by taking the limit as the maximum dimension of the excluded region tends to zero.

Since the present problem is a second (or Neumann) boundary-value problem, it is important to determine the values of the gradient of ϕ on the boundary. To find this limit, the point $\underline{r}_o$ is excluded from the surface Σ by surrounding it with different shapes $s(\underline{r}_o, \lambda)$, where λ characterizes the dimensions of the region. With the same notation as used previously, one seeks

$$\lim_{\underline{r} \to \underline{r}_o} \nabla\phi(\underline{r}) = \lim_{\eta \to o} \nabla\phi(\underline{r}_o + \eta\underline{e}) \equiv (\nabla\phi)^{\pm}$$

For a point on the boundary of a solid of finite thickness

$$(\nabla\phi)^{\pm} = \frac{1}{2\pi} \lim_{\lambda \to 0} \left[\iint_{\Sigma - s(\underline{r}_o, \lambda)} \frac{\underline{r}_o \cdot \underline{s}}{|\underline{r}_o \cdot \underline{s}|^3} (\underline{n} \cdot \nabla\phi) ds \right] + \tag{2-19a}$$

[*]The $\pm$ superscripts here denote different sides of the surface as well as the limit operation when appropriate.

26

$$+ \frac{1}{2\pi} \lim_{\lambda \to o} \left[\oiint_{\Sigma - s(\underline{r}_o, \lambda)} \phi \left(\frac{\underline{n}}{|\underline{r}_o - \underline{s}|^3} - \frac{3(\underline{r}_o - \underline{s}) \cdot \underline{n}}{|\underline{r}_o - \underline{s}|^5} (\underline{r}_o - \underline{s}) \right) ds - K_s \frac{\phi_o \underline{n}_o}{\lambda} \right] \qquad \text{(2-19a)}$$
<div align="right">Cont'd</div>

where $\underline{n}_o = \underline{n}(\underline{r}_o)$, and $\phi_o = \phi(\underline{r}_o)$.

When $s(\underline{r}_o, \lambda)$ is the region of Σ interior to a right circular cylinder of radius λ with axis $\underline{n}_o$, then $K_s = 2\pi$; when $s(\underline{r}_o, \lambda)$ is the region of Σ interior to a square of half-side λ with axis $\underline{n}_o$, then $K_s = 4\sqrt{2}$; when $s(\underline{r}_o, \lambda)$ is the region of Σ interior to a rectangle, two sides of which are distant λ from $\underline{r}_o$ and the other two sides of which are an arbitrary finite distance from $\underline{r}_o$, then $K_s = 4$. We call the first integral in Equation (2-19a) a Cauchy principal-value integral.

For a point on a boundary in the flow field

$$(\nabla \phi)^+ + (\nabla \phi)^- = \frac{1}{2\pi} \lim_{\lambda \to o} \left[\oiint_{\Sigma - s(\underline{r}_o, \lambda)} \frac{\underline{r}_o - \underline{s}}{|\underline{r}_o - \underline{s}|^3} (\underline{n} \cdot \nabla \phi) \, ds \right]$$

$$+ \frac{1}{2\pi} \lim_{\lambda \to o} \left[\oiint_{\Sigma - s(\underline{r}_o, \lambda)} \phi \left(\frac{\underline{n}}{|\underline{r}_o - \underline{s}|^3} - \frac{3(\underline{r}_o - \underline{s}) \cdot \underline{n}}{|\underline{r}_o - \underline{s}|^5} (\underline{r}_o - \underline{s}) \right) ds \right.$$

$$\left. - \frac{\underline{n}_o^+ \phi_o^+ + \underline{n}_o^- \phi_o^-}{\lambda} K_s \right] \qquad \text{(2-19b)}$$

The limit operation indicated in Equations (2-19) is considered to define a singularity in the mathematical literature (Tychonov and Samarski)[45] while in the aeronautical literature (Mangler,[46] Ashley and Landahl)[47] such forms are accepted. In Chapter 5, a form of the expression for velocity is obtained for which only Cauchy principal values are needed so that numerical analysis can be performed on the more convenient form.

The values of the gradient on the boundary are generally to be interpreted as $\nabla F(\underline{r})|_{\underline{r} \to \underline{r}_o} = (\nabla F)^{\pm}$. This expression is not equal to $\nabla F(\underline{r}_o) \equiv \nabla(F^{\pm})$ since the normal components are not equal. Generally the normal component is given by a separate boundary condition, and one need not explicitly consider the distinction. Throughout the text the notation for differentials of functions known on the surface $\nabla(F^{\pm})$ is indicated, rather than the field value evaluated on the body $(\nabla F)^{\pm}$. Although this notation sometimes indicates a ridiculous result if interpreted literally, it is used since it permits a shorthand-like notation to be developed.

[46]Mangler, K.W., "Improper Integrals in Theoretical Aerodynamics," Aeronautical Research Council, Current Papers 94 (1952).

[47]Ashley, H. and M. Landahl, "Aerodynamics of Wings and Bodies," Addison-Wesley Publishing Co., Inc., Reading, Mass. (1965).

The surface Σ consists of the Z bounding surfaces of $S_B \cup S_V$ (where S_B is the blade surface, and S_V the shed vortex surface) and the surface for $|\underline{r}| \to \infty$. At this point it is necessary to suppose that the integral over the bounding surface at infinity gives at most a constant. (This supposition will be proven.) Hence, to within this additive constant, the potential for the propeller can be written

$$\phi(\underline{r}) = \frac{1}{4\pi} \sum_{b=0}^{Z-1} \oiint_{S_b} \left\{ \phi(\underline{s})\underline{n}(\underline{s}) \cdot \nabla_s \frac{1}{|\underline{r}-\underline{s}|} - \frac{1}{|\underline{r}-\underline{s}|} \underline{n}(\underline{s}) \cdot \nabla_s \phi(\underline{s}) \right\} dS \qquad (2\text{-}20)$$

where S_b is one of the M bounding surfaces

$$S_b = S_{V+} \cup S_{B+} \cup S_{B-} \cup S_{V-}.$$

The boundary condition in Equation (2-10) can be used to simplify Equation (2-20) since the second part of the integral becomes

$$\oiint_{S_b} \frac{1}{|\underline{r}-\underline{s}|} \underline{n} \cdot \nabla_s \phi \, dS = - \oiint_{S_b} \frac{\underline{q}_0 \cdot \underline{n}}{|\underline{r}-\underline{s}|} \, dS$$

$$= - \oiint_{S_B^+ \cup S_B^-} \frac{\underline{q}_0 \cdot \underline{n}}{|\underline{r}-\underline{s}|} \, dS \qquad (2\text{-}21)$$

The reduction in area in Equation (2-21) follows because $\underline{q}_0$ is continuous at S, and $\underline{n}$ (on S_V^+) = $-n$ (on S_V^-). The normal on S_V^+ is directed oppositely to that on S_V^-, and hence Equation (2-20) can be written

$$\phi(\underline{r}) = \frac{1}{4\pi} \sum_{b=0}^{Z-1} \oiint_{S_{B+} \cup S_{B-}} \left\{ \phi(\underline{s})\underline{n} \cdot \nabla_s \frac{1}{|\underline{r}-\underline{s}|} + \frac{\underline{q}_0 \cdot \underline{n}}{|\underline{r}-\underline{s}|} \right\} dS$$

$$+ \frac{1}{4\pi} \sum_{b=0}^{Z-1} \oiint_{S_{V+}} \left\{ \phi_+ - \phi_- \right\} \underline{n}_+ \cdot \nabla_s \frac{1}{|\underline{r}-\underline{s}|} \, dS \qquad (2\text{-}22)$$

28

The circulation[*] in a fluid is defined as the integral

$$\Gamma = \oint \underline{q} \cdot d\underline{\ell}$$

$$= \oint (\underline{q}_0 + \nabla_\phi) \cdot d\underline{\ell} \tag{2-23}$$

where $d\underline{\ell}$ is the vector arc length along the closed curve which completely encircles the shed vorticity. Since $\underline{q}_0$ is a continuous point function, it contributes nothing to the integral in Equation (2-23). For a curve which lies entirely within the irrotational flow except at the one point at which it cuts the shed vortex sheet

$$\Gamma\left(\underline{r}_{S_V}\right) = \left\{ \phi^+ - \phi^- \right\} \underline{r} \in S_V \tag{2-24}$$

Further simplification is possible by considering the continuous vortex sheet to be composed of lines of constant circulation which leave the trailing edge of the blade at the point $T(z)$.

In Figure 4, from curve C_2, the circulation about the blade at $T(z)$ is given by

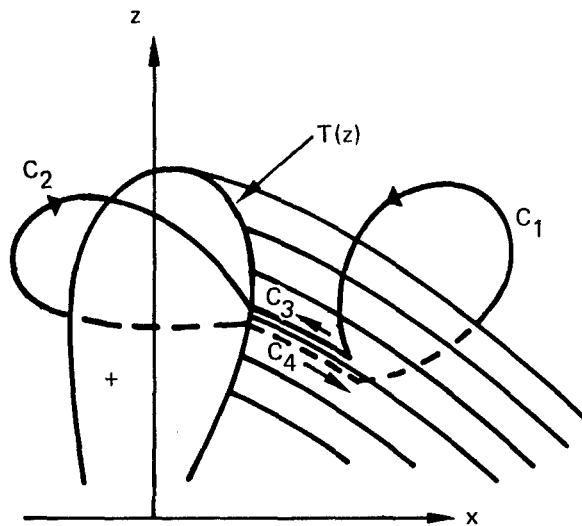$$\Gamma(T(z)) = \phi^+(T(z)) - \phi^-(T(z)) \tag{2-25}$$

Figure 4 — Schematic of Vortex Sheet
for Determining Circulation

[*]The word circulation will be associated with the scalar jump in potential across a surface as in Equation (2-24), and the word vorticity will be associated with the vector jump in velocity across a surface. If $\underline{\Lambda}$ is the vorticity vector then $\underline{\Lambda} = \underline{n} \times (\underline{q}^+ - \underline{q}^-) = \underline{n} \times \nabla (\phi^+ - \phi^-) = \underline{n} \times \nabla\Gamma$, where $\underline{n}$ is the + unit normal; see Reference 48.

[48]Milne-Thomson, L.M., "Theoretical Hydrodynamics," Fifth Edition, The Macmillan Company, New York (1968).

Now the circulation at $\underline{r} \in S_v$ is determined from the curve C_1. This curve is connected to C_2 by the curves C_3 and C_4 lying along a line of constant circulation. Hence, the total curve is simply connected and

$$
\begin{aligned}
0 &= \int_{C_3} \nabla \phi \cdot d\underline{\ell} + \int_{C_4} \nabla \phi \cdot d\underline{\ell} + \Gamma(\underline{r} \in S_v) - \Gamma(T(z)) \\
&= \int_{C_3} \nabla(\phi^+ - \phi^-) \cdot d\underline{\ell} + \Gamma(\underline{r} \in S_v) - \Gamma(T(z))
\end{aligned}
\tag{2-26}
$$

By definition, C_3 lies along a curve of constant circulation and from Equation (2-24), the integrand in Equation (2-26) is

$$
\nabla\Gamma \cdot \underline{t}_1 = \frac{\partial \Gamma}{\partial t_1} = 0
\tag{2-27}
$$

where $\underline{t}_1$ is a unit vector along the lines of constant circulation. Hence

$$
\Gamma(\underline{r} \in S_v) = \Gamma(T(z))
\tag{2-28}
$$

Conditions are sought which describe the position vector of this line of constant circulation which leaves the trailing edge from the point $\underline{r}_T \in T(z)$. To emphasize that this point is located at the blade, let it be written z_0. The position vector of the line of constant circulation can be described as

$$
\begin{aligned}
\underline{\zeta} &= \underline{\zeta}(z_0, \theta; \theta_b)^* \\
&= f_1(z_0, \theta; \theta_b) \underline{e}_\varpi(\theta) + f_2(z_0, \theta; \theta_b) \underline{i}
\end{aligned}
\tag{2-29}
$$

where z_0 is the parameter describing the starting position of the line,

θ is the independent variable, and

$\theta_b = \dfrac{2\pi b}{Z}$ is the parameter describing the individual vortex sheets.

The functions $f_1(z_0, \theta; \theta_b)$ and $f_2(z_0, \theta; \theta_b)$ are the radius and axial position of the line, respectively. The parameter z_0 ranges from zero to the propeller radius, and the variable θ ranges from the trailing edge $\theta_{TE}(z_0)$ to ∞. If $f_1 = z_0$, then no contraction of the shed vorticity takes place.

To establish differential equations** governing the position of the line, Equations (2-10) and (2-15) will be used together with the definition that the strength of the circulation is constant along the line. Since the rate of change of Γ is zero along the line,

---

*Alternatively, one could take $\underline{\zeta} = \underline{\zeta}(z_0, x; \theta_b)$. However, the usual representation given in Equation (2-29) was more convenient.

**The derivation here parallels that given by Ciolkowski[49] and Thurber.[7]

[49]Ciolkowski, S.I., "The Swept-Back Wing," Ph.D. Thesis, New York University, University Microfilms 24,694 (1955).

$$\nabla \Gamma(\underline{r}) \cdot \frac{d\underline{\zeta}}{d\theta} = 0 \tag{2-30}$$

Since the vortex sheet is actually continuous, the function $\underline{\zeta}(z_0, \theta)$ may be considered a function of two independent variables which describe the surface. Lines of constant circulation are obtained by holding z_0 constant. Tangent vectors in the surface S_V are found by constructing;

$$\underline{t}_1 = \frac{\partial \underline{\zeta}}{\partial \theta} \tag{2-31}$$

$$\underline{t}_2 = \frac{\partial \underline{\zeta}}{\partial z_0} \tag{2-32}$$

see, e.g., Wills.[43]

A vector normal to the sheet S_V (but not a unit normal) is given by

$$\underline{N} = \underline{t}_1 \times \underline{t}_2 = \frac{\partial \underline{\zeta}}{\partial \theta} \times \frac{\partial \underline{\zeta}}{\partial z_0} \tag{2-33}$$

which is assumed to be non-zero.

Hence, Equation (2-10) can be expressed

$$\left(\underline{q}_0 + \nabla \phi \right) \cdot \underline{N} = 0 \tag{2-34}$$

Since $\Gamma = \left\{ \phi^+ - \phi^- \right\}_{\underline{r} \in S_V}$, Equation (2-34) gives two equations:

$$\nabla \Gamma \cdot \underline{N} = 0 \tag{2-35}$$

$$\underline{N} \cdot \left[2\underline{q}_0 + \nabla \left\{ \phi^+ + \phi^- \right\} \right] = 0 \tag{2-36}$$

Let $\psi \equiv \left\{ \phi^+ + \phi^- \right\}_{\underline{r} \in S_V}$. Then Equation (2-36) is

$$\underline{N} \cdot (2\underline{q}_0 + \nabla \psi) = 0 \tag{2-37}$$

Now Equation (2-15) can be written as

$$\nabla \Gamma \cdot (\underline{q}_0 + 1/2 \nabla \psi) = 0 \tag{2-38}$$

It would appear that, since only two unknowns, f_1 and f_2, are sought, the scalar Equations (2-27) or (2-30) and (2-37) would be sufficient to establish differentials of the trajectory. However, derivatives with respect to z_0 enter into the equations and are not desirable. For a more elegant form of the differential equation for $\underline{\zeta}$, Equation (2-35) must be used.

Equations (2-35) and (2-30) show that

$$\nabla\Gamma \times (\underline{t}_1 \times \underline{N}_1) = (\nabla\Gamma \cdot \underline{N}) \underline{t}_1 - (\nabla\Gamma \cdot \underline{t}_1) \underline{N} = 0 \qquad (2\text{-}39)$$

Since Equation (2-39) is zero, any multiple of it is also zero. Hence,

$$(2\underline{q}_0 + \nabla\psi) \times (\nabla \Gamma \times (\underline{t}_1 \times \underline{N})) = 0 \qquad (2\text{-}40)$$

In another form this equation is

$$\left\{ (2\underline{q}_0 + \nabla\psi) \cdot (\underline{t}_1 \times \underline{N}) \right\} \nabla\Gamma - \left[(2\underline{q}_0 + \nabla\psi) \cdot \nabla\Gamma \right] \underline{t}_1 \times \underline{N} = 0$$

Equation (2-38) simplifies this equation to be

$$\left\{ \left(2\underline{q}_0 + \nabla\psi \right) \cdot \left(\underline{t}_1 \times \underline{N} \right) \right\} \nabla\Gamma = 0$$

This equation holds everywhere on the sheet. Since

$\nabla\Gamma \neq 0$ everywhere, it requires that

$$(2\underline{q}_0 + \nabla\psi) \cdot (\underline{t}_1 \times \underline{N}) = 0 \qquad (2\text{-}41)$$

Thus for the orthogonal base vector system $(\underline{t}_1, \underline{N}, \underline{t}_1 \times \underline{N})$, the average velocity at the vortex sheet, $(\underline{q}_0 + 1/2\nabla\psi)$, has no $\underline{N}$ component from Equation (2-37) and no $\underline{t}_1 \times \underline{N}$ component from Equation (2-41). Hence the average velocity is parallel to the curves of constant circulation, and the equation for $\underline{\zeta}$ can be constructed from two of the three scalar equations which make up

$$(2\underline{q}_0 + \nabla\psi) \times \underline{t}_1 = 0 \qquad (2\text{-}42)$$

The vector $\underline{t}_1$ is

$$\underline{t}_1 = \frac{\partial f_1}{\partial \theta} \underline{e}_{\widetilde{\omega}} + f_1 \underline{e}_\theta + \frac{\partial f_2}{\partial \theta} \underline{i}$$

and on the shed vortex sheet

$$(2\underline{q}_0 + \nabla\psi)\Big|_{\underline{r} = \underline{\zeta}} = \frac{\partial \psi}{\partial \widetilde{\omega}} \underline{e}_{\widetilde{\omega}} + \left(2\Omega f_1 + \frac{1}{f_1} \frac{\partial \psi}{\partial \theta} \right) \underline{e}_\theta + \left(2U + \frac{\partial \psi}{\partial x} \right) \underline{i}$$

Hence, Equation (2-42) in component form is

$$f_1 \left(2U + \frac{\partial \psi}{\partial x} \right) - \left(2\Omega f_1 + \frac{1}{f_1} \frac{\partial \psi}{\partial \theta} \right) \frac{\partial f_2}{\partial \theta} = 0 \qquad (2\text{-}43)$$

$$\frac{\partial f_2}{\partial \theta} \frac{\partial \psi}{\partial \widetilde{\omega}} - \left(2U + \frac{\partial \psi}{\partial x} \right) \frac{\partial f_1}{\partial \theta} = 0 \qquad (2\text{-}44)$$

32

$$\frac{\partial f_1}{\partial \theta}\left(2\,\Omega f_1 + \frac{1}{f_1}\frac{\partial \psi}{\partial \theta}\right) - f_1\frac{\partial \psi}{\partial \widetilde{\omega}} = 0 \tag{2-45}$$

Thus from Equation (2-43)

$$\frac{\partial f_2}{\partial \theta} = \frac{U + 1/2\,\dfrac{\partial \psi}{\partial x}}{\Omega + \dfrac{1}{2 f_1^{\,2}}\dfrac{\partial \psi}{\partial \theta}} \tag{2-46}$$

and from Equation (2-45)

$$\frac{\partial f_1}{\partial \theta} = \frac{\dfrac{1}{2}\dfrac{\partial \psi}{\partial \widetilde{\omega}}}{\Omega + \dfrac{1}{2 f_1^{\,2}}\dfrac{\partial \psi}{\partial \theta}} \tag{2-47}$$

Equations (2-46) and (2-47) are nonlinear coupled integro-differential equations for the radial and axial position of the lines of constant circulation.

The integral over the shed vortex sheet in the expression for ϕ, Equation (2-22), can be simplified using the coordinates z_0, θ used to describe the vortex sheet; see Figure 4. First, in the expression

$$\nabla_s \frac{1}{|r\text{-}\underline{s}|} = \frac{r\text{-}\underline{s}}{|r\text{-}\underline{s}|^3}$$

the position of the circulation element is used for $\underline{s}$ so the integration is performed for constant circulation strength. Second, the value of the vector surface area element $\underline{n}\,dS$ is given by

$$\begin{aligned}
\underline{n}dS &= \underline{t}_1 \text{X}\ \underline{t}_2\ dz_0\ da \\
&= \frac{\partial \underline{\zeta}}{\partial a} \text{X} \frac{\partial \underline{\zeta}}{\partial z_0}\ dz_0\ da
\end{aligned} \tag{2-48}$$

where a is a dummy variable for θ; see, e.g., Wills.[43] With these changes, the integral over a shed vortex sheet becomes

$$\phi_{b,V} \equiv \frac{+1}{4\pi} \int_0^R \Gamma(z_0)\,dz_0 \int_{a_{TE(z_0)}}^{\infty} \left(\frac{\partial \underline{\zeta}}{\partial a} \text{X} \frac{\partial \underline{\zeta}}{\partial z_0}\right) \cdot \frac{r\text{-}\underline{\zeta}}{|r\text{-}\underline{\zeta}|^3}\,da \tag{2-49}$$

where b denotes an individual blade.

Hence, ϕ becomes:

$$\phi(\underline{r}) = \frac{1}{4\pi} \sum_{b=0}^{Z-1} \iint_{S_B} \phi(\underline{s})\underline{n} \circ \frac{\underline{r}\text{-}\underline{s}}{|\underline{r}\text{-}\underline{s}|^3} \, dS + \sum_{b=0}^{Z-1} \phi_{b,V}(\underline{r})$$

$$+ \frac{1}{4\pi} \sum_{b=0}^{Z-1} \iint_{S_B} \frac{\underline{q}_0 \cdot \underline{n}}{|\underline{r}\text{-}\underline{s}|} \, ds$$

(2-50)

As described in Chapter 1, the propeller geometry is traditionally defined in terms of blade sections lying on cylinders of constant radius. The nose-tail line lies on the cylinder, and, hence, blade shape is measured from a helical surface of radially varying pitch. On the cylindrical surface $\widetilde{\omega} = $ constant, a left-handed coordinate system (to define section geometry in the traditional orientation) is constructed with ξ_1 on the surface of the cylinder and is measured positively in the downstream direction along the constant pitch of the nose-tail line. The variable ξ_2 is normal to the ξ_1 axis and points in the upstream direction. Unit orthogonal vectors $(\underline{e}_1, \underline{e}_2, \underline{e}_{\widetilde{\omega}})$ are in the $(\xi_1, \xi_2, \widetilde{\omega})$ direction, respectively, but the coordinate system is only locally orthogonal; this coordinate system is detailed in Chapter 1. Although the pitch is assumed to be that of the nose-tail line, it is not necessary in the following development and will not be used that way in later chapters.

The blade shape is given by

$$\left. \begin{array}{l} \xi_2 = E(\xi_1, \widetilde{\omega}) \\[2mm] \quad = E_c(\xi_1, \widetilde{\omega}) \pm E_T(\xi_1, \widetilde{\omega}) \end{array} \right\} \quad c_2(\widetilde{\omega}) \leqslant \xi_1 \leqslant c_1(\widetilde{\omega}), 0 \leqslant \widetilde{\omega} \leqslant R \qquad (2\text{-}51)$$

where E_c is the camberline function and E_T is the thickness function; hence, the position vector of a point on the surface is given by

$$\underline{s} = (\mathcal{R} + \xi_1 \sin \varphi_p - E \cos \varphi_p) \underline{i} - \widetilde{\omega} \sin \left(\theta_b + W \right.$$

$$+ \frac{\xi_1 \cos \varphi_p + E \sin \varphi_p}{\widetilde{\omega}} \right) \underline{j} + \widetilde{\omega} \cos \left(\theta_b + W + \frac{\xi_1 \cos \varphi_p + E \sin \varphi_p}{\widetilde{\omega}} \right) \underline{k} \qquad (2\text{-}52)$$

where $\varphi_p(\widetilde{\omega})$ is the pitch angle of the blade-section reference line,

$\mathcal{R}(\widetilde{\omega})$ is the rake, and

$W(\widetilde{\omega})$ is the warp.

A normal is given by; see Chapter 1

$$\underline{N} = \pm \left\{ \frac{\partial \underline{s}}{\partial \xi_1} \times \frac{\partial \underline{s}}{\partial \widetilde{\omega}} \right\}$$

$$= \pm \left[\underline{e}_2 - \frac{\partial E}{\partial \xi_1} \underline{e}_1 + \left\{ (sin\ \varphi_p - \frac{\partial E}{\partial \xi_1} cos\ \varphi_p) \cdot \left(\frac{\xi_1\ cos\ \varphi_p + E\ sin\ \varphi_p}{\widetilde{\omega}} - \widetilde{\omega} \frac{dW}{d\widetilde{\omega}} \right) \right. \right.$$

$$\left. + \frac{d\mathcal{R}}{d\widetilde{\omega}} \left(cos\ \varphi_p + \frac{\partial E}{\partial \xi_1} sin\ \varphi_p \right) \right. \tag{2-53}$$

$$\left. \left. + \left(\xi_1 + E \frac{\partial E}{\partial \xi_1} \right) \frac{d\varphi_p}{d\widetilde{\omega}} - \frac{\partial E}{\partial \widetilde{\omega}} \right\} \underline{e}_{\widetilde{\omega}} \right]$$

where the + sign refers to the S_{B+} surface, i.e., suction or back side; and the - sign, to the S_{B-} surface, i.e., pressure or face side. The vector element of area is

$$\underline{n}ds = \underline{N}\ d\xi_1\ d\widetilde{\omega} \tag{2-54}$$

These expressions can be substituted into Equation (2-50) to give precise limits on the integration. Because of nonlinearities, no conceptual simplifications result unless the expressions are linearized.

The explicit form of the normal allows the body boundary condition to be simplified. The free-stream velocity can be resolved to

$$\underline{q}_0 = |\underline{q}_0|\ cos\ (\varphi_p - \beta) \underline{e}_1 + |\underline{q}_0|\ sin\ (\varphi_p - \beta) \underline{e}_2$$

so that on the body, the boundary condition is

$$\underline{N} \cdot \nabla \phi = \mp \sqrt{U^2 + \Omega^2\ \widetilde{\omega}^2} \left\{ sin\ (\varphi_p - \beta) - \frac{\partial E}{\partial \xi_1} cos\ (\varphi_p - \beta) \right\} \tag{2-55}$$

where $\quad \beta = tan^{-1} \dfrac{U}{\Omega\widetilde{\omega}}$

Equations (2-49), (2-50), (2-46), (2-47) and (2-55) constitute the exact formulation. Equations (2-46) and (2-47) are nonlinear in ϕ. Although Equation (2-55) is linear in ϕ, an integral equation results in both the design and performance applications. Fortunately, however, the integral equation can be reduced to a quadrature in appropriate cases when the solution is expanded in a perturbation series. These perturbation solutions are the subject of Chapters 3 and 4.

With ϕ known, the pressure can be computed from Equation (2-14)

$$p = \frac{\rho}{2} \left\{ K - U^2 - (2\underline{q}_0 + \nabla\phi) \cdot \nabla\phi \right\}$$

and then the force on the propeller can be found from

$$\underline{F} = \sum_{b=0}^{Z-1} \oiint_{S_B} p(-\underline{n})ds$$

$$= \frac{\rho}{2} \sum_{b=0}^{Z-1} \oiint_{S_B} [2\underline{q}_0 + \nabla\phi) \cdot \nabla\phi] \underline{n}ds \qquad (2\text{-}56)$$

In particular, the thrust is

$$T = -\underline{F} \cdot \underline{i} = -\frac{\rho}{2} Z \oiint_{S_B} [(2\underline{q}_0 + \nabla\phi) \cdot \nabla\phi] \underline{i} \cdot \underline{n}ds \qquad (2\text{-}57)$$

Equation (2-54) can be used to give an explicit formula for calculating thrust. The $\underline{i}$ component of Equation (2-53) is

$$\underline{N} \cdot \underline{i} = \mp \left\{ \cos\varphi_p + \sin\varphi_p \frac{\partial E}{\partial\xi_1} \right\}$$

$$= \mp \left\{ \cos\varphi_p + \sin\varphi_p \frac{\partial E_c}{\partial\xi_1} \right\} - \sin\varphi_p \frac{\partial E_T}{\partial\xi_1} \qquad (2\text{-}58)$$

Hence

$$T = \frac{\rho Z}{2} \int_0^R d\widetilde{\omega} \int_{c_2 (\widetilde{\omega})}^{c_1 (\widetilde{\omega})} \left[\left(p^- - p^+ \right) \left(\cos\varphi_p + \sin\varphi_p \frac{\partial E_c}{\partial\xi_1} \right) \right.$$

$$\left. + \left(p^- + p^+ \right) \sin\varphi_p \frac{\partial E_T}{\partial\xi_1} \right] d\xi_1$$

or in terms of ϕ:

$$T = \frac{\rho}{2} Z \int_0^R d\widetilde{\omega} \int_{c_2 (\widetilde{\omega})}^{c_1 (\widetilde{\omega})} \left[\left\{ 2\underline{q}_0 \cdot \nabla (\phi^+ - \phi^-) + \nabla\phi^+ \cdot \nabla\phi^+ - \nabla\phi^- \cdot \nabla\phi^- \right\} \cdot \right.$$

$$\left(\cos\varphi_p + \sin\varphi_p \frac{\partial E_c}{\partial\xi_1} \right) + \left\{ 2\underline{q}_0 \cdot \nabla (\phi^+ + \phi^-) + \nabla\phi^+ \cdot \nabla\phi^+ \right.$$

$$\left. + \nabla\phi^- \cdot \nabla\phi^- \right\} \sin\varphi_p \frac{\partial E_T}{\partial\xi_1} \right] d\xi_1$$

where ϕ^+ and ϕ^- are the values of ϕ on the suction and pressure side of the blade at the points of intersection of the line ξ_1, $\widetilde{\omega}$ and the blade. By analogy with Equation (2-25), the circulation at the points of intersection of the line ξ_1, $\widetilde{\omega}$ and the blade is defined as

$$\Gamma_B(\xi_1, \widetilde{\omega}) \equiv \phi(\xi_1, E^+, \widetilde{\omega}) - \phi(\xi_1, E^-, \widetilde{\omega}) \equiv \phi^+ - \phi^-$$

$$= \int^{\xi_1, \widetilde{\omega}} (\nabla\phi^+ \cdot d\underline{\ell}^+ - \nabla\phi^- \cdot d\underline{\ell}^-) \qquad (2\text{-}59)$$

where the integration starts at a point on the edge of the lifting surface or wake and goes to the point ξ_1, $\widetilde{\omega}$. Similar to Equation (2-37), we define

$$\psi_B(\xi_1, \widetilde{\omega}) \equiv \phi^+ + \phi^-$$

$$= \int^{\xi_1, \widetilde{\omega}} (\nabla\phi^+ \cdot d\underline{\ell}^+ + \nabla\phi^- \cdot d\underline{\ell}^-) \qquad (2\text{-}60)$$

which gives

$$T = \frac{\rho}{2} Z \int_0^R d\widetilde{\omega} \int_{c_2}^{c_1} \left[\left\{ 2\underline{q}_0 \cdot \nabla\Gamma_B + \nabla\phi_B \right\} \left(\cos\varphi_p + \sin\varphi_p \frac{\partial E_c}{\partial\xi_1} \right) \right.$$

$$\left. + (2q_0 \cdot \nabla\psi_B + \nabla\phi^+ \cdot \nabla\phi^+ + \nabla\phi^- \cdot \nabla\phi^-) \sin\varphi_p \frac{\partial E_T}{\partial\xi_1} \right] d\xi_1 \qquad (2\text{-}61)$$

The thrust coefficient is

$$C_T \equiv \frac{T}{1/2\, \rho U^2\, \pi R^2} = \frac{Z}{\pi U^2} \int_0^1 d\frac{\widetilde{\omega}}{R} \left[2\cos\varphi_p \sqrt{U^2 + \Omega^2\, \widetilde{\omega}^2} \cos(\varphi_p - \beta) \cdot \Gamma(\widetilde{\omega}) \right.$$

$$+ 2\sqrt{U^2 + \Omega^2\, \widetilde{\omega}^2}\, \sin\varphi_p \int_{c_2/R}^{c_1/R} \left\{ \cos(\varphi_p - \beta) \left(\frac{\partial\Gamma_B}{\partial\xi_1} \frac{\partial E_c}{\partial\xi_1} \right. \right.$$

$$+ \frac{\partial\psi_B}{\partial\xi_1} \frac{\partial E_T}{\partial\xi_1} \Bigg) + \sin(\varphi_p - \beta)\, \underline{e}_2 \cdot \left(\nabla\psi_B \frac{\partial E_T}{\partial\xi_1} + \cot\varphi_p\, \nabla\Gamma_B \right.$$

$$+ \nabla\Gamma_B \frac{\partial E_c}{\partial\xi_1} \Bigg) \Bigg\} d\frac{\xi_1}{R} + \cos\varphi_p \int_{c_2/R}^{c_1/R} \nabla\psi_B \cdot \nabla\Gamma_B\, d\frac{\xi_1}{R} + \sin\varphi_p \cdot \qquad (2\text{-}62)$$

$$\int_{c_2/R}^{c_1/R} \left(\nabla\psi_B \cdot \nabla\Gamma_B \frac{\partial E_c}{\partial\xi_1} + \left\{ (\nabla\phi^+)^2 + (\nabla\phi^-)^2 \right\} \frac{\partial E_T}{\partial\xi_1} \right) d\frac{\xi_1}{R} \Bigg]$$

Similarly the moment acting on the propeller blades is

$$\underline{M} = \sum_{b=0}^{Z-1} \oiint_{S_B} p(\underline{s} \times (-\underline{n})) dS$$

$$= \frac{\rho}{2} \sum_{b=0}^{Z-1} \oiint_{S_B} \left[(2\underline{q}_0 + \nabla\phi) \circ \nabla\phi \right] (\underline{s} \times \underline{n}) dS \tag{2-63}$$

And the moment about the i axis is

$$Q = \underline{M} \circ \underline{i} = \frac{\rho}{2} Z \oiint_{S_B} \left[(2\underline{q}_0 + \nabla\phi) \cdot \nabla\phi \right] \underline{i} \cdot (\underline{s} \times \underline{n}) dS \tag{2-64}$$

This equation is not of fundamental use in the following development and is not further reduced.

Before the previous formulation can be considered the complete solution, two points assumed in the development must be checked: first, that the integration over the region at infinity, which was neglected in going from Equation (2-18) to Equation (2-19), gives at most a constant; second, either that the solution is unique or that further conditions to establish uniqueness need be specified.

To examine the integration over the boundary at infinity, an area consisting of a finite cylinder of radius $\overline{W}$ with ends at $x = \pm \overline{X}$ is considered. The integration over this area as $\overline{X}, \overline{W} \to + \infty$ is to be evaluated. By uniqueness proofs[45] for nonlifting problems, the integrals of ϕ and $\nabla\phi$ are zero for that portion of the solution arising from the integration over the body. Any constant arising from integration over the wake also gives zero on the cylinder and the upstream surface. However, the downstream surface must be investigated in detail since neither ϕ nor $\nabla\phi$ go to zero as $x \to + \infty$.

At the downstream surface the vortex sheet rolls up as it does for wings; see Cummings.[50] However, the total circulation remains constant and the lines of constant circulation become asymptotic to regular helical vortices of constant radius and pitch. The integral over the downstream surface requires evaluation of the two quantities

$$J_1 = \lim_{\overline{X} \to \infty} \left| \int_{-\infty}^{\infty} dy' \int_{-\infty}^{\infty} \phi(\overline{X}, y', z') \left(\underline{i} \cdot \frac{\underline{r} - \underline{s}}{|\underline{r} - \underline{s}|^3} \right) dz' \right| \tag{2-65}$$

and

[50]Cummings, D., "Vortex Interactions in a Propeller Wake," Massachusetts Institute of Technology, Naval Architecture Department Report 68-12 (Jun 1968).

$$J_2 = \lim_{\underline{X} \to \infty} \left| \int_{-\infty}^{\infty} dy' \int_{-\infty}^{\infty} \frac{\partial \phi}{\partial x} \frac{1}{|\underline{r} - \underline{s}|} \, dz' \right| \tag{2-66}$$

where

$$\underline{r} = \overline{\underline{X}} \, \underline{i} + y \, \underline{j} + z \, \underline{k}$$

$$\underline{s} = y' \, \underline{j} + z' \, \underline{k}$$

and the bar through the integral sign means the vortex itself is excluded; ϕ and ϕ_x are undefined on the vortex surface, except in the limit.

In Appendix A, the form of the potential for a vortex distribution on a regular helix is examined, and it is shown that both ϕ and ϕ_x have the same form far downstream. Since the velocities are known to exist in the sense of a Cauchy principal-value,[11,13,14] we assume the potential does also. In particular, this means both ϕ and ϕ_x are bounded in the fluid.

The region of integration can be divided into two regions; one bounded by a circle of radius A and the other one the area outside this circle and going to infinity. By taking A sufficiently large, integration over the area exterior to the circle can be made to yield as small a value as desired, since ϕ and its derivatives go to zero. In the interior of the circle, the boundedness of ϕ and the power of $\overline{\underline{X}}$ in the deonimnator insure that the limit as $\overline{\underline{X}} \to \infty$ gives a zero value for the integral. Thus the integral over the surface bounding the fluid does not contribute to the expression for ϕ given in Equation (2-19) and the statement to that effect just previous to Equation (2-19) is justified.

To examine uniqueness of the potential, two different solutions are assumed to satisfy Laplace's equation and the boundary conditions. From these a third solution is constructed by subtracting them. This third solution also satisfies Laplace's equation and has zero normal velocity on the fixed body. However, unless the two solutions have the same circulation, the difference solution will have a shed vortex sheet with a finite value of normal velocity on it. Hence, the two solutions must have the same value of circulation in addition to satisfying the boundary conditions. Identical positions for the shed vortex sheet are assumed. Then the difference solution has no shed vortex sheet, and $\phi \to 0$ for $|\underline{r}| \to \infty$.

Green's first identity in the form

$$\iiint_V (\phi \nabla^2 \phi) + \nabla \phi \cdot \nabla \phi) d\tau = \iint_\Sigma \phi \, \underline{n} \cdot \nabla \phi \, dS \tag{2-67}$$

then shows that

$$\iiint_V \nabla \phi \cdot \nabla \phi \, d\tau = 0 \tag{2-68}$$

Since $\nabla \phi \cdot \nabla \phi$ is a positive-definite form, it follows that $\nabla \phi = 0$. and hence, that ϕ (the difference of any two solutions with identical circulation) can be at most a constant throughout the fluid. Therefore, any two solutions of the problem which have identical shed vortex sheets differ at most by an unessential constant; thus the solution is unique.

CHAPTER 3
REGULAR PERTURBATIONS IN PROPELLER THEORY

A—GENERAL FIRST-ORDER SOLUTION

In this chapter, the regular-perturbation problem is examined and the application of the formulation to both design and performance calculations is discussed.

For the regular-perturbation problem, the propeller is assumed to deviate little from a helical reference surface of variable radial pitch angle $\varphi_p(\widetilde{\omega})$. (This is the same description as in Chapter 2.) In design this surface might be the approximate position of the shed vortex system, and in performance calculations it would be the geometrical pitch surface. On the cylindrical surface $\widetilde{\omega} =$ constant, a left-handed coordinate system $(\xi_1, \xi_2, \widetilde{\omega})$ is constructed (as was done in Chapters 1 and 2) with ξ_1 along the intersection of the cylinder with the reference surface so that ξ_1 increases with increasing x. The variable ξ_2 is on the surface, normal to the ξ_1 axis, so that ξ_2 increases with increasing θ. The cylinder is rolled out in Figure 5. Unit vectors $(\underline{e}_1, \underline{e}_2, \underline{e}_{\widetilde{\omega}})$ are in the $(\xi_1, \xi_2, \widetilde{\omega})$ direction, respectively.
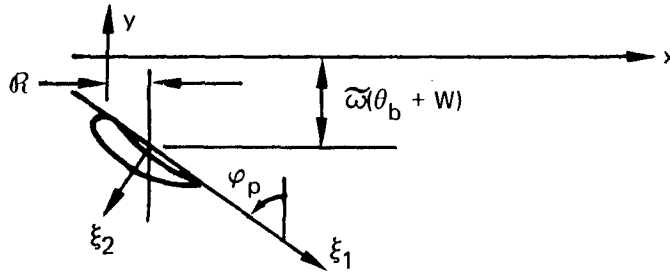

Figure 5 — Coordinate System for
Describing Blade Shape

In terms of these new independent variables, the position vector is (Chapter 1)

$$
\begin{aligned}
\underline{r} = &\left(\Re + \xi_1 \sin \varphi_p - \xi_2 \cos \varphi_p \right) \underline{i} - \widetilde{\omega} \sin\left(\theta_b + W \right. \\
&\left. + \frac{\xi_1 \cos \varphi_p + \xi_2 \sin \varphi_p}{\widetilde{\omega}} \right) \underline{j} + \widetilde{\omega} \cos\left(\theta_b + W \right. \\
&\left. + \frac{\xi_1 \cos \varphi_p + \xi_2 \sin \varphi_p}{\widetilde{\omega}} \right) \underline{k}
\end{aligned}
\tag{3-1}
$$

The blade is assumed to be described as

$$\xi_2 = \epsilon \, E(\xi_1, \, \tilde{\omega}) \tag{3-2}$$

$$= \epsilon \, E_c(\xi_1, \, \tilde{\omega}) \pm \epsilon \, E_T(\xi_1, \, \tilde{\omega}) \tag{3-3}$$

where E is the function describing the blade thickness and camber for the appropriate restrictions on the independent variables ξ_1 and $\tilde{\omega}$,

ϵ is a small parameter describing the departure from the surface $\xi_2 = 0$,

E_c is the camberline function, and

E_T is the thickness function.

The description of the blade offsets differs from the presentations in Chapters 1 and 2 by explicitly making them $0(\epsilon)$.

The position vector of a point on the blade surface is given by

$$
\begin{aligned}
\underline{s}(\xi_1, \, \tilde{\omega}) = & \left(\Re + \xi_1 \sin \varphi_p - \epsilon \, E \cos \varphi_p \right) \underline{i} - \tilde{\omega} \sin \left(\theta_b + W \right. \\
& + \frac{\xi_1 \cos \varphi_p + \epsilon \, E \sin \varphi_p}{\tilde{\omega}} \right) \underline{j} + \tilde{\omega} \cos \left(\theta_b + W \right. \\
& + \frac{\xi_1 \cos \varphi_p + \epsilon \, E \sin \varphi_p}{\tilde{\omega}} \right) \underline{k}
\end{aligned}
\tag{3-4}
$$

Two tangent vectors to the blade surface are given by

$$\underline{t}_1 = \frac{\partial \underline{s}}{\partial \xi_1}$$

$$\underline{t}_2 = \frac{\partial \underline{s}}{\partial \tilde{\omega}}$$

Hence a vector normal to the blade surface can be constructed

$$
\begin{aligned}
\underline{N} & = \pm \left\{ \underline{t}_1 \times \underline{t}_2 \right\} \\
& = \pm \left[\underline{e}_2 - \epsilon \frac{\partial E}{\partial \xi_1} \underline{e}_1 + \left\{ \left(\sin \varphi_p - \epsilon \frac{\partial E}{\partial \xi_1} \cos \varphi_p \right) \circ \right. \right.
\end{aligned}
\tag{3-5}
$$

41

$$\left(\frac{\xi_1 \cos \varphi_p + \epsilon E \sin \varphi_p}{\widetilde{\omega}} - \widetilde{\omega} \frac{dW}{d\widetilde{\omega}} \right) + \frac{d\Omega}{d\widetilde{\omega}} \left(\cos \varphi_p + \epsilon \frac{\partial E}{\partial \xi_1} \sin \varphi_p \right)$$

$$\left. + \xi_1 \frac{d\varphi_p}{d\widetilde{\omega}} - \epsilon \left[\frac{\partial E}{\partial \widetilde{\omega}} + \epsilon^2 E \frac{\partial E}{\partial \xi_1} \frac{d\varphi_p}{d\widetilde{\omega}} \right\} e \widetilde{\omega} \right] \qquad \begin{array}{l}(3\text{-}5)\\ \text{Cont'd}\end{array}$$

Note that even for $\varphi_p = \Omega = W = 0$ and $E = E(\xi_1)$ a term appears in the $e\widetilde{\omega}$ direction. This is because the cross sections are measured on the surface of cylinders of different radius. For $\widetilde{\omega} \to \infty$ the radial component of the normal vanishes for the stated conditions.

The boundary condition on the body, Equation (2-55), gives two equations

$$1/2 \left(\underline{N}+ \cdot \nabla \phi+ - \underline{N}- \cdot \nabla \phi- \right) = -\sqrt{U^2 + \omega^2 \, \Omega^2} \left\{ \sin (\varphi_p - \beta) \right.$$

$$\left. - \epsilon \frac{\partial E_c}{\partial \xi_1} \cos (\varphi_p - \beta) \right\} \qquad (3\text{-}6)$$

and

$$1/2 \left(\underline{N}+ \cdot \nabla \phi+ + \underline{N}- \cdot \nabla \phi- \right) = \sqrt{U^2 + \omega^2 \, \Omega^2} \; \epsilon \frac{\partial E_T}{\partial \xi_1} \cos (\varphi_p - \beta) \qquad (3\text{-}7)$$

The further assumption is made that

$$(\varphi_p - \beta) = 0(\epsilon) \qquad (3\text{-}8)$$

(This assumption is necessary only in design, since it insures that the camber and the potential are $0(\epsilon)$.)

As yet no approximations beyond the inviscid, incompressible fluid and the steady velocities have been made. However, to obtain the regular perturbation solution only the terms to order ϵ are retained. Hence, a point on the surface is given by

$$\underline{s} = \underline{s}_0 + \epsilon \underline{s}_1 + 0(\epsilon^2)$$

$$= (\Omega + \xi_1 \sin \varphi_p)\underline{i} - \widetilde{\omega} \sin \left(\theta_b + W \frac{\xi_1 \cos \varphi_p}{\widetilde{\omega}} \right) \underline{j}$$

$$+ \widetilde{\omega} \cos \left(\theta_b + W+ \frac{\xi_1 \cos \varphi_p}{\widetilde{\omega}} \right) \underline{k} + \epsilon \left\{ -E \cos \varphi_p \underline{i} \right. \qquad (3\text{-}9)$$

$$- \widetilde{\omega} \cos \left(\theta_b + W + \frac{\xi_1 \cos \varphi_p}{\widetilde{\omega}} \right) \frac{E \sin \varphi_p}{\widetilde{\omega}} \; \underline{j}$$

$$\left. - \widetilde{\omega} \sin \left(\theta_b + W + \frac{\xi_1 \cos \varphi_p}{\widetilde{\omega}} \right) \frac{E \sin \varphi_p}{\widetilde{\omega}} \; \underline{k} \right\} + 0(\epsilon^2)$$

42

and the normal to the blade surface is

$$\underline{N} = \underline{N}_0 + \epsilon\,\underline{N}_1 + 0\,(\epsilon^2)$$

$$= \pm \left[\underline{e}_2 + \left\{ \xi_1 \frac{dP}{d\widetilde{\omega}}\,\frac{(\cos^2\varphi_p)}{2\pi\widetilde{\omega}} + \frac{d\mathfrak{R}}{d\widetilde{\omega}}\cos\varphi_p - \widetilde{\omega}\frac{dW}{d\widetilde{\omega}}\sin\varphi_p \right\} \underline{e}_{\widetilde{\omega}} \right.$$

$$+ \epsilon \left\{ -\frac{\partial E}{\partial \xi_1}\underline{e}_1 + \left(\frac{\partial E}{\partial \xi_1} \left[\sin\varphi_p \frac{d\mathfrak{R}}{d\widetilde{\omega}} + \cos\varphi_p\,\widetilde{\omega}\frac{dW}{d\widetilde{\omega}} \right. \right.$$

$$\left. \left. \left. - \cos\varphi_p\frac{\xi_1\cos\varphi_p}{\widetilde{\omega}} \right] + E\frac{\sin^2\varphi_p}{\widetilde{\omega}} - \frac{\partial E}{\partial \widetilde{\omega}} \right) \underline{e}_{\widetilde{\omega}} \right\} + 0\,(\epsilon^2) \right]$$

(3-10)

The potential function due to the blade disturbance will vanish as $\epsilon \to 0$ (since then the thickness and camber vanish) and $\varphi_p \to \beta$. Hence, the potential function can be expanded in a perturbation series with first term $0\,(\epsilon)$. In particular, the potential on the blade surface is expressed in a perturbation series[*]

$$\phi(\xi_1, \epsilon E, \widetilde{\omega}) = \epsilon\,\phi(\xi_1, 0, \widetilde{\omega}) + 0\,(\epsilon^2)$$

(3-11)

Because ϕ is $0\,(\epsilon)$, only zero-order terms in the integral over the blade in Equation (1-50) need be retained. The equation is then

$$\oiint_{S_B} \phi(\underline{s})\underline{n}\cdot\frac{\underline{r}\text{-}\underline{s}}{|\underline{r}\text{-}\underline{s}|^3}\,ds = \epsilon\oiint_{S_{B_0}} \phi(\xi_1, 0, \widetilde{\omega})\frac{\underline{N}_0\cdot(\underline{r}\text{-}\underline{s})}{|\underline{r}\text{-}\underline{s}_0|^3}\,d\xi_1\,d\widetilde{\omega}$$

$$+ 0\,(\epsilon^2)$$

$$= \epsilon\iint_{S_{B_0}^+}\left\{\phi^+ - \phi^-\right\}\cdot\frac{\underline{N}_0^+\cdot(\underline{r}\text{-}\underline{s}_0)}{|\underline{r}\text{-}\underline{s}|^3}\,d\xi_1\,d\widetilde{\omega} + 0\,(\epsilon^2)$$

(3-12)

---

[*]Actually it is the difference in velocity across the blade, Equation (3-13), which should be taken $0\,(\epsilon)$, which is necessarily true only in design. If $\varphi_p-\beta \neq 0\,(\epsilon)$, as would be true in performance calculations, then an integral equation must first be solved to find the pressure distribution corresponding to an uncambered, thin lifting surface at an angle of attack. The remaining problem corresponding to the camber and thickness is then $0\,(\epsilon)$.

43

where S_{B_0} is the projection of the blade outline on the surface $\xi_2 = 0$

$$\underline{N+}_0 \cdot (\underline{r-s}_0) = (\Re \quad X) \cos \varphi_p \quad \sin \varphi_p \left\{ y \cos \theta + z \sin \theta \right\}$$

$$+ \left(\xi_1 \frac{dP}{d\widetilde{\omega}} \frac{\cos^2 \varphi_p}{2\pi\widetilde{\omega}} - \widetilde{\omega} \frac{dW}{d\widetilde{\omega}} \sin \varphi_p + \cos \varphi_p \frac{d\Re}{d\widetilde{\omega}} \right) \cdot$$

$$\left\{ z \cos \theta - y \sin \theta \right\} - \widetilde{\omega} \left(\xi_1 \frac{d\varphi_p}{d\widetilde{\omega}} - \widetilde{\omega} \frac{dW}{d\widetilde{\omega}} \sin \varphi_p + \cos \varphi_p \frac{d\Re}{d\widetilde{\omega}} \right)$$

$$|\underline{r-s}_0|^3 = \left\{ (x - \Re - \xi_1 \sin \varphi_p)^2 + (y + \widetilde{\omega} \sin \theta)^2 \right.$$

$$\left. + (z - \widetilde{\omega} \cos \theta)^2 \right\}^{3/2}$$

and $\qquad \theta = \theta_b + W + \dfrac{\xi_1 \cos \varphi_p}{\widetilde{\omega}}$

As in Chapter 2, the jump in potential across the blade surface can be interpreted as a local circulation. In terms of the velocity jump across the surface it is given by Equation (2-59)

$$\Gamma_B (\xi_1, \widetilde{\omega}) = \left\{ \phi+ - \phi- \right\}$$

$$= \int^{\xi_1, \widetilde{\omega}} (\nabla \phi+ \circ d\underline{\ell}+ - \nabla \phi- \circ d\underline{\ell}-)$$

$$= \epsilon \int_{LE}^{(\xi_1, \widetilde{\omega})} (\underline{q}+ - \underline{q}-) \cdot d\underline{\ell}_0 + 0 (\epsilon^2) \qquad (3\text{-}13)$$

where the path starts from any point along the leading edge and

$$\Gamma(z_0) = \epsilon \int_{LE}^{TE(z_0)} (\underline{q}+ - \underline{q}-) \cdot d\underline{\ell}_0 + 0 (\epsilon^2)$$

Similarly, the integral in Equations (2-21) and (2-50) reduces to

$$\frac{1}{4\pi} \oiint_{S_{B_0}} \frac{\underline{q}_0 \cdot \underline{N}}{|\underline{r-s}|} d\xi_1 d\widetilde{\omega} =$$

$$\frac{\epsilon U}{2\pi} \iint_{S_{B_0}+} \left\{ 1 + \frac{\Omega^2 \widetilde{\omega}^2}{U^2} \right\}^{1/2} \frac{\dfrac{\partial E_T}{\partial \xi_1}}{|\underline{r-s}_0|} \cos (\varphi_p - \beta) \ d\xi_1 d\widetilde{\omega} + 0 (\epsilon^2) \qquad (3\text{-}14)$$

The position vector of the shed vortex sheet is determined by Equations (2-46) and (2-47), which to first-order in ϵ become

$$f_2(z_0, \theta) = f_2^{(0)}(z_0, \theta) + \epsilon f_2^{(1)}(z_0, \theta) + 0(\epsilon^2)$$

$$= X_{TE}(z_0) + \frac{U}{\Omega}(\theta - \theta_{TE}(z_0)) \tag{3-15}$$

$$+ \epsilon\, 1/2 \int_{\theta_{TE}}^{\theta} \left\{ \frac{\psi_x(\underline{\zeta}_0)}{\Omega} - \frac{U}{\Omega^2 z_0^2} \psi_\theta(\underline{\zeta}_0) \right\} d\alpha + 0(\epsilon^2)$$

$$f_1(z_0, \theta) = f_1^{(0)}(z_0, \theta) + \epsilon f_1^{(1)}(z_0, \theta) + 0(\epsilon^2) \tag{3-16}$$

$$= z_0 + 1/2\,\Omega \int_{\theta_{TE}}^{\theta} \epsilon\ \psi_{\widetilde{\omega}}(\underline{\zeta}_0) d\alpha + 0(\epsilon^2)$$

Hence

$$\underline{\zeta} = \underline{\zeta}_0 + \epsilon\,\underline{\zeta}_1 + 0(\epsilon^2)$$

$$= z_0\,\underline{e}_{\widetilde{\omega}} + (x_{TE}(z_0) + \frac{U}{\Omega}(\theta - \theta_{TE}(z_0))\,\underline{i}$$

$$+ \epsilon\left[(1/2\,\Omega \int_{\theta_{TE}}^{\theta} \psi_{\widetilde{\omega}}(\underline{\zeta}_0)\, d\alpha)\,\underline{e}_{\widetilde{\omega}} + (1/2 \int_{\theta_{TE}}^{\theta} \left\{ \frac{\psi_x(\underline{\zeta}_0)}{} \right. \right. \tag{3-17}$$

$$\left. \left. - \frac{U}{\Omega^2 z_0^2}\ \psi_\theta(\underline{\zeta}_0) \right\} d\alpha)\,\underline{i} \right] + 0(\epsilon^2)$$

However, since $\Gamma(z_0)$ in Equation (2-40) is of order ϵ the first-order solution for the potential of the shed vortex sheet requires only $\underline{\zeta}_0$. The zero order normal to the shed vortex sheet becomes:

$$\underline{N}_0^+ \equiv \frac{\partial \underline{\zeta}_0}{\partial \theta} \times \frac{\partial \underline{\zeta}_0}{\partial z_0} = (+z_0\,\underline{e}_\theta + \frac{U}{\Omega}\,\underline{i}) \times (\underline{e}_{\widetilde{\omega}} + \frac{\partial}{\partial z_0}\left(X_{TE} \right.$$

$$\left. - \frac{U\theta_{TE}}{\Omega} \right)\underline{i})$$

$$= - z_0\,\underline{i} + z_0 \frac{\partial}{\partial z_0}\left(X_{TE} - \frac{U\theta_{TE}}{\Omega} \right)\underline{e}_{\widetilde{\omega}} + \frac{U}{\Omega}\,\underline{e}_\theta \tag{3-18}$$

45

and the dot product in the infinite integral is

$$\underline{N}_0^+ \cdot (\underline{r}\text{-}\underline{\xi}_0) = z_0 \, [\, x_{TE} + \frac{U}{\Omega} \, (a \cdot \theta_{TE}) \quad x] + \widetilde{\omega} \, [\sin \theta \, \{ z_0 \sin a$$

$$\cdot \frac{\partial}{\partial z_0} \left(x_{TE} \quad \frac{U\theta_{TE}}{\Omega} \right) + \cos a \frac{U}{\Omega} \} + \cos \theta \, \{ z_0 \cos a \frac{\partial}{\partial z_0} \qquad (3\text{-}19)$$

$$\left(x_{TE} \quad \frac{U\theta_{TE}}{\Omega} \right) \quad \sin a \, U/\Omega \}] \quad z_0^2 \frac{\partial}{\partial z_0} \left(x_{TE} \quad \frac{U\theta_{TE}}{\Omega} \right)$$

and the denominator is

$$|\underline{r}\text{-}\underline{\xi}_0|^3 = \left[\{ x \quad \left(x_{TE} + \frac{U}{\Omega} \, (a \cdot \theta_{TE}) \right) \}^2 + \widetilde{\omega}^2 + z_0^2 \qquad (3\text{-}20) \right.$$

$$\left. - 2 \, \widetilde{\omega} z_0 \cos (\theta - a + \theta_{TE}) \right]^{3/2}$$

where the position vector of an arbitrary point in space is expressed in cylindrical coordinates. This is done to facilitate the integration since past experience[11,13,14] indicates that in some cases the integration can be done analytically for such a representation.

Putting together the previously described pieces, one finds the total first-order potential for the disturbance due to the blades, omitting the ϵ

$$\phi(\underline{r}) = \frac{1}{4\pi} \sum_{b=0}^{Z-1} \iint_{S_{B_0}^+} d\xi_1 d\widetilde{\omega} \cdot$$

$$\frac{\left(\int_{LE}^{\xi_1, \widetilde{\omega}} (\underline{q}^+ - \underline{q}^-) \circ d\underline{\ell}_0 \right) \underline{N}_0^+ \cdot (\underline{r}\text{-}\underline{s}_0) - 2 \sqrt{U^2 + \Omega^2 \widetilde{\omega}^2} \frac{\partial E_T}{\partial \xi_1} \cos (\varphi_p - \beta) |\underline{r}\text{-}\underline{s}_0|^2}{|\underline{r}\text{-}\underline{s}_0|^3} \qquad (3\text{-}21)$$

$$+ \frac{1}{4\pi} \sum_{b=0}^{Z-1} \int_0^R \Gamma(z_0) dz_0 \int_{\infty_{TE}}^\infty \left(\frac{\partial \underline{\xi}_0}{\partial a} \times \frac{\partial \underline{\xi}_0}{\partial z_0} \right) \cdot \frac{(\underline{r}\text{-}\underline{\xi}_0)}{|\underline{r}\text{-}\underline{\xi}_0|^3} da$$

This equation is the first-order solution for the regular-perturbation problem. In the next two sections, the use of this equation in design and performance predictions is discussed, and in the last section the second-order solution is outlined.

The force on the propeller blade, Equation (2-56), is to first-order in ϵ

$$\underline{F} = \epsilon \iint_{S_{B_0}^+} (\underline{q}_0 \cdot \nabla \Gamma_B) \, \underline{N}_0^+ d\xi_1 \, d\widetilde{\omega} \qquad (3\text{-}22)$$

46

and the thrust produced by all the blades is

$$T = - \sum_{b=0}^{Z-1} \underline{i} \cdot \underline{F} = \epsilon \rho Z \int_0^R \cos \varphi_p \sqrt{U^2 + \Omega^2 \widetilde{\omega}^2} \cos (\varphi_p - \beta) \Gamma(\widetilde{\omega}) d\widetilde{\omega} \qquad (3\text{-}23)$$

The torque can be computed in a similar manner but it is not used in the following sections.

A second-order theory follows by straightforward application of the previously described procedure when thickness and camber are expanded in perturbation series. The second-order effects include consideration of the first-order position of the shed vortex position, Equation (3-17). Second-order design theory is discussed in Section D.

B—DESIGN PROBLEM

For the design problem considered here the total thrust produced by the Z-blades is specified at one operating point, as well as the following geometrical data:

1. Blade outline

2. Chordwise thickness function and radial thickness ratio

3. Number of blades

4. Position of blade-reference line

The designer also specifies, to within a scale factor, the chordwise difference in pressure, i.e., the pressure on the upper surface minus the pressure on the lower surface, which reduces to

$$p^- - p^+ = \frac{\rho}{2} \left\{ (\underline{q}+)^2 - (\underline{q}-)^2 \right\}$$

Since $\underline{q} = \underline{q}_0 + \nabla \phi$, the pressure difference is

$$p^- - p^+ = -\rho \left\{ \underline{q}_0 \cdot \nabla (\phi^- - \phi^+) - 1/2[(\nabla \phi+)^2 - (\nabla \phi^-)^2] \right\}$$

$$= +\rho \left\{ \underline{q}_0 \cdot \nabla \Gamma_B + 1/2 \nabla \psi_B \cdot \nabla \Gamma_B \right\}$$

Also, since $\underline{q}_0$ has a zero-order component only along $\underline{e}_1$, the significant term of $\nabla \Gamma_B$ is the $\underline{e}_1$ component. The velocity difference $\nabla \Gamma_B$ can be resolved into the three orthogonal components (γ, μ, σ),

$$\nabla \Gamma_B = \gamma \underline{e}_1 + \mu \underline{N}_0^+ + \sigma (\underline{N}_0^+ \times \underline{e}_1)$$

From the boundary condition, Equation (3-7), the component of μ is known to first order

$$\mu = 2 \epsilon \sqrt{U^2 + \widetilde{\omega}^2 \Omega^2} \frac{\partial E_T}{\partial \xi_1} \cos (\varphi_p - \beta) / (\underline{N}_0^+ \cdot \underline{N}_0^+) + 0 (\epsilon^2)$$

However, to $0(\epsilon)$, no use is made of this knowledge.

47

Now since $\nabla \Gamma_B = O(\epsilon)$, $\nabla \psi_B = O(\epsilon)$, $\sin (\varphi_p - \beta) = O(\epsilon)$, and $\underline{q}_0 = |\underline{q}_0| \cos (\varphi_p - \beta) \underline{e}_1 + |\underline{q}_0| \sin (\varphi_p - \beta) \underline{e}_2$ the pressure distribution is

$$\frac{p^- - p^+}{\rho} = \sqrt{U^2 + \Omega^2 \widetilde{\omega}^2} \, (\epsilon \gamma^{(1)} \cos (\varphi_p - \beta) + O(\epsilon^2))$$

Hence to first order, the chordwise component of the velocity difference is related to the pressure difference across the blade by the equation

$$\gamma^{(1)} = \frac{p^- - p^+}{\rho \sqrt{U^2 + \Omega^2 \widetilde{\omega}^2} \cos (\varphi_p - \beta)} \tag{3-24}$$

For the first-order problem, no information need be specified about the other components of the velocity difference.[*]

---

[*]The component σ can be found from $\nabla \Gamma_B$ since Γ_B is known in terms of $\gamma^{(1)}$ stated previously. An alternative is to note that when a tangential discontinuity in velocity exists across a surface, one can define the surface as a vortex sheet with a vorticity distribution given by

$$\underline{\Lambda} = \underline{n} \times (\underline{q}^+ - \underline{q}^-) = \frac{\underline{N}_0^+}{|\underline{N}_0^+|} \times (\gamma \underline{e}_1 + \sigma (\underline{N}_0^+ \times \underline{e}_1))$$

$$= |\underline{N}_0^+| \, \sigma \underline{e}_1 + \frac{\gamma}{|\underline{N}_0^+|} (\underline{N}_0^+ \times \underline{e}_1)$$

Since $\underline{\Lambda}$ must satisfy

$$\nabla \cdot \underline{\Lambda} = 0$$

the component σ can be found from the partial differential equation governing the components. The equivalence of both these approaches is demonstrated in Chapter 5.

The local circulation, which is the quantity needed in the calculations, is given by Equation (2-59) or to first-order by Equation (3-13). Since the chordwise component of velocity difference is known, $d\underline{\ell}$, the tangent vector in Equation (2-59), can be taken as

$$d\underline{\ell} = \underline{t}_1 \, d\xi_1 = \frac{\partial \underline{s}}{\partial \xi_1} \, d\xi_1 = \left(\underline{e}_1 + \epsilon \frac{\partial E}{\partial \xi_1} \underline{e}_2\right) d\xi_1$$

Hence Equation (2-59) becomes

$$\Gamma_B = \int_{c_2}^{\xi_1} \left\{ \nabla (\phi^+ - \phi^-) \cdot \left(\underline{e}_1 + \epsilon \frac{\partial E_c}{\partial \xi_1} \underline{e}_2\right) \right.$$
$$\left. + \nabla (\phi^+ + \phi^-) \cdot \left(\epsilon \frac{\partial E_T}{\partial \xi_1} \underline{e}_2\right) \right\} d\xi_1$$

$$= \int_{c_2}^{\xi_1} \left\{ \left[\gamma \underline{e}_1 + \mu \underline{N}_0^+ + \sigma (\underline{N}_0^+ \times \underline{e}_1) \right] \cdot \left(\underline{e}_1 + \epsilon \frac{\partial E_c}{\partial \xi_1} \underline{e}_2\right) \right.$$
$$\left. + \nabla \psi_B \cdot \underline{e}_2 \frac{\partial E_T}{\partial \xi_1} \right\} d\xi_1$$

$$= \int_{c_2}^{\xi_1} \left(\gamma + \epsilon \frac{\partial E_c}{\partial \xi_1} (\mu + \sigma \underline{e}_2 \cdot (\underline{N}_0^+ \times \underline{e}_1)) + \nabla \psi_B \cdot \underline{e}_2 \epsilon \frac{\partial E_T}{\partial \xi_1} \right) d\xi_1$$

When the quantities are expanded in a perturbation series, one finds

$$\Gamma_B = \epsilon \int_{c_2}^{\xi_1} \gamma^{(1)} \, d\xi_1 + \epsilon^2 \int_{c_2}^{\xi_1} \left(\gamma^{(2)} + \frac{\partial E_c}{\partial \xi_1} \left(\mu^{(1)} + \sigma^{(1)} \underline{e}_2 \cdot \right. \right.$$
$$\left. \left. \cdot (\underline{N}_0^+ \times \underline{e}_1) \right) + \nabla \psi_{(b)}^{(1)} \cdot \underline{e}_2 \frac{\partial E_T}{\partial \xi_1} \right) d\xi_1 + 0(\epsilon^3)$$

where

$$-\underline{e}_2 \cdot (\underline{N}_0^+ \times \underline{e}_1) = \xi_1 \frac{dP\left(\cos^2 \varphi_p\right)}{d\widetilde{\omega}} \frac{1}{2\pi\widetilde{\omega}} - \widetilde{\omega} \frac{dW}{d\widetilde{\omega}} \sin \varphi_p + \cos \varphi_p \frac{d\Re}{d\widetilde{\omega}}$$

and $\underline{e}_2 \cdot \nabla \psi_B^{(1)} = 2v$; v is from Equation (3-26). For the first-order problem, only the leading term stated previously is needed

$$\Gamma_B^{(1)} = \epsilon \int_{c_2}^{\xi_1} \gamma^{(1)} \, d\xi_1$$

When Equation (3-24) is integrated over the chord, the total bound circulation distribution, still with the unknown scale factor, is obtained. This unknown factor can be determined from the equation for thrust, Equation (3-23). Hence everything needed to calculate the first-order perturbation potential is known.

What is not yet known, however, is the magnitude of the camber and the blade pitch which will produce the specified thrust. To obtain these values, the boundary condition, Equation (3-6) is used. To first order, this equation is

$$\frac{\partial E_c}{\partial \xi_1} = \sin (\varphi_p - \beta) - 1/2 \frac{\underline{N}_0^+ \cdot \nabla \psi}{\sqrt{U^2 + \tilde{\omega}^2 \Omega^2}} \tag{3-25}$$

where ψ is a principal-value integral given by Equation (2-18).

For conceptual consistency the blade trailing edge must lie on the reference surface so that the trailing vortices spring from the trailing edge. Thus

$$E_c = \int_{c_2}^{\xi_1} \frac{\partial E_c}{\partial \xi_1} \, d\xi_1 - \int_{c_2}^{c_1} \frac{\partial E_c}{\partial \xi_1} \, d\xi_1 = \int_{c_1}^{\xi_1} \frac{\partial E_c}{\partial \xi_1} \, d\xi_1$$

This camberline will consist of a shape measured from the nose-tail line and, in general, an angle of attack. This angle is added to the pitch angle of the reference surface to give the total blade pitch. This incremental angle is called the ideal angle of attack.

The knowledge of the camberline completes the first approximation for the design problem. The regular perturbation solution involves an integration to find the slope of the camberline and then a straightforward integration of this slope to find the shape. However, a new term appears in Equation (3-25) which should be explicitly mentioned before proceeding with the analysis.

From the equation for ψ in Equation (2-18), one sees that Equation (3-21) gives $1/2 \, \psi$ when the principal value for points on the blade reference surface is taken. Hence, if the gradient of ϕ in Equation (3-21) gives the velocity

$$\nabla \phi = u \underline{e}_1 + v \underline{e}_2 + w \underline{e}_{\tilde{\omega}} \tag{3-26}$$

and if for $\underline{r} \rightarrow \underline{r}_0$

$$\frac{1}{2} \nabla \psi_B = u(\xi_1, 0, \tilde{\omega}) \underline{e}_1 + v(\xi_1, 0, \tilde{\omega}) \underline{e}_2 + w(\xi_1, 0, \tilde{\omega}) \underline{e}_{\tilde{\omega}}$$

then Equation (3-25) becomes

50

$$\sqrt{U^2 + \tilde{\omega}^2 \, \Omega^2} \left(\frac{\partial E_c}{\partial \xi_1} - \sin \, (\varphi_p \; \beta) \right) = \nu \, (\xi_1, \, 0, \, \tilde{\omega})$$

$$+ \left[\frac{d\beta}{d\tilde{\omega}} \cos \varphi_p + \tilde{\omega} \frac{dW}{d\tilde{\omega}} \sin \varphi_p - \xi_1 \left(\frac{dP}{d\tilde{\omega}} \frac{\cos^2 \varphi_p}{2\pi\tilde{\omega}} \right) \right] w(\xi_1, \, 0, \, \tilde{\omega})$$

(3-27)

In the literature, intuitive arguments are used to derive only the first term on the right-hand side of Equation (3-27). The formal procedure presented here indicates that another term also contributes to the camberline shape. For the term containing a multiple of the distance from the reference line, the effect will be most pronounced for points near the blade edge.

In the discussion section of Chapter 5, an estimate of the contribution from this term is made. In addition, other aspects of the design problem which simplify the integrals are discussed.

C—PERFORMANCE CALCULATIONS

To determine the performance of a propeller over a given J-range, it is assumed that the position vector of a point on the surface is given, that is, the geometry is completely specified. The unknowns of interest are the thrust and torque as a function of J and possibly the pressure distribution. The pressure distribution near the leading edge will not generally be accurate because $\left. \dfrac{\epsilon \, \partial E_T}{\partial \xi_1} \right|_{LE}$ is in general infinite and hence not of order ϵ as assumed in the derivation. In the design problem, this point was not critical but in performance calculations it will generally give results for the pressure distribution which are not uniformly valid at the leading edge. However, it is integrable and hence the total thrust can be found.

In calculating the propeller performance, the circulation is unknown, and the zero-order position of the shed vortex sheet is known. Modes for the chordwise distribution of velocity given in Equation (3-24) can be assumed which satisfy the Kutta condition and which have variable spanwise coefficients. Then, in principle, the integral equation formulation in Equation (3-25) can be solved for the spanwise coefficients. Sugai[40] was able to successfully evaluate numerically such a procedure. Murray[33] used an iteration procedure, starting with blade-element theory (Glauert[51]) with a reduction factor found necessary for convergence. As already mentioned, Murray's performance calculations did not converge to the values set in his design.

Presumably the exact solution in Equation (2-50) could be used as the integral equation without much increase in complexity but no one has done this yet.

---

[51]Glauert, H., "Airplane Propellers," Division L, Aerodynamic Theory, Edited by W.F. Durand, J. Springer, pp. 169-360 (1935); also published by Dover Publications, Inc., New York (1963).

Rather than solve an integral equation it would be preferable to obtain a solution which could be constructed as quadratures as was done in the design problem. Such an expression is found in the next chapter.

D—SECOND-ORDER DESIGN THEORY

The second-order theory follows by retaining terms to order ϵ^2 in the previous development. Most of the second-order effects are known from the first-order solution; however, the second-order increment in circulation must be evaluated. This is found by considering the second-order thrust

$$T = T_1(\epsilon\Gamma^{(1)} + \epsilon^2\Gamma^{(2)}) + \epsilon^2 T_2 \tag{3-28}$$

where $T_1(\epsilon\Gamma^{(1)})$ is given by Equation (3-23) and

$$T_2 = \frac{\rho Z}{2} \int_0^R d\tilde{\omega} \int_{c_2}^{c_1} \left[\nabla\psi_B^{(1)} \cdot \nabla\Gamma_{(B)}^{(1)} \cos\varphi_p + 2\sqrt{U^2 + \Omega^2\tilde{\omega}^2} \right.$$

$$\cdot \left\{ \sin(\varphi_p - \beta)\cos\varphi_p \, \underline{e}_2 \cdot \nabla\Gamma_B^{(1)} + \cos(\varphi_p - \beta)\sin\varphi_p \tag{3-29} \right.$$

$$\left. \left. \cdot \left(\frac{\partial\Gamma_B^{(1)}}{\partial\xi_1} \frac{\partial E_c^{(1)}}{\partial\xi_1} + \frac{\partial\psi_B^{(1)}}{\partial\xi_1} \frac{\partial E_T}{\partial\xi_1} \right) \right) \right] d\xi_1$$

All quantities in this integral are known from the first-order solution. Since in design the thrust is set and since $T_1(\epsilon\Gamma^{(1)})$ is the set value, the second-order terms must vanish:

$$\epsilon^2 T_1(\Gamma^{(2)}) + \epsilon^2 T_2 = 0$$

which fixes the value of $\Gamma^{(2)}$

$$\Gamma^{(2)}(\tilde{\omega}) = -\int_{c_2}^{c_1} \left[1/2 \frac{\nabla\psi_B^{(1)} \cdot \nabla\Gamma_B^{(1)}}{\sqrt{U^2 + \Omega^2\tilde{\omega}^2}} \frac{1}{\cos(\varphi_p - \beta)} \right. \tag{3-30}$$

$$\left. + \tan\varphi_p \left(\frac{\partial\Gamma_B^{(1)}}{\partial\xi_1} \frac{\partial E_c^{(1)}}{\partial\xi_1} + \frac{\partial\psi_B^{(1)}}{\partial\xi_1} \frac{\partial E_T}{\partial\xi_1} \right) + \tan(\varphi_p - \beta)\underline{e}_2 \cdot \nabla\Gamma_B^{(1)} \right] d\xi_1$$

In design the form of the chordwise circulation is assumed to remain constant, i.e., $\gamma(\xi_1, \tilde{\omega})$ in Equation (3-24) is a fixed chordwise variation; however, the amplitude of the function may change. The scale is fixed by the magnitude of the bound circulation. If γ is normalized to give unity when integrated over the chord

$$\int_{c_2}^{c_1} \gamma(\xi_1, \tilde{\omega}) \, d\xi_1 = 1$$

then the scale factor will be just the total bound circulation. In this case

$$(\underline{q}^+ - \underline{q}^-) \cdot \underline{e}_1 = (\Gamma^{(1)}(\tilde{\omega}) + \epsilon \Delta\Gamma^{(2)}(\tilde{\omega})) \gamma^*(\xi_1, \tilde{\omega})$$

and

$$\Gamma_B^{(1)} = \Gamma^{(1)}(\tilde{\omega}) \cdot \int_{c_2(\tilde{\omega})}^{\xi_1} \gamma^*(\xi_1, \tilde{\omega}) \, d\xi_1 \qquad (3\text{-}31)$$

where $\gamma^*(\xi_1, \tilde{\omega})$ is the normalized value of Equation (3-24). Now we have previously found that

$$\Gamma_B = \epsilon \int_{c_2}^{\xi_1} \gamma^{(1)} \, d\xi_1 + \epsilon^2 \int_{c_2}^{\xi_1} \left[\gamma^{(2)} + \frac{\partial E_c}{\partial \xi_1} (\mu^{(1)} + \sigma^{(1)} \underline{e}_2 \cdot (\underline{N}_0^+ \times \underline{e}_1)) \right.$$
$$\left. + \underline{e}_2 \cdot \nabla \psi_B^{(1)} \frac{\partial E_T}{\partial \xi_1} \right] d\xi_1 \qquad (3\text{-}32)$$

Thus

$$\Gamma(\tilde{\omega}) = \epsilon \Gamma^{(1)} + \epsilon^2 \left[\Delta\Gamma^{(2)} + \int_{c_2}^{c_1} \left\{ \frac{\partial E_c}{\partial \xi_1} (\mu^{(1)} + \sigma^{(1)} \underline{e}_2 \cdot (\underline{N}_0^+ \times \underline{e}_1)) \right. \right.$$
$$\left. \left. + \underline{e}_2 \cdot \nabla \psi_B^{(1)} \frac{\partial E_T}{\partial \xi_1} \right\} d\xi_1 \right]$$

Hence

$$\Delta\Gamma^{(2)} = \Gamma^{(2)} - \int_{c_2}^{c_1} \left\{ \frac{\partial E_c}{\partial \xi_1} (\mu^{(1)} + \sigma^{(1)} \underline{e}_2 \cdot (\underline{N}_0^+ \times \underline{e}_1)) \right.$$
$$\left. + \underline{e}_2 \cdot \nabla \psi_B^{(1)} \frac{\partial E_T}{\partial \xi_1} \right\} d\xi_1 \qquad (3\text{-}33)$$

All quantities appearing under the integral sign in Equations (2-49) and (2-50) are expanded in perturbation series and the second-order contribution found. The necessary expansions have been given previously and in Part A. In these calculations it is assumed that the thickness function is given and constant at order ϵ. The quantity sought is the second-order correction to the camber. This is obtained from the boundary condition on the blade set in Equations (2-10) and (3-6). Because of the length of the expression, it is not given explicitly but it follows directly from the previously described development.

CHAPTER 4
SINGULAR PERTURBATIONS IN PROPELLER THEORY

As described in the introduction, the singular perturbation problem examines the solution as the chordlength goes to zero. At a fixed point $\underline{r} = (x,y,z)$ in the flow field relative to the propeller, the chordlength-to-diameter ratio $\bar{\epsilon}$ goes to zero. Since the geometry is unchanged except for chordlength, the blade forces go to zero in this limit. Hence the flow disturbance vanishes as the lifting surface vanishes. The solution in this case is just a lifting line (as the chordlength goes to zero, thickness effects give a second-order dipole distribution rather than a first-order source distribution and hence will appear in the higher-order terms of the solution). This is the outer flow. The flow near the body is the inner flow and can be found by stretching the coordinates near the body so that the flow field is magnified sufficiently to recover the necessary details. In the inner limit the stretched variables are held constant as the chordlength goes to zero.

A—FIRST-ORDER TERMS

Outer Flow

The starting point is the outer flow which is found by straightforward linearization of the exact solution given by Equation (2-50). Both ϕ and Γ will be of the same order in the integrals of Equations (2-49) and (2-50). However the integral over the blade area is of higher-order than the integral over the shed vortex sheet because the area of integration goes to zero with the chordlength. The zero-order integration over the shed vortex sheet reduces to the lifting-line results, i.e., $a_{TE}(\bar{\epsilon}T(z_0)) \to \theta_b = \dfrac{2\pi b}{Z}$, with the zero-order position of the vortex sheet. Formally, the circulation is expressed in a perturbation series of the form

$$\Gamma(z_0, \bar{\epsilon}) = \delta_1(\bar{\epsilon}) \, \Gamma^{(1)}(z_0) + \delta_2(\bar{\epsilon}) \, \Gamma^{(2)}(z_0) + \cdots \qquad (4\text{-}1)$$

where $\bar{\epsilon}$ is the maximum chordlength-to-diameter ratio and $\delta_n(\bar{\epsilon})$ is an ordered set of linearly independent gage functions, with the property $\delta_{n+1} = o(\delta_n)$ as $\bar{\epsilon} \to 0$. A general form for them is $\bar{\epsilon}^{a_n^1} \left((ln)^{a_n^2} \cdot \bar{\epsilon} \right)^{a_n^3} e^{-a_n^4/\bar{\epsilon}}$ where a_n^m are constants. Normally the terms with $a_n^4 \neq 0$ are considered transcendentally small and are ignored. The coefficients a_n^m will be found as the solution evolves. The position vector of the curves of constant circulation in the shed vortex sheet is also expanded in a perturbation series

$$\underline{\zeta}(z_0, 0; \bar{\epsilon}) = \underline{\zeta}_0(z_0, 0) + \delta_1(\bar{\epsilon}) \underline{\zeta}_1(z_0, 0) + \delta_2(\bar{\epsilon}) \underline{\zeta}_2(z_0, 0) + \cdots \tag{4-2}$$

From Equation (2-46) and (2-47) the zero-order solution for a blade-reference line lying along a radial line in the $x = 0$ plane* is

$$\underline{\zeta}_0 = z_0 \, \underline{e}_{\widetilde{\omega}}(\theta) + \frac{U}{\Omega}(\theta - \theta_b) \, \underline{i} \tag{4-3}$$

and consequently the normal is given by

$$\frac{\partial \underline{\zeta}}{\partial \theta} \times \frac{\partial \underline{\zeta}}{\partial z_0} = \left(z_0 \, \underline{e}_\theta + \frac{U}{\Omega} \underline{i} \right) \times \underline{e}_{\widetilde{\omega}} + 0 \, (\delta_1)$$

$$= - z_0 \underline{i} + \frac{U}{\Omega} \underline{e}_\theta + 0(\delta_1) \tag{4-4}$$

Hence for the outer flow, the lowest-order solution in Equation (3-50) is

$$\phi(x, y, z; \bar{\epsilon}) = \delta_1 \, \phi_1(r) \pm \cdots$$

$$\phi_1(r) = \frac{1}{4\pi} \int_0^R \Gamma^{(1)}(z_0) \, G(\underline{r}, z_0) \, dz_0 \tag{4-5}$$

where $G(\underline{r}, z_0) =$

$$\sum_{b=0}^{Z-1} \int_{\theta_b}^{\infty} \frac{\left[x - \frac{U}{\Omega}(a - \theta_b) \right] z_0 - \frac{U}{\Omega} \widetilde{\omega} \sin(\theta - a)}{\left\{ \left[x - \frac{U}{\Omega}(a - \theta_b) \right]^2 + \widetilde{\omega}^2 + z_0^2 - 2 \widetilde{\omega} z_0 \cos(\theta - a) \right\}^{3/2}} \, da$$

$$= \sum_{b=0}^{Z-1} \int_0^{\infty} \left\{ - z_0 \frac{\partial}{\partial x} + \frac{U}{\Omega z_0} \frac{\partial}{\partial \theta} \right\} \frac{1}{r} \, d\gamma \tag{4-6}$$

where

$$r = \sqrt{(x - \frac{U}{\Omega}\gamma)^2 + \widetilde{\omega}^2 + z_0^2 - 2 z_0 \widetilde{\omega} \cos(\theta - \gamma - \theta_b)}$$

---

*The reason for this restriction on the reference line will be explained when the inner flow is examined.

This expression is also derived in Appendix A from the Biot-Savart Law applied to an elemental horseshoe vortex. Isay[35] presents a similar equation which he bases on the work of Yamazaki.[19]

Equation (2-50) also contains another term which appears to be of order $\bar{\epsilon}$; the integration of the source terms over the boundary. The first-order effect in these integrals reduces to an integration over the radius and an integration of the thickness slope over the chord. Since only closed profiles are considered, this integration is zero, and the contribution is second order. In the outer flow one expects dipoles rather than sources which is confirmed in the previous statement.

Inner Flow

Unfortunately, the potential is not uniquely determined since the circulation is unknown. The circulation is determined by details at the body and hence must be determined from an inner flow for which the body boundary condition is not lost as the limit of zero chordlength is taken. Because the spanwise scale is not changed as $\bar{\epsilon} \rightarrow 0$, a stretching is needed for only the chordwise variables. A suitable stretching for the reference blade along the z axis is

$$\bar{x} = x/\bar{\epsilon} \text{ and } \bar{y} = y/\bar{\epsilon} \quad 0 < z < R \quad (4\text{-}7)$$

where $\bar{x}$ and $\bar{y}$ are held constant as $\bar{\epsilon} \rightarrow 0$. The z variable remains unchanged.

The previously described transformation applied to the Laplace equation gives

$$\frac{\partial \phi}{\partial \bar{x}^2} + \frac{\partial \phi}{\partial \bar{y}^2} = -\bar{\epsilon}^2 \frac{\partial^2 \phi}{\partial z^2} \quad (4\text{-}8)$$

Now it can be seen why rake and warp have been excluded from the analysis: If rake were included, a displacement varying with z would have to be made in x before the stretching in Equation (4-7) could be performed. This displacement would introduce a term of order $\bar{\epsilon}$ on the right-hand side of Equation (4-8). Rake would be equivalent to sweep in wings, which has been considered by Thurber.[7] If warp were included, a displacement in y would be necessary. A displacement in either x or y prior to stretching would also lead to a transformed Laplace equation with a term of order $\bar{\epsilon}$, unless the displacement were constant. The second-order right-hand side means that the first two nontrivial solutions are governed by a two-dimensional Laplace equation with the spanwise variable a parameter. Experience with wing perturbation problems indicates that the first term governed by Poisson's equation is a practical limit to the number of terms in the series.

The potential in terms of the inner variables must also be expanded in a perturbation series. The potential in the inner region will be

$$\phi \ (x, y, z; \bar{\epsilon}) = \phi(\bar{\epsilon}\bar{x}, \epsilon\bar{y}, z; \bar{\epsilon}) = \Phi(\bar{x}, \bar{y}, z; \bar{\epsilon})$$

$$= \bar{\epsilon}\Phi_1(\bar{x}, \bar{y}, z) + \nu_2(\bar{\epsilon})\Phi_2(\bar{x}, \bar{y}, z) + \cdots \quad (4\text{-}9)$$

The inner potential is of order $\bar{\epsilon}$ because the velocities in the inner flow are required to be bounded as $\bar{\epsilon} \rightarrow 0$.

The inner boundary condition in Equation (2-10)

$$\underline{n} \cdot \nabla \phi = - \underline{q}_0 \cdot \underline{n} \quad for \ \underline{r} \in S_B$$

has to be expressed in terms of inner variables. Instead of the $\bar{x}$ and $\bar{y}$ defined in Equation (4-9), it is convenient to use variables measured along and perpendicular to the chordline in the $\bar{x},\bar{y}$ plane. The chordline is at an angle $\varphi_B(z)$ relative to the $\bar{y}$ axis and passes through the reference line, the z axis. The variable ξ_1 measured along the chordline is positive in the downstream direction, and the variable ξ_2 is normal to the ξ_1 axis, positive in upstream direction. This coordinate system has been examined in Chapter 1 and is shown in Figure 6 below.
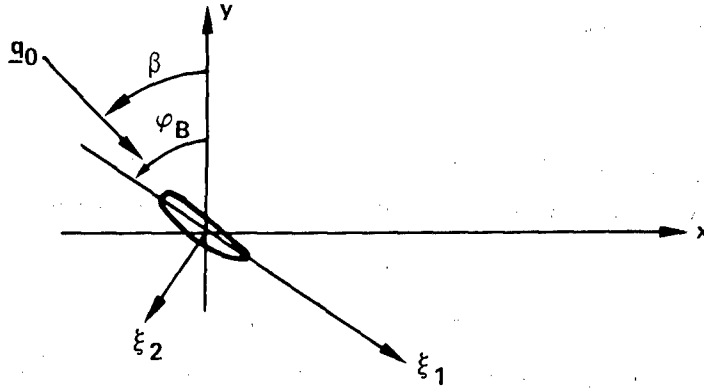
Figure 6 — Geometry in Plane at Fixed z

The variables ξ_1 and ξ_2 are related to x and y by

$$x = \xi_1 \ sin \ \varphi_B(z) - \xi_2 \ cos \ \varphi_B(z)$$

$$y = - \xi_1 \ cos \ \varphi_B(z) - \xi_2 \ sin \ \varphi_B(z) \tag{4-10}$$

Obviously if a hub existed on such a propeller, a complicated expression in (x,y,z) would be needed for its geometrical specification. For narrow blades considered here, this problem is not significant.

The shape is assumed to be given relative to the reference surface by a shape function (Chapter 1)

$$\xi_2 = E(\xi_1, z) \tag{4-11}$$

Substituting this expression into the previous equations for x and y, and taking the appropriate differential, one can find a normal (Chapter 1)

$$\underline{N} = \pm \left(\frac{\partial \underline{s}}{\partial \xi_1} \times \frac{\partial \underline{s}}{\partial z} \right) \tag{4-12}$$

where

$$\underline{s} = \underline{s}\,(\xi_1,\ E(\xi_1,\ z),z)$$

$$\underline{N} = \pm \left[\underline{e}_2 - \frac{\partial E}{\partial \xi_1}\underline{e}_1 + \left(\xi_1 \frac{d\varphi_B}{dz} - \frac{\partial E}{\partial z} + E\frac{\partial E}{\partial \xi_1}\frac{d\varphi_B}{dz} \right)\underline{k} \right] \tag{4-13}$$

where

$$\underline{e}_1 = \underline{i}\ sin\ \varphi_B - \underline{j}\ cos\ \varphi_B$$

$$\underline{e}_2 = -\ \underline{i}\ cos\ \varphi_B - \underline{j}\ sin\ \varphi_B$$

For the body boundary condition, the normal component of the free-stream velocity is needed:

$$\underline{q}_0 \cdot \underline{N} = \sqrt{U^2 + \Omega^2\,z^2}\ \left\{ sin\ (\varphi_B - \beta) - \frac{\partial E}{\partial \xi_1}\ cos\ (\varphi_B - \beta) \right\}$$

$$+\ \Omega y\ \left(\xi_1 \frac{d\varphi_B}{dz} - \frac{\partial E}{\partial z} + E\frac{\partial E}{\partial \xi_1}\frac{d\varphi_B}{dz} \right) \tag{4-14}$$

where

$$tan\ \beta = \frac{U}{\Omega z}$$

The $(\xi_1,\ \xi_2)$ variables are linear combinations of the x,y variables and thus a stretching of x,y is also a stretching of $\xi_1,\ \xi_2$. Let the stretched $\xi_1,\ \xi_2$ variables be $\sigma_1,\ \sigma_2$. In Chapter 1, the transformation of the partial derivatives in the normal was discussed. It was shown that

$$E(\xi_1,\ z;\ \overline{\epsilon}) = \overline{\epsilon}\ E\left(\frac{\xi_1}{\overline{\epsilon}},z \right) = \overline{\epsilon}\ E(\sigma_1,\ z)$$

$$\frac{\partial E}{\partial \xi_1}\bigg|_{\xi_1 = \overline{\epsilon}\sigma_1} = 0(1) \tag{4-15}$$

$$\frac{\partial E}{\partial z}\bigg|_{\xi_1 = \overline{\epsilon}\sigma_1} = 0(\overline{\epsilon})$$

With these relations the transformation of the right-hand side of Equation (4-14) becomes

$$
\underline{q}_0 \cdot \underline{N} = \sqrt{U^2 + \Omega^2 z^2} \left\{ \sin{(\varphi_B - \beta)} - \frac{\partial E}{\partial \xi_1} (\sigma_1, z) \cos{(\varphi_B - \beta)} \right\}
$$

$$
+ \bar{\epsilon}^2 \Omega \bar{y} \left(\sigma_1 \frac{d\varphi_B}{dz} - \frac{\partial E}{\partial z} + E \frac{\partial E}{\partial \xi_1} \frac{d\varphi_B}{dz} \right) \tag{4-16}
$$

where $\bar{y}$ is given by Equation (4-7). The normal in Equation (4-13) transforms to

$$
\underline{N} = \pm \left\{ \underline{e}_2 - \frac{\partial E}{\partial \xi_1} \underline{e}_1 \right\} \pm \bar{\epsilon} \left(\sigma_1 \frac{d\varphi_B}{dz} - \frac{\partial E}{\partial z} + E \frac{\partial E}{\partial \xi_1} \frac{d\varphi_B}{dz} \right) \underline{k} \tag{4-17}
$$

The transformation of Equation (2-10), using inner variables (σ_1, σ_2, z), then becomes

$$
\frac{1}{\bar{\epsilon}} \left(\frac{\partial \Phi}{\partial \sigma_2} - \frac{\partial E}{\partial \xi_1} \frac{\partial \Phi}{\partial \sigma_1} \right) + \bar{\epsilon} \left(\sigma_1 \frac{d\varphi_B}{dz} - \frac{\partial E}{\partial z} + E \frac{\partial E}{\partial \xi_1} \frac{d\varphi_B}{dz} \right)
$$

$$
\circ \left[\frac{\partial \Phi}{\partial z} + \frac{d\varphi_B}{dz} \left(\sigma_1 \frac{\partial \Phi}{\partial \phi_1} - \sigma_2 \frac{\partial \Phi}{\partial \sigma_2} \right) \right] =
$$

$$
- \sqrt{U^2 + \Omega^2 z^2} \left\{ \sin{(\varphi_B - \beta)} - \frac{\partial E}{\partial \xi_1} \cos{(\varphi_B - \beta)} \right\} \tag{4-18}
$$

$$
- \bar{\epsilon}^2 \Omega \bar{y} \left(\sigma_1 \frac{d\varphi_B}{dz} - \frac{\partial E}{\partial z} + E \frac{\partial E}{\partial \xi_1} \frac{d\varphi_B}{dz} \right)
$$

In this section only the first-order terms are considered. Hence for $\Phi = \bar{\epsilon} \Phi_1$ the equation for Φ_1 is

$$
\frac{\partial^2 \Phi_1}{\partial \sigma_1^2} + \frac{\partial^2 \Phi_1}{\partial \sigma_2^2} = 0 \tag{4-19a}
$$

with the body boundary condition, on $\sigma_2 = E(\sigma_1, z)$, $0 < z < R$

$$
\frac{\partial \Phi_1}{\partial \sigma_2} - \frac{\partial E}{\partial \xi_1} \frac{\partial \Phi_1}{\partial \sigma_1} = - V_1 \left(\sin{\alpha_1} - \frac{\partial E}{\partial \xi_1} \cos{\alpha_1} \right) \tag{4-19b}
$$

where
$$V_1(z) = \sqrt{U^2 + \Omega^2 z^2}$$

$$\alpha_1(z) = \varphi_B(z) - \beta(z)$$

The remaining boundary condition far from the body has to be found by matching with the outer flow. This process will be formalized in the following section, but intuitively it is expected that the potential in the outer flow will match the inner flow as the outer variables $\sqrt{x^2 + y^2} \to 0$, $0 < z < R$ and the inner variables $\sqrt{\sigma_1^2 + \sigma_2^2} \to \infty$, $0 < z < R$. In the outer flow, as an observer approaches the reference blade, the flow should look locally like a two-dimensional line vortex with higher-order effects caused by the induced velocities from the trailing vortex system. Hence for the first-order inner potential, the far-field boundary condition is that the flow look like a line vortex. (Subsequent matching will confirm this hypothesis.)

The inner potential could in principle be found from an inner expansion of the exact potential given in Chapter 2. Germain[52] reports such procedures applied to wings lead to considerable difficulty and that it is simpler to solve the posed two-dimensional problem of Equation (4-19). In fact, using complex variables and conformal mapping of a circular cylinder, one can state the solution immediately:

$$\Phi_1(\sigma_1, \sigma_2, z) = V_1 \, Re \left\{ f(\sigma_1 + i\sigma_2) \, e^{-i\alpha_1} + a^2 \frac{e^{i\alpha_1}}{f(\sigma_1 + i\sigma_2)} \right.$$

$$\left. + i \frac{\Gamma}{2\pi V_1} \ln \frac{f(\sigma_1 + i\sigma_2)}{a} - (\sigma_1 + i\sigma_2) \, e^{-i\alpha_1} \right\} \tag{4-20}$$

where

$$f(\sigma_1 + i\sigma_2) = \sigma_1 + i\sigma_2 + \sum_{n=0}^{\infty} \frac{a_n(z)}{(\sigma_1 + i\sigma_2)^n}$$

is the inverse mapping function

$a_n(z)$ are complex numbers depending on the section shape

$a(z)$ is the radius of the transformed circular cylinder

$\Gamma(z) = 4\pi a(z) V_1(z) \sin(\alpha_1(z) - \alpha_0(z))$ is the value of the circulation when the Kutta condition is satisfied and

$\alpha_0(z)$ is the angle of zero lift of the profile section

[52]Germain, P., "Recent Evolution in Problems and Methods in Aerodynamics," Journal of the Royal Aeronautical Society, Vol. 71, No. 682, pp. 673-691 (1967).

Several techniques exist for finding the mapping function for a given section geometry. Most of these are discussed by Thwaites.[53] It is not necessary at this time to examine the techniques for obtaining these coefficients, but they are considered known in terms of the geometry. Specifications of the circulation renders the two-dimensional problem unique. In a review of the planar wing problem, Ogilvie,[54] points out that the inner expansion can be taken as a Laurent series but doing so adds no new information or insight to the direct solution from conformal mapping given previously.

Although the solution indicated in Equation (4-20) is the required solution, in anticipation of the matching discussed in the next section, the form of the solution at large distances from the body will be examined. Figure 7 shows complex number $\sigma_1 + i\sigma_2$, given by $\mu e^{i\omega}$
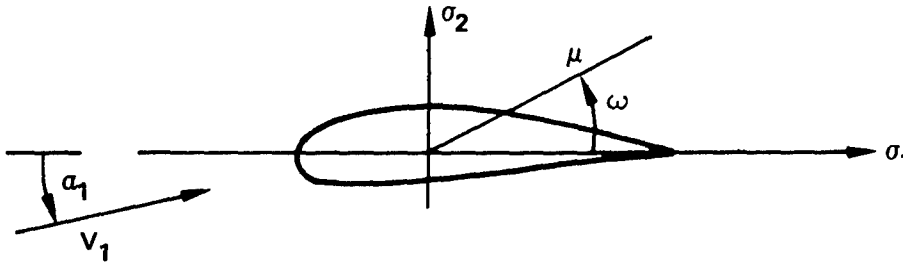
Figure 7 — Profile Coordinates for Inner Flow

Hence

$$\mu = \sqrt{\sigma_1^2 + \sigma_2^2} \; , \; \omega = tan^{-1} \frac{\sigma_2}{\sigma_1}$$

The expansion is straightforward, except for the log term

[53]Thwaites, B., "Incompressible Aerodynamics," Oxford University Press, England (1960).

[54]Ogilvie, T.F., "Singular Perturbation Problems in Ship Hydrodynamics," University of Michigan, Department of Naval Architecture, Report 096 (Oct 1970).

$$\ln \frac{f(\mu e^{i\omega})}{a} = \ln \frac{\mu e^{i\omega}}{a} + \ln \left(1 + \frac{a_0}{\mu e^{i\omega}} + \frac{a_1}{\mu^2 e^{2i\omega}} + \cdots \right.$$

$$= \ln \frac{\mu}{a} + i\omega + \left(\frac{a_0}{\mu} e^{-i\omega} + \frac{a_1 - 1/2 a_0^2}{\mu^2} e^{-2i\omega} + \cdots \right)$$

Hence for large μ, the expansion is

$$\frac{\Phi_1(\sigma_1, \sigma_2, z)}{V_1(z)} = -2 a \sin (\alpha_1 - \alpha_0) (\omega + \omega_0(z)) + Re \left\{ \frac{a_1}{\mu} e^{-i(\alpha_1 + \omega)} \right.$$

$$+ \frac{a_2}{\mu^2} e^{-i(\alpha + 2\omega)} + \cdots + \frac{a^2 e^{i(\alpha_1 - \omega)}}{\mu} \left[1 - \frac{a_0}{\mu e^{i\omega}} + \frac{a_0^2 - a_1}{\mu^2 e^{2i\omega}} + \cdots \right]$$

$$+ 2 i a \sin (\alpha_1 - \alpha_0) \left[\frac{a_0}{\mu e^{i\omega}} + \frac{a_1 - 1/2 a_0^2}{\mu^2 e^{2i\omega}} \right.$$

$$\left. \left. + \frac{a_2 - 1/2 a_0 a_1 + \dfrac{a_0^3}{3}}{\mu^3 e^{3i\omega}} + \cdots \right] \right\}$$

where $\omega_0(z)$ is arbitrary.

By grouping terms, one finds

$$\frac{\Phi_1}{V_1} = -2a \sin (\alpha_1 - \alpha_0) \left(\omega + \omega_0(z) \right) + \sum_{n=1}^{\infty} \left(\frac{a}{\mu} \right)^n k_n (\alpha_1, z) \qquad (4\text{-}21)$$

where $k_1(\alpha_1, z) = a \cos (\alpha_1 - \omega) + Re \left[\frac{a_1}{a} e^{-i(\alpha_1 + \omega)} + 2i \sin (\alpha_1 - \alpha_0) a_0 e^{-i\omega} \right]$

$$k_2(\alpha_1, z) = Re \left\{ \frac{a_2}{a^2} e^{-i(\alpha_1 + 2\omega)} + a_0 e^{i(\alpha_1 - 2\omega)} + \frac{2i}{a} \sin (\alpha_1 - \alpha_0) e^{-2i\omega} (a_1 - 1/2 a_0^2) \right\}$$

$$k_3(\alpha_1, z) = Re \left\{ \frac{a_3}{a^3} e^{-i(\alpha_1 + 3\omega)} + \frac{a_0^2 - a_1}{a} e^{-i(\alpha_1 - 3\omega)} \right.$$

$$\left. + \frac{2i}{a^2} \sin (\alpha_1 - \alpha_0) e^{-3i\omega} (a_2 - 1/2 a_0 a_1 + 1/3 a_0^2) \right\}$$

etc.

The first term is a vortex; the second, a dipole. Then the higher-order terms are listed. No source terms appear, as expected, since none are in the first-order outer solution.

Matching

The two expressions for ϕ are the leading terms of asymptotic expansions valid in different domains of the flow field. For the reference blade, the outer solution is valid everywhere in the flow field, *except* $z \leqslant R, \sqrt{x^2 + y^2} \leqslant C_0$. The inner solution is valid for $z < R, \sqrt{\bar{x}^2 + \bar{y}^2} \leqslant C_1$ or $\sqrt{x^2 + y^2} \leqslant C_1 \bar{\epsilon}$. For an overlap domain to exist, one must assume that the domain of validity of the outer solution can be extended to $\sqrt{x^2 + y^2} \geqslant C_0 (\bar{\epsilon})$ where $\lim\limits_{\bar{\epsilon} \to 0} \frac{\bar{\epsilon}}{C_0(\bar{\epsilon})} \to \infty$. This extension of the region of validity is discussed by Kaplan[4] and Cole.[5] In this assumed overlap region, the x and y variables are taken as

$$x = \bar{\bar{x}} \, g(\bar{\epsilon})$$

$$y = \bar{\bar{y}} \, g(\bar{\epsilon})$$

(4-22)

where $\bar{\bar{x}}$ and $\bar{\bar{y}}$ are constants of $O(1)$, and $g(\bar{\epsilon})$ is the function which places x and y in the intermediate region. To insure x and y are in the intermediate region, $g(\bar{\epsilon})$ must satisfy

$$\left. \begin{array}{c} g(\bar{\epsilon}) \to 0 \\ \dfrac{\bar{\epsilon}}{g(\bar{\epsilon})} \to 0 \end{array} \right\} \ as \ \bar{\epsilon} \to 0$$

The x and y are the outer variables, and the inner variables are obtained from Equation (4-7) as

$$\left. \begin{array}{c} \bar{x} = \dfrac{x}{\bar{\epsilon}} = \bar{\bar{x}} \dfrac{g(\bar{\epsilon})}{\bar{\epsilon}} \\ \\ \bar{y} = \dfrac{x}{\bar{\epsilon}} = \bar{\bar{y}} \dfrac{g(\bar{\epsilon})}{\bar{\epsilon}} \end{array} \right\}$$

(4-23)

From the definition of an asymptotic sequence, e.g., Erdélyi,[55] the two solutions can be matched to order $\mu_N(\bar{\epsilon})$ if

$$\lim_{\bar{\epsilon} \to 0} \frac{\sum_{n=1}^{N} \delta_n(\bar{\epsilon})\, \phi_n(\overline{\overline{xg}}, \overline{\overline{yg}}, z) - \sum_{n=1}^{N} \nu_n(\bar{\epsilon})\, \Phi_n(\overline{\overline{x}}\, \tfrac{g}{\bar{\epsilon}}, \overline{\overline{y}}\, \tfrac{g}{\bar{\epsilon}}, z)}{\mu_N(\bar{\epsilon})} = 0 \qquad (4\text{-}24)$$

$$(N = 1, 2 \cdots)$$

Hence the dominant terms can be matched if

$$\lim_{\bar{\epsilon} \to 0} \frac{\delta_1(\bar{\epsilon})\, \phi_1(\overline{\overline{xg}}, \overline{\overline{yg}}, z) - \bar{\epsilon}\, \Phi_1(\overline{\overline{x}}\, \tfrac{g}{\bar{\epsilon}}, \overline{\overline{y}}\, \tfrac{g}{\bar{\epsilon}}, z)}{\mu_1(\bar{\epsilon})} = 0$$

A match to order $\bar{\epsilon}$, i.e., $\mu_1(\bar{\epsilon}) = \bar{\epsilon}$, is possible by selecting $\delta_1(\bar{\epsilon}) = \bar{\epsilon}$ and by requiring the following equality to hold

$$\lim_{g \to 0} \phi_1(\overline{\overline{xg}}, \overline{\overline{yg}}, z) = \Phi_1(\infty, \infty, z) \qquad (4\text{-}25)$$

The matching principle given by Van Dyke[3] expresses the same requirements as described previously in a more concise form.

The matching principle will be used later but for now a much simpler argument can be used to find the circulation in the outer flow. The argument is that the spanwise circulation must be independent of the chordwise stretching.

Thus

$$\Gamma^{(1)}(z) = 4\pi a(z)\, V_1(z)\, \sin\left(\alpha_1(z) - \alpha_0(z)\right) \qquad (4\text{-}26)$$

Hence the outer solution is completely determined to the first order. There are no incompatibilities; consequently, the first-order solution is complete.

---

[55]Erdélyi, A., "Asymptotic Expansions," Dover Publications, Inc., New York (1956).

A composite solution, not necessarily unique but uniformly valid throughout the flow field, can be directly written down. To within an arbitrary constant of z, which to second order is only a parameter in the inner flow, the first-order composite solution is the sum of the inner solution plus the outer solution minus the common part. The common part is either side of the equality in Equation (4-25), and from the inner solution in Equation (4-21) it is seen to be

$$\phi_{c.p.} = \bar{\epsilon} \, \Phi_1(\infty, \infty, z)$$

$$= \begin{cases} 0 & z > R \\[2ex] - \bar{\epsilon} \, V_1(z) \, 2a(z) \sin\left(\alpha_1(z) - \alpha_0(z)\right) \left(\omega + \omega_0(z)\right) & 0 < z < R \end{cases}$$

Hence the composite solution is

$$\phi_c = \begin{cases} \hat{\epsilon} \, \phi_1(x, y, z) & z > R \\[2ex] \bar{\epsilon} \, \phi_1(x, y, z) + \hat{\epsilon}\Phi_1(\sigma_1, \sigma_2, z) \\[1ex] \qquad + 2 \, \hat{\epsilon} \, V_1 a \, \sin(\alpha_1 - \alpha_0) \, (\omega + \omega_0) \end{cases} \Bigg\} \quad 0 < z < R \qquad (4\text{-}27)$$

Use of the matching principle will show that $\omega_0(z)$ is such that $\omega + \omega_0 = tan^{-1}y/x$. This is shown in Equations (4-34) and (4-45). Such a composite solution is useful in finding information in the flow field such as field-point velocities. Since this overall view of the flow field is not required in the present analysis, it is not considered again; however, similar expressions valid to higher order can be obtained just as easily when the individual higher-order solutions are known. Composite solutions are discussed at some length by both Van Dyke[3] and Cole.[5]

The circulation to first order corresponds to what is known as blade-element theory.[51] Its usefulness is restricted to narrow propellers with light loads. The second-order terms derived in Section B will modify the circulation distribution with higher-order effects and will extend the usefulness of the solution.

B—SECOND-ORDER TERMS

Outer Flow

The second-order terms in the outer flow will arise from three sources. The first will be from the integration over the blade. Although this could be extracted by a Taylor expansion from the exact formulation in Equation (2-50), it is simpler to assume that a distribution of dipoles in the x and y direction will be the required singularity system. Once again, if the assumed form is not correct then the matching will not be possible. The second term in the outer series will be from the second-order term in the circulation expansion in Equation (4-1). This will appear in an equation similar to Equation (4-5). The last second-order contribution will appear because of the first-order modification to the position of the vortex sheet. Since this last term is too complex to treat analytically, an approximation will be made to simplify

66

it. For this term it is necessary to know the expression for $\underline{\zeta}_1(z_0, \theta)$ in Equation (4-2). To obtain $\underline{\zeta}_1$, the first-order effects in Equations (2-46) and (2-47) must be included. If, on the vortex sheet, $1/2 \, \psi_x \equiv u_a$, $\frac{1}{2\tilde{\omega}}\psi_\theta \equiv u_t$ and $1/2\,\psi_{\tilde{\omega}} \equiv w$ then the zero- and first-order terms for the position of lines of constant circulation can be found from

$$f_1 \sim z_0 + \frac{\overline{\epsilon}}{\Omega} \int_{\theta_b}^{\theta} w(\underline{\zeta}_0)\, da \tag{4-28}$$

$$f_2 \sim z_0 \int_{\theta_b}^{\theta} \frac{U + \overline{\epsilon}\, u_a^{(1)}\, (\underline{\zeta}_0)}{\Omega z_0 + \overline{\epsilon}\, u_t^{(1)}\, (\underline{\zeta}_0)}\, da \tag{4-29}$$

where the second term is left in the inconsistent form because of the approximation to be made. Since there is little hope of analytically integrating Equation (4-29), one seeks a reasonable approximation. The main contribution of the modified position of the shed vorticity will be from points close to the line. Hence a Taylor series expansion of the velocity is called for; however, for even greater simplicity, all but the first term is ignored, that is, the velocities are evaluated at the lifting line. Hence

$$f_2 \approx z_0 \frac{U + \overline{\epsilon}\, u_a^{(1)}\, (z_0)}{\Omega z_0 + \overline{\epsilon}\, u_t^{(1)}\, (z_0)}\, (\theta - \theta_b)$$

The quantity $z_0 \dfrac{U + \overline{\epsilon}\, u_a^{(1)}\, (z_0)}{\Omega z_0 + \overline{\epsilon}\, u_t^{(1)}\, (z_0)}$ is $\dfrac{1}{2\pi}$ times the pitch of the shed vortex at the lifting line. This pitch is often called the hydrodynamic pitch and it is denoted by $P_i(z_0)$. Hence

$$f_2 \approx \frac{P_i(z_0)}{2\pi}\, (\theta - \theta_b) \tag{4-30}$$

It is possible to propose a slightly better model for the integral in Equation (4-29) since the induced velocity both at the lifting line and the value far downstream are known (the value for $x \to \infty$ is twice that

67

at the lifting line). Numerical calculations[17] have been performed for which the information necessary to propose a variation in the induced velocities as a function of x or θ could be obtained. However, the previous assumption is universally[*] made and considerably simplifies the calculations.

A similar universal and significantly simplifying approximation is to ignore the contraction of lines of constant circulation. This means the radial velocity in Equation (4-28) is approximated by zero. Any other constant approximation for it would lead to negative values for the radial position, clearly an unacceptable occurrence. Here too, alternatives to this crude approximation would be the numerical calculations or results of actuator-disk theory. These alternatives produce complications not essential to the continuation of the present investigation, and we accept the approximations as customarily used.

These two approximations involved in the higher-order description of the shed vortex position are defined as the basis of moderately-loaded propeller theory.[13]

Hence to the first-order, the approximate position vector is

$$\underline{\zeta} = z_0 \underline{e}_{\widetilde{\omega}} + \frac{P_i(z_0)}{2\pi} (\theta - \theta_b) \underline{i} \qquad (4\text{-}31)$$

$$\approx \underline{\zeta}_0 + \bar{\epsilon}\, \underline{\zeta}_1$$

Since this approximation merely replaces the constant $\dfrac{U}{\Omega}$ in Equation (4-3) by $\dfrac{P_i(z_0)}{2\pi}$, no further insight is added to the problem by considering this term and from now on it will be ignored. That no essential modification to the theory results is not obvious in the formulation of the velocity potential but can be seen in the calculation of induced velocities by the Biot-Savart Law;[**] see Appendix B. However, the calculation of induced velocities is usually done with expressions derived for constant P_i.

Thus only the modification of the blade-element circulation distribution and the dipole distribution comprise the direct second-order outer potential. Although a general gage function $\delta_2(\bar{\epsilon})$ must be assumed for the circulation distribution, second-order terms from the blade integration in Equation (2-50) are easily seen to be order $\bar{\epsilon}^2$. (Change the chordwise integration to inner variables and expand the expression in a Taylor series.) Thus the two-term outer solution is

---

[*]Notable exceptions are Erickson et al.[56] and Cummings,[50] who calculate vortex interactions for lifting-line theory.

[56]Erickson, J.E. et al., "A Theory for VTOL Propeller Operation in a Static Condition," Curtiss-Wright Corporation, Caldwell, N.J. (Oct 1965).

[**]The vorticity vector $\underline{\Lambda} = \underline{n} \times \nabla \Gamma$ has no additional term from the $\underline{e}_{\widetilde{\omega}}$ component of $\underline{n}$, since $\underline{e}_{\widetilde{\omega}} \times \nabla \Gamma = 0$.

$$\phi\ (\underline{r};\ \bar{\epsilon}) = \bar{\epsilon}\phi_1(\underline{r}) + \delta_2(\bar{\epsilon})\ \phi_{12}(\underline{r}) + \bar{\epsilon}^2\ \phi_2(\underline{r}) \tag{4-32}$$

where ϕ_1 is given by Equation (4-5), and

$$\phi_{12}(\underline{r}) = \frac{1}{4\pi} \int_0^R \Gamma^{(2)}\ (z_0)\ G(\underline{r},\ z_0)\ dz_0$$

$$\phi_2(\underline{r}) = \frac{1}{4\pi} \sum_{b=0}^{Z-1} \int_0^R \frac{x\mu_1(z_0) + (y + z_0 \sin\theta_b)\ \mu_2(z_0)\ dz_0}{\left[x^2 + (y + z_0 \sin\theta_b)^2 + \left(z - z_0 \cos\theta_b\right)^2\right]^{3/2}} \tag{4-33}$$

where $\Gamma^{(2)}\ (z_0)$ is the next term in the circulation expansion in Equation (4-1), and $\mu_1(z)$ and $\mu_2(z_0)$ are the dipole strengths. All three of these are unknown.

To match with the inner flow, one needs the asymtotic sequences which results when Equation (4-22) is substituted into the two-term expression for ϕ. By an indirect procedure described in Appendix B, the expansion of ϕ is found to be

$$\phi(g\bar{\bar{x}},\ g\bar{\bar{y}},\ z;\ \bar{\epsilon}) = F_0(z;\ \bar{\epsilon}) - \frac{1}{2\pi}[\bar{\epsilon}\Gamma^{(1)} + \delta_2\ \Gamma^{(2)}]\ \tan^{-1}\frac{\bar{\bar{y}}}{\bar{\bar{x}}}$$

$$+ \bar{\epsilon}g[\bar{\bar{x}}\ u_a^{(1)}\ (z) + \bar{\bar{y}}\ u_t^{(1)}\ (z)] \tag{4-34}$$

$$+ \frac{\bar{\epsilon}^2}{4\pi g}\ \frac{\bar{\bar{x}}\mu_1\ (z) + \bar{\bar{y}}\mu_2\ (z)}{\bar{\bar{x}}^2 + \bar{\bar{y}}^2} + H.O.T.$$

where $u_a^{(1)}\ (z)$ and $u_t^{(1)}\ (z)$ are the axial and tangential velocities at the lifting line as induced by the first-order circulation distribution.

Inner Flow

For the second term in the inner flow, the governing equations must be examined. From Equation (4-18), the boundary condition on the body can be determined. One substitutes the two-term inner expansion

$$\phi(\bar{x},\ \bar{y},\ z;\ \bar{\epsilon}) = \bar{\epsilon}\Phi_1\ (\sigma_1,\ \sigma_2;\ z) + \nu_2\Phi_2(\sigma_1,\ \sigma_2;\ z) \tag{4-35}$$

into that equation and finds that Φ_2 satisfies

69

$$\frac{v_2}{\bar{\epsilon}} \left(\frac{\partial \Phi_2}{\partial \sigma_2} - \frac{\partial E}{\partial \xi_1} \frac{\partial \Phi_2}{\partial \sigma_1} \right) = O(\bar{\epsilon}^2) \tag{4-36}$$

on $\sigma_2 = E(\sigma_2; z)$, $0 < z < R$

Obviously, it is most convenient to take $\lim\limits_{\bar{\epsilon} \to 0} \bar{\epsilon}^3/v_2 = 0$ so that the body boundary condition becomes

$$\frac{\partial \Phi_2}{\partial \sigma_2} - \frac{\partial E}{\partial \xi_1}(\sigma_1; z) \frac{\partial \Phi_2}{\partial \sigma_1} = 0 \tag{4-37}$$

on $\sigma_2 = E(\sigma_1; z)$, $0 < z < R$

Similarly, in the flow field, Equation (4-8) requires Φ_2 to satisfy a two-dimensional Laplace equation. As yet the boundary condition at $\sqrt{\sigma_1^2 + \sigma_2^2} \to \infty$ is unknown and must be determined by matching. The simplest problem for which the two-dimensional flow cannot pass through the body is that associated with an airfoil at an angle of attack to the flow. Hence as $\sqrt{\sigma_1^2 + \sigma_2^2} \to \infty$ one assumes that the potential behaves like

$$\Phi_2(\sigma_1, \sigma_2; z) \sim \sigma_1 V_2(z) \cos \alpha_2(z) + \sigma_2 V_2(z) \sin \alpha_2(z) \tag{4-38}$$

where $V_2(z)$ and $\alpha_2(z)$ are unknown. This two-dimensional problem is also easily solved, using complex variables and conformal mapping. With the same notation as in Equations (4-20) and (4-21) the second-order inner potential is

$$\frac{\Phi_2}{V_2} = \sigma_1 \cos \alpha_2 + \sigma_2 \sin \alpha_2 - 2 a \sin (\alpha_2 - \alpha_0) (\omega + \omega_0 (z))$$

$$+ \sum_{n=1}^{\infty} \left(\frac{a}{\mu} \right)^n k_n(\alpha_2, z) \tag{4-39}$$

where $\omega_0(z)$ is arbitrary, and the $k_n(\alpha, z)$ are given in Equation (4-21). In order to find the necessary form of this expression for matching, one substitutes

$$\sigma_1 = \bar{\bar{\sigma}}_1 \, g/\bar{\epsilon} \quad \text{and} \quad \sigma_2 = \bar{\bar{\sigma}}_2 \, g/\bar{\epsilon} \tag{4-40}$$

70

into the expression for Φ_2 and obtains

$$\frac{\Phi_2}{V_2} = g/\bar{\epsilon}\,(\bar{\bar{\sigma}}_1 \cos a_2 + \bar{\bar{\sigma}}_2 \sin a_2) - 2a \sin (a_2 - a_0)\,(\omega + \omega_0'\,(z))$$

$$+\frac{\bar{\epsilon}}{g\bar{\bar{\mu}}}\,k_1\,(a_2,\,z) + 0(\bar{\epsilon}/g)^2 \qquad (4\text{-}41)$$

Combining this expression with the one for Φ_1, one finds the expansion for Φ has the form

$$\Phi(\bar{\bar{\sigma}}_1\,g/\bar{\epsilon},\,\bar{\bar{\sigma}}_2\,g/\bar{\epsilon},\,z;\,\bar{\epsilon}) = F_1(z,\,\bar{\epsilon})$$

$$+\,\bar{\epsilon}\,V_1 \left[-2a \sin (a_1 - a_0)\,(\omega + \omega_0) + \frac{\bar{\epsilon}\,k_1(a_1,\,z)}{g(\bar{\bar{x}}^2 + \bar{\bar{y}}^2)^{1/2}} + \cdots \right]$$

$$+\,v_2\,V_2 \Big[g/\bar{\epsilon}\,(\sigma_1 \cos a_2 + \sigma_2 \sin a_2)$$

$$-\,2a \sin (a_2 - a_0)\,(\omega + \omega_0) + \cdots \Big] \qquad (4\text{-}42)$$

In the next section the actual matching will be performed.

Matching

In this section the coefficients and gage functions are to be selected so that the two expressions for ϕ will be matched. In Equation (4-24) the matching condition is given for the general case. One now seeks to use this expression to match Equations (4-34) and (4-42). First, one notes that $k_1(a_1,z)$ in Equation (4-42) is a linear combination of $\cos \omega$ and $\sin \omega$ hence also a linear combination of

$$\frac{x}{\sqrt{x^2 + y^2}} \quad \text{and} \quad \frac{y}{\sqrt{x^2 + y^2}}$$, and this term is known from the first-order matching. By inspection this term will cancel with the dipole-distribution terms in Equation (4-34), thus implicitly giving the solution for their strength:

$$V_1(z)\,k_1(a_1,\,z) = \frac{\bar{\bar{x}}\,\mu_1(z) + \bar{\bar{y}}\,\mu_2(z)}{[\bar{x}^2 + \bar{\bar{y}}^2]^{1/2}} \qquad (4\text{-}43)$$

Hence, the matching is reduced to the expression

$$\lim_{\bar{\epsilon}\to 0} \frac{\left[\begin{array}{l} -\dfrac{\delta_2}{2\pi}\,\Gamma^{(2)}\,tan^{-1}\dfrac{\bar{\bar{y}}}{\bar{\bar{x}}} + \bar{\epsilon}\,g[\bar{\bar{x}}\,u_a^{(1)}\,(z) + \bar{\bar{y}}\,u_t^{(1)}\,(z)] + \cdots \\[3mm] -\ \nu_2\,V_2\left[\dfrac{g}{\epsilon}\,(\bar{\bar{\sigma}}_1\,\cos\,\alpha_2 + \bar{\bar{\sigma}}_2\,\sin\,\alpha_2) \\[3mm] \qquad -\ 2a\,\sin\,(\alpha_2-\alpha_0)\,(\omega+\omega_0) + \cdots\right] \end{array}\right]}{\mu_2(\bar{\epsilon})} = 0 \tag{4-44}$$

where $\mu_2(\bar{\epsilon})$ is such that terms not explicitly given vanish in the limit.

This matching is possible by selecting

$$\nu_2 = \epsilon^2$$

$$\delta_2 = \nu_2(\bar{\epsilon}) = \bar{\epsilon}^2 \tag{4-45}$$

$$\omega + \omega_0 = tan^{-1}\,\bar{\bar{y}}/\bar{\bar{x}}$$

for which

$$\bar{\bar{x}}\,u_a^{(1)}\,(z) + \bar{\bar{y}}\,u_t^{(1)}\,(z) = V_2\,(\bar{\bar{\sigma}}_1\,\cos\,\alpha_2 + \bar{\bar{\sigma}}_2\,\sin\,\alpha_2) \tag{4-46}$$

$$\Gamma^{(2)}\,(z) = 4\pi\,a(z)\,V_2(z)\,\sin\,(\alpha_2 - \alpha_0) \tag{4-47}$$

To determine the performance of the propeller, the circulation distribution must be known explicitly. That is, both $V_2(z)$ and $\alpha_2(z)$ must be determined in Equation (4-47). To find these terms we use Equations (4-46) and (4-10);

$$\sigma_1(u_a^{(1)}\,\sin\,\varphi_B - u_t^{(1)}\,\cos\,\varphi_B) - \sigma_2(u_a^{(1)}\,\cos\,\varphi_B + u_t^{(1)}\,\sin\,\varphi_B)$$

$$= \sigma_1\,V_2\,\cos\,\alpha_2 + \sigma_2\,V_2\,\sin\,\alpha_2$$

Hence

$$V_2^2 = u_a^{(1)2} + u_t^{(1)2} \tag{4-48}$$

and

72

$$\tan \alpha_2 = -\frac{u_a^{(1)} \cos \varphi_B + u_t^{(1)} \sin \varphi_B}{u_a^{(1)} \sin \varphi_B - u_t^{(1)} \cos \varphi_B} \qquad (4\text{-}49)$$

Thus the second-order solution is complete. In the next section, formulas for the propeller performance are given.

C—PERFORMANCE

Determination of the circulation from the given profile coordinates shows that the singular-perturbation problem gives a quadrature for the performance. However, the appropriate form of the integral for the thrust and torque has not been determined yet.

The expression for thrust is given by Equation (2-57)

$$T = -\frac{\rho}{2} Z \oiint_{S_B} [2 \underline{q}_0 + \nabla \phi] \cdot \nabla \phi] \; \underline{i} \cdot \underline{n} \; ds$$

In lifting-line theory the expression for thrust is usually obtained from the outer flow. Here we derive the appropriate expression from the inner flow since, in the preceding equation, the inner potential is the appropriate one to use. Now

$$\underline{i} \circ \underline{n} \; ds = \underline{i} \cdot \left(\pm \underline{e}_2 \mp \frac{\partial E}{\partial \xi_1} \underline{e}_1 \right) d\xi_1 \; dz$$

$$= \mp \bar{\epsilon} \left(\cos \varphi_B + \frac{\partial E}{\partial \xi_1} \sin \varphi_B \right) d\sigma_1 \; dz$$

$$\underline{q}_0 = \sqrt{U^2 + \Omega^2 z^2} \; [\cos (\varphi_B - \beta) \; \underline{e}_1 + \sin (\varphi_B - \beta) \; \underline{e}_2] + \Omega y \underline{k}$$

$$= V_1(z) \; [\cos \alpha_1 \; \underline{e}_1 + \sin \alpha_1 \; \underline{e}_2] + \bar{\epsilon} \; \Omega \bar{y} \underline{k}$$

$$\nabla \phi = \nabla \Phi (\sigma_1, \sigma_2, z; \bar{\epsilon})$$

$$= \frac{1}{\bar{\epsilon}} \left(\underline{e}_1 \frac{\partial}{\partial \sigma_1} + \underline{e}_2 \frac{\partial}{\partial \sigma_2} \right) (\bar{\epsilon} \; \Phi_1 + \bar{\epsilon}^2 \; \Phi_2 + H.O.T.) + O(\bar{\epsilon}) \; \underline{k}$$

see Chapter 1 for the gradient in inner variables.

Thus to the first-order in $\bar{\epsilon}$, the integrand

$$(2 \underline{q}_0 + \nabla \phi) \cdot \nabla \phi$$

involves only two-dimensional quantities, i.e., z is a parameter. By inspection, the integrand can be changed to

73

$$\left(\underline{q}_{0\ 2D} + \nabla_2 \Phi \right)^2$$

since $|q_{0\ 2D}|^2$ is a constant with respect to the chordwise integration and, hence, integrates to give zero.

In two-dimensional wing theory, one defines

$$\left.\begin{array}{c} \oint \mp (\underline{q}_{0\ 2D} + \nabla_2 \Phi)^2 \, d\sigma_1 = -\dfrac{2}{\rho} F_N \\[2em] \oint \mp (\underline{q}_{0\ 2D} + \nabla_2 \Phi)^2 \dfrac{\partial E}{\partial \xi_1} \, d\sigma_1 = -\dfrac{2}{\rho} F_c \end{array}\right\} \tag{4-50}$$

where F_N and F_c are the forces normal to and along the chord. If one defines

$$\beta_i = \tan^{-1} \frac{U + \bar{e} u_a^{(1)} + \cdots}{\Omega z - (\bar{e} u_t^{(1)} + \cdots)} \tag{4-51}$$

then

$$F_N = L \cos (\varphi_B - \beta_i)$$

$$F_c = L \sin (\varphi_B - \beta_i)$$

where L is the lift of the blade section.

Hence the thrust coefficient becomes

$$C_T = \frac{T}{\dfrac{\rho}{2} U^2 \pi R^2} = \frac{2 Z}{\pi U^2 R^2 \rho} \int_0^R \bar{e} L \, [\cos \varphi_B \cos (\varphi_B - \beta_i)$$

$$+ \sin \varphi_B \sin (\varphi_B - \beta_i)] \, dz$$

$$= \frac{2 Z}{\pi U^2 R^2 \rho} \int_0^R \bar{e} L \cos \beta_i \, dz \tag{4-52}$$

The lift is given by

$$L = \rho \sqrt{(U + \bar{e} u_a^{(1)} + \cdots)^2 + (\Omega z - (\bar{e} u_t^{(1)} + \cdots))^2} \ \Gamma(z; \bar{e}) \tag{4-53}$$

Hence

$$C_T = \frac{2Z}{\pi U^2 R^2} \int_0^R (\bar{\epsilon} \, \Gamma^{(1)} + \bar{\epsilon}^2 \, \Gamma^{(2)} + \cdots)(\Omega z - (\bar{\epsilon} \, u_t^{(1)} + \cdots)) \, dz$$

and by retaining terms to only second-order, one has

$$C_T = \frac{2Z}{\pi U^2 R^2} \int_0^R \left((\bar{\epsilon} \, \Gamma^{(1)} + \bar{\epsilon}^2 \, \Gamma^{(2)}) \, \Omega z - \bar{\epsilon}^2 \, \Gamma^{(1)} \, u_t^{(1)} \right) \, dz \qquad (4\text{-}54)$$

By a similar series of steps, one finds the power coefficient

$$C_P = \frac{\Omega \, (\underline{M} \cdot \underline{i})}{\frac{\rho}{2} \pi U^3 R^2}$$

$$= \frac{2Z}{\pi U^3 R^2} \int_0^R \Omega z \left((\bar{\epsilon} \, \Gamma^{(1)} + \bar{\epsilon}^2 \, \Gamma^{(2)}) \, U + \bar{\epsilon}^2 \, \Gamma^{(1)} \, u_a^{(1)} \right) dz \qquad (4\text{-}55)$$

CHAPTER 5
DISCUSSION

A—COMMENTS ON RESULTS

The lifting-line analysis is essentially the same as that given in the literature, except for notation. One apparent difference is that the two-dimensional sections are defined on sections cut by a plane perpendicular to the straight blade-reference line. However, a Taylor expansion of the shape defined on a cylinder shows that to second-order they are the same since the difference $z - \tilde{\omega}$ is $O(\bar{\epsilon}^2)$. Of course higher-order terms would show the effect of the new section definition.

The lifting-line analysis was developed for propellers with a straight lifting line. If the blade-reference line were raked or warped, the outer-flow potential could be easily found. The overall solution, however, would not be as given in Chapter 4, because the second-order problem would include solution of Poisson's rather than Laplace's equation. The appropriate solution for such cases could probably be obtained, but the lifting-line analysis is appropriate only for propellers with narrow blades and hence is not useful for marine propellers. For marine propellers, the most important analysis is the lifting-surface formulation, and the rest of this discussion will concern this problem.

In the preceding chapters, the expressions for velocity were left in the form of the gradient operating on an integral. This is because they are principal-value integrals, and, if the differential would be taken inside some of the integrals (Equation (2-19)), they would not exist in the mathematical sense; see Tychonov and Samarski.[45] The singularities which result when the operator is taken inside the integral are usually called Hadamard singularities, and as shown in Equation (2-19), the finite part of the integral is defined in terms of limit operations. However, if the expression for $\underline{q}$ is integrated by parts, the order of the singularity will be reduced for the limit $\underline{r} \to s$, and the integrals will exist as Cauchy principal values. (For a principal-value integral the region surrounding $\underline{r}_0$ must be excluded from the integral, and the limit with the maximum dimension of the excluded region going to zero must be taken; for a Cauchy principal-value integral, restrictions are placed on the shape of the region excluding $\underline{r}_0$).

In evaluating the expressions numerically, either formulation of the problem is acceptable since both expressions involve a region surrounding the singularity which requires special consideration. In fact, Sparenberg,[25] Pien and Strom-Tejsen,[31] and Tsakonas and Jacobs[41] treat the higher-order singularity, while Pien,[30] Kerwin,[27,28] Yamazki,[20] and Murray[33] work with principal-value integrals. Sparenberg[25] presents an analysis for both points of view.

B—EXPRESSIONS FOR VELOCITY AS INTEGRALS OF FIRST-ORDER SINGULARITIES

Equation (3-21) for the perturbation potential consists of three terms

$$\phi = \phi_s + \phi_T + \phi_v \qquad (5\text{-}1)$$

In this equation ϕ_s is an integral over the surface of the blades corresponding to the lifting aspect of the propeller

$$\phi_s(\underline{r}) = \frac{1}{4\pi} \sum_{b=0}^{Z-1} \iint_{S_{B_0}^+} \frac{\Gamma_B(\xi_1, \widetilde{\omega}) \, \underline{N}_{0s}^+ \cdot (\underline{r} - \underline{s}_0)}{|\underline{r} - \underline{s}_0|^2} \, d\xi_1 \, d\widetilde{\omega} \qquad (5\text{-}2)$$

and ϕ_T is also an integral over the surface of the blades; however, due to the blade thickness

$$\phi_T(\underline{r}) = -\frac{1}{2\pi} \sum_{b=0}^{Z-1} \iint_{S_{B_0}^+} \frac{\sqrt{U^2 + \omega^2 \, \Omega^2} \, \cos(\varphi_p - \beta)}{|\underline{r} - \underline{s}_0|} \frac{\partial E_T}{\partial \xi_1} \, d\xi_1 \, d\widetilde{\omega} \qquad (5\text{-}3)$$

and ϕ_v is an integral over the shed vortex sheet

$$\phi_v = \frac{1}{4\pi} \sum_{b=0}^{Z-1} \int_0^R \Gamma(z_0) \, dz_0 \int_{\alpha_{TE}}^{\infty} \underline{N}_{0v}^+ \cdot \frac{\underline{r} - \underline{s}_0}{|\underline{r} - \underline{s}_0|^3} \, d\alpha \qquad (5\text{-}4)$$

where $\Gamma_B(c_1(\widetilde{\omega}), \widetilde{\omega}) = \Gamma(\widetilde{\omega})$

$\underline{N}_{0s}^+$ is given in Equation (3-10) and

$\underline{N}_{0v}^+$ is given in Equation (3-18)

In the following work, the expressions will be considered without the effects of rake or warp since they are less complicated and permit comparison with results in the literature. The formulation with rake and warp can be obtained similarly.

In design, the detailed geometry of the propeller is to be determined. Since this is so, the position of the trailing edge can be chosen to simplify the integrals. With neither rake nor warp the blade-reference lines are the θ_b values $(\theta_b = \frac{2\pi}{Z} b)$. If the trailing edge of the blade is chosen to lie on the helical surface passing through this line, then in Equation (3-17)

$$\underline{s}_0 = z_0 \, \underline{e}_{\widetilde{\omega}} + \frac{U}{\Omega}(\theta - \theta_b) \underline{i} \; ; \; \theta \leqslant \theta_{TE}(z_0) \qquad (5\text{-}5)$$

i.e., $x_{TE} = \dfrac{U}{\Omega} \, \theta_{TE}$. Then Equation (3-18) reduces to Equation (4-4), etc. The expression for ϕ_v reduces to

$$\phi_v(r) = \frac{1}{4\pi} \sum_{b=0}^{Z-1} \int_0^R \Gamma(z_0) \, dz_0 \int_{a_{TE}(z_0)}^{\infty} \left\{ -z_0 \frac{\partial}{\partial x} + \frac{U}{\Omega z_0} \frac{\partial}{\partial \theta} \right\} \frac{1}{r} d\gamma$$

(5-6)

where r is given in Equation (4-6). From the results of Appendix B, the velocities computed from this expression can be seen to equal those derived from the Biot-Savart Law for a bound vortex along the blade trailing edge and a shed vortex sheet trailing downstream from it. The position vector of the trailing edge is

$$\underline{\ell} = x_{TE}(\widetilde{\omega}) \, \underline{i} + \widetilde{\omega} \, \underline{e}_{\widetilde{\omega}} (\theta_{TE}(\widetilde{\omega}) + \theta_b)$$

(5-7)

Hence a vector tangent to the trailing edge is

$$\underline{t} = \frac{d\underline{\ell}}{d\widetilde{\omega}} = \frac{dx_{TE}}{d\widetilde{\omega}} \, \underline{i} + \underline{e}_{\widetilde{\omega}} (\theta_{TE} + \theta_b) + \widetilde{\omega} \left(\frac{d\underline{e}_{\widetilde{\omega}}}{d\theta} \right)_{\theta_{TE} + \theta_b} \frac{d\theta_{TE}}{d\widetilde{\omega}}$$

$$= x_{TE} \, \underline{i} + \underline{e}_{\widetilde{\omega}} (\theta_{TE} + \theta_b) + \widetilde{\omega} \, \underline{e}_{\theta} \, \theta'_{TE}$$

(5-8)

Thus the velocity is

$$\underline{q}_v = \frac{1}{4\pi} \sum_{b=0}^{Z-1} \int_0^R \Gamma(z_0) \frac{\underline{t} \times (\underline{r} - \underline{\ell})}{|\underline{r} - \underline{\ell}|^3} \, dz_0$$

$$+ \frac{1}{4\pi} \sum_{b=0}^{Z-1} \int_0^R \frac{d\Gamma}{dz_0} \, dz_0 \int_{\theta_{TE}}^{\infty} \underline{I} \, d\gamma$$

(5-9)

where $\underline{I}$ is given in Equation (B-10) of Appendix B. In the preceding integral, z_0 is a dummy variable for $\widetilde{\omega}$. As shown in Appendix B this form is the same as that found in the literature, and hence the detailed explicit form used for the numerical analysis is not repeated here.

When the pitch of the blade-reference surface and the shed vortex sheet are the same, Pien[36] found that significant savings in computing time could be obtained by rearranging the limits of the infinite integral so that it would need to be calculated only once. Naturally this left an integral over a finite

78

region to be evaluated for each new position on the blade. For points everywhere on the blade except the trailing edge, the preceding expression is a straightforward quadrature without singularities in the integrand. When Pien's procedure is used, Cauchy principal-value integrals occur, but apparently these are easier to handle than the repeated infinite integral.

The preceding expression for the induced velocity is usually modified to include the moderately-loaded assumption discussed in Chapter 4 which consists of replacing the ζ_0 expression by the approximate one for $\zeta_0 + \bar{\epsilon} \zeta_1$, given in Equation (4-31), which is derived from lifting-line theory. Although an argument can be made for this approximation in lifting-line analysis, no justification is given for its use in lifting-surface theory. In any event, only a portion of the second-order effects are considered with this modification; see Section D of Chapter 3.

The expression for the potential due to blade thickness can be written

$$\phi_T(\underline{r}) = -\frac{1}{2\pi} \sum_{b=0}^{Z-1} \int_0^R \sqrt{U^2 + \widetilde{\omega}^2\, \Omega^2}\, \cos(\varphi_p - \beta)\, d\widetilde{\omega} \cdot \int_{c_2(\widetilde{\omega})}^{c_1(\widetilde{\omega})} \frac{\partial E_T/\partial \xi_1}{|\underline{r} - \underline{s}_0|}\, d\xi_1 \quad (5\text{-}10)$$

where

$$\underline{r} - \underline{s}_0 = (x - \xi_1 \sin\varphi_p)\, \underline{i} + \left(y + \widetilde{\omega} \sin\left(\theta_b + \frac{\xi_1 \cos\varphi_p}{\widetilde{\omega}}\right)\right) \underline{j}$$

$$+ \left(z - \widetilde{\omega} \cos\left(\theta_b + \frac{\xi_1 \cos\varphi_p}{\widetilde{\omega}}\right)\right) \underline{k}$$

Hence $\underline{q}_T = \nabla \phi_T$ is given by

$$\underline{q}_T = \frac{1}{2\pi} \sum_{b=0}^{Z-1} \int_0^R \sqrt{U^2 + \widetilde{\omega}^2\, \Omega^2}\, \cos(\varphi_p - \beta)\, d\widetilde{\omega} \cdot \int_{c_2}^{c_1} \frac{\frac{\partial E_T}{\partial \xi_1}(\underline{r} - \underline{s}_0)}{|\underline{r} - \underline{s}_0|^3}\, d\xi_1 \quad (5\text{-}11)$$

For points on the blade $\underline{r} \to \underline{s}_0$, only a principal-value integral must be evaluated.

Since this expression is the same as that found in the literature, it is convenient to make the necessary changes to demonstrate the equivalence. The changes are that the blade surface is described by $\widetilde{\omega}$, θ instead of ξ_1, $\widetilde{\omega}$, and that pitch $P(\widetilde{\omega})$ instead of pitch angle $\varphi_p(\widetilde{\omega})$ is used. This is the description used by Kerwin.[27,28] In addition, the term $\cos(\varphi_p - \beta)$ is ignored, and constant pitch is assumed since the blade normal is taken to be $\underline{e}_2$.

For constant pitch and neither rake nor warp, the only component of velocity in the boundary condition of Equation (3-27) is

$$v = \nabla\phi \cdot \underline{e}_2 \quad (5\text{-}12)$$

For points on the blade described by (r, ϕ),

$$x = r \ tan \ \varphi_p(r) \quad \phi = \frac{P(r)}{2\pi} \ \phi$$

$$y = - r \ sin \ \phi$$

$$z = r \ cos \ \phi$$

the component v can be written

$$v(r, \phi) = \int_0^R \sqrt{(\frac{P(\widetilde{\omega})}{2\pi})^2 + \widetilde{\omega}^2} \ d\widetilde{\omega} \int_{\theta_{LE}}^{\theta_{TE}} \sigma(\widetilde{\omega}, \theta) \ G_T \ d\theta \tag{5-13}$$

where

$$\sigma(\widetilde{\omega}, \theta) = U \ \sqrt{\frac{\left(\frac{P(\widetilde{\omega})}{2\pi}\right)^2 + \widetilde{\omega}^2}{P(\widetilde{\omega})/2\pi}} \ \frac{\partial E_T}{\partial \xi_1} \Big|_{\widetilde{\omega}, \ \theta} \tag{5-14}$$

and

$$G_T = \frac{1}{2\pi} \ \frac{P(\widetilde{\omega})/2\pi}{\sqrt{\left(\frac{P(\widetilde{\omega})}{2\pi}\right)^2 + \widetilde{\omega}^2}} \ \sum_{b=0}^{Z-1} \left[\frac{\frac{P(\widetilde{\omega})}{2\pi} \frac{\theta - P(r)}{2\pi} \phi_r - \frac{P(\widetilde{\omega})}{2\pi} \widetilde{\omega} \ sin \ (\theta_b + \theta - \phi)}{\left[\left(\frac{P(r) \ \phi - P(\omega) \ \theta}{2\pi}\right)^2 + r^2 + \widetilde{\omega}^2 - 2 \ \widetilde{\omega} r \ cos \ (\theta_b + \theta - \phi)\right]^{3/2}} \right]$$

$$\tag{5-15}$$

Except for notation, this agrees with Kerwin's expression. Kerwin uses $2E_T$ for his thickness distribution, so there is also a difference factor of 2. When the pitch is constant, G_T is a function of $(\theta - \phi)$.

The remaining term to be examined is the integral over the lifting surface. The velocity from this component of ϕ is given by

$$q_s = \nabla \phi_s$$

$$= \frac{1}{4\pi} \sum_{b=0}^{Z-1} \iint_{S_{B_0^+}} \Gamma_B(\underline{s}_0) \, \nabla_r \left(\frac{\underline{n}_0^+ s \cdot (\underline{r}-\underline{s}_0)}{|\underline{r}-\underline{s}_0|^3} \right) ds \tag{5-16}$$

$$= \frac{1}{4\pi} \sum_{b=0}^{Z-1} \iint_{S_{B_0^+}} \Gamma_B(\underline{s}_0) \left\{ \frac{\underline{n}_0^+ s}{|\underline{r}-\underline{s}_0|^3} - 3 \frac{\underline{n}_0^+ \cdot (\underline{r}-\underline{s}_0)}{|\underline{r}-\underline{s}_0|^5} (\underline{r}-\underline{s}_0) \right\} ds$$

When $\underline{r} - \underline{s}_0 \to 0$, the singularity in this expression is second-order rather than first-order as in principal-value integrals; see Equation (2-19).

To integrate by parts, the gradient of the kernel in Equation (5-16) must be expanded and rearranged

$$\nabla_r \left(\frac{\underline{n} \cdot (\underline{r}-\underline{s})}{|\underline{r}-\underline{s}|^3} \right) = (\underline{n} \cdot \nabla_r) \frac{\underline{r}-\underline{s}}{|\underline{r}-\underline{s}|^3} + \underline{n} \times \left(\nabla_r \times \frac{\underline{r}-\underline{s}}{|\underline{r}-\underline{s}|^3} \right)$$

But for an arbitrary vector A,

$$\underline{n} \times (\nabla \times \underline{A}) = (\underline{n} \times \nabla) \times \underline{A} - (\underline{n} \cdot \nabla) \underline{A} - \underline{n} (\nabla \cdot \underline{A})$$

Now, since

$$\nabla \cdot \left(\frac{\underline{r}-\underline{s}}{|\underline{r}-\underline{s}|^3} \right) = 0 \quad (\underline{r}-\underline{s} \neq 0)$$

the preceding expression becomes

$$\nabla_r \left(\frac{\underline{n} \cdot (\underline{r}-\underline{s})}{|\underline{r}-\underline{s}|^3} \right) = (\underline{n} \times \nabla_r) \times \frac{\underline{r}-\underline{s}}{|\underline{r}-\underline{s}|^3} = -(\underline{n} \times \nabla_s) \times \frac{\underline{r}-\underline{s}}{|\underline{r}-\underline{s}|^3}$$

To actually perform the integration by parts, we determine that

$$(\underline{n} \times \nabla_s) \times \left(\Gamma_B \frac{\underline{r}-\underline{s}}{|\underline{r}-\underline{s}|^3} \right) = \Gamma_B (\underline{n} \times \nabla_s) \times \frac{\underline{r}-\underline{s}}{|\underline{r}-\underline{s}|^3} + (\underline{n} \times \nabla_s \, \Gamma_B) \times \frac{\underline{r}-\underline{s}}{|\underline{r}-\underline{s}|^3}$$

Hence the velocity is

$$q_s = \frac{1}{4\pi} \sum_{b=0}^{Z-1} \iint_{S_{B_0^+}} \left\{ \left(\underline{n}_{0_s}^+ \times \nabla_s \, \Gamma_B \right) \times \frac{\underline{r} - \underline{s}_0}{|\underline{r} - \underline{s}_0|^3} \right.$$

$$\left. - \left(\underline{n}_{0_s}^+ \times \nabla_s \right) \times \left(\Gamma_B \, \frac{\underline{r} - \underline{s}_0}{|\underline{r} - \underline{s}_0|^3} \right) \right\} ds \tag{5-17}$$

One of Stokes' theorems is[48]

$$\iint_s \left(\underline{n} \times \nabla \right) \times \underline{A} \; ds = \oint_c d\underline{\ell} \times \underline{A}$$

where c is the curve bounding s, and $d\underline{\ell}$ is along the curve in the usual orientation. Thus the expression for velocity is

$$q_s = \frac{1}{4\pi} \sum_{b=0}^{Z-1} \left\{ \iint_{S_{B_0^+}} \left(\underline{n}_{0_s}^+ \times \nabla_s \, \Gamma_B \right) \times \frac{\underline{r} - \underline{s}_0}{|\underline{r} - \underline{s}_0|^3} \; ds \right.$$

$$\left. - \oint_c \Gamma_B \, d\underline{\ell} \times \frac{\underline{r} - \underline{\ell}}{|\underline{r} - \underline{\ell}|^3} \right\}$$

Now Γ_B is zero at the blade leading edge; and $\Gamma_{(\widetilde{\omega})}$, at the trailing edge. The arc element along the blade outline is

$$d\underline{\ell} = \frac{d\underline{\ell}}{d\widetilde{\omega}} d\widetilde{\omega}$$

$$= \underline{t} \, d\widetilde{\omega}$$

Hence

$$q_s = \frac{1}{4\pi} \sum_{b=0}^{Z-1} \left\{ \iint_{S_{B_0^+}} \left(\underline{n}_{0_s}^+ \times \nabla_s \, \Gamma_B \right) \times \frac{\underline{r} - \underline{s}_0}{|\underline{r} - \underline{s}_0|^3} \; ds \right.$$

$$\left. - \int_0^R \Gamma_{(z_0)} \underline{t} \times \frac{\underline{r} - \underline{\ell}}{|\underline{r} - \underline{\ell}|^3} \; dz_0 \right\} \tag{5-18}$$

82

The line integral cancels a similar contribution from the trailing vortex sheet in Equation (5-9), and the surface integral is the Biot-Savart Law with a vorticity distribution:

$$\underline{\Lambda} = \underline{n} \times \nabla_s \, \Gamma_B$$

$$= \underline{n} \times (\underline{q}^+ - \underline{q}^-)$$

Since the conversion is general, it would also be possible to express velocities from the nonlinear results of Chapter 2 in terms of a vorticity distribution. To interpret the results in such a manner, it will be necessary to define an inner surface of the blade which has zero flow velocity. Then the vorticity will be simply $\underline{n} \times \nabla \phi$. Since no further insight is provided with this approach, it is not pursued further.

The explicit expressions for the linearized velocity in the case of the general propeller geometry can be found in a straightforward manner. Since the results will eventually be compared with equations found in the literature, the geometrical restrictions appropriate for those cases will be made. These are that the propeller is neither raked nor warped and that the pitch is constant. For constant pitch

$$\underline{n} = \underline{N}^+ = \underline{e}_2$$

and for neither rake nor warp

$$\underline{n} \times \nabla \Gamma_B = \underline{e}_2 \times \left[\frac{\partial \Gamma_B}{\partial \xi_1} \, \underline{e}_1 + \left(\frac{\partial \Gamma_B}{\partial \widetilde{\omega}} + \frac{\xi_1 \cos^2 \varphi_p}{\widetilde{\omega}} \, \frac{\partial \Gamma_B}{\partial \xi_1} \right) \underline{e}_{\widetilde{\omega}} \right]$$

Hence

$$\underline{\Lambda} = \frac{\partial \Gamma_B}{\partial \xi_1} \, \underline{e}_{\widetilde{\omega}} - \left(\frac{\partial \Gamma_B}{\partial \widetilde{\omega}} + \frac{\xi_1 \cos^2 \varphi_p}{\widetilde{\omega}} \, \frac{\partial \Gamma_B}{\partial \xi_1} \right) \underline{e}_1$$

Now since

$$\Gamma_B = \int_{c_2(\widetilde{\omega})}^{\xi_1} \gamma(\eta, \widetilde{\omega}) \, d\eta$$

one finds

$$\underline{\Lambda} = \gamma \underline{e}_{\widetilde{\omega}} - \left(\frac{\partial}{\partial \widetilde{\omega}} \int_{c_2}^{\xi_1} \gamma \, d\eta + \frac{\xi_1 \cos^2 \varphi_p}{\widetilde{\omega}} \, \gamma \right) \underline{e}_1 \tag{5-19}$$

This is the form of the vorticity vector required in the coordinate systems developed here. However, in the literature it is more common to work with cylindrical polar coordinates $(\tilde{\omega}, \theta, x)$. In this system the parametric representation of the helical blade-reference surface is given by

$$\left.\begin{aligned}
x &= \tilde{\omega}\,\tan\varphi_p \quad \theta = \frac{P}{2\pi}\theta \\
y &= -\,\tilde{\omega}\sin\theta \\
z &= \tilde{\omega}\cos\theta
\end{aligned}\right\} \tag{5-20}$$

For the surface coordinate system $u^1, u^2 = \tilde{\omega}, \theta$, the metric coefficients are[43]

$$g_{ij} = \begin{bmatrix} 1 & 0 \\ & \\ 0 & \left(\dfrac{P}{2\pi}\right)^2 + \tilde{\omega}^2 \end{bmatrix} \tag{5-21}$$

Hence for constant pitch, the gradient of Γ_B in this coordinate system is

$$\underline{n} \times \nabla\Gamma_B = \underline{e}_2 \times \left[\underline{e}_{\tilde{\omega}}\frac{\partial\Gamma_B}{\partial\tilde{\omega}} + \frac{\underline{e}_1}{\sqrt{(\frac{P}{2\pi})^2 + \tilde{\omega}^2}}\frac{\partial\Gamma_B}{\partial\theta} \right]$$

Now since

$$\Gamma_B = \int_{\theta_{LE}(\tilde{\omega})}^{\theta} \sqrt{(\frac{P}{2\pi})^2 + \tilde{\omega}^2}\,\gamma d\theta$$

one finds

$$\underline{n} \times \nabla\Gamma_B = \underline{e}_2 \times \left[\gamma\underline{e}_1 + \frac{\partial}{\partial\tilde{\omega}}\left(\int_{\theta_{LE}}^{\theta} \sqrt{\left(\frac{P}{2\pi}\right)^2 + \tilde{\omega}^2}\,\gamma d\theta\right)\underline{e}_{\tilde{\omega}} \right]$$

and hence

$$\underline{\Lambda} = \gamma\underline{e}_{\tilde{\omega}} - \frac{\partial}{\partial\tilde{\omega}}\left(\int_{\theta_{LE}}^{\theta} \sqrt{\left(\frac{P}{2\pi}\right)^2 + \tilde{\omega}^2}\,\gamma d\theta\right)\underline{e}_1 \tag{5-22}$$

This is the same expression obtained by Kerwin,[51] although he used the result in a different manner.

84

Explicit formulas for calculating the velocity from the Biot-Savart Law are given in the next section and hence are not repeated here.

C—COMPARISON WITH OTHER FORMULATIONS

In the past, linearized propeller lifting-surface formulations have been developed from three viewpoints—a postulated vorticity distribution (Pien,[30] Kerwin,[26,27] and Murray[33]), an acceleration potential (Sparenberg,[25] Hanaoka,[32] Pien and Strom-Tejsen[31]), or a velocity potential (Yamazaki[18-24]). Both velocity potential and acceleration potential formulations are based on the equations of motion, while the vortex distribution formulation is based on laws derived from the governing equations. Of course, all solutions should be equivalent so the development is only a matter of personal preference.

The details of the formulation of the velocity-potential function are not given by Yamazaki. However, examination of the potential reveals it to be compatible with the velocity potential derived from the acceleration potential. Such solutions are given in terms of the pressure difference across the blade (for constant pitch propellers, this is equivalent to the radial component of bound vorticity; see the footnote following Equation (3-24)) and an infinite integral to a variable point on the blade.

In the acceleration potential method formulated by Sparenberg, the linearization is on the basis of only the axial component of q_0; other velocity components are assumed small relative to it. However, since the propeller also has a rotational velocity, it is not clear such an assumption is justified. Hanaoka linearizes about the total free-stream speed and converts his expression for the linearized acceleration potential to one for the velocity potential. For steady flow, his Equation (3-8) is the same as the lifting portion of Equation (3-21), when the pitch of the blade-reference surface and the shed vortex wake are identical.

The formulation on the basis of the vorticity distribution is now almost classical. The vorticity vector is specified on the body and shed vortex sheet, and the velocity distribution can be calculated from the Biot-Savart Law. For a surface distribution of vorticity, the Biot-Savart equation gives the induced velocity as

$$\underline{q}_i = \frac{1}{4\pi} \iint_{S_0} \frac{\underline{\Lambda} \times (\underline{r} - \underline{s})}{|\underline{r} - \underline{s}|^3}\, dS \tag{5-23}$$

where $\underline{\Lambda}$ is the vorticity vector, and S_0 is the approximate blade surfaces plus the shed vortex sheets.

Across the shed vortex sheet

$$\underline{q}^+ - \underline{q}^- = \nabla(\phi^+ - \phi^-) = \nabla\Gamma(\widetilde{\omega})$$

$$= \frac{\partial \Gamma}{\partial \widetilde{\omega}}\, \underline{e}_{\widetilde{\omega}}$$

and the normal to this sheet is, (from Equation (3-18))

$$\underline{N} = \frac{\widetilde{\omega}}{\cos \beta} \; \underline{n} = \frac{\widetilde{\omega}}{\cos \beta} \left(- \cos \beta \, \underline{i} + \sin \beta \, \underline{e}_\theta \right)$$

hence the vorticity vector is

$$\underline{\Lambda} = \underline{n} \times (\underline{q}^+ - \underline{q}^-) = - \frac{\partial \Gamma}{\partial \widetilde{\omega}} \left(\sin \beta \, \underline{i} + \cos \beta \, \underline{e}_\theta \right)$$

where $\tan \beta = {}^U/{}_{\Omega\widetilde{\omega}}$.

Since $\underline{s} = \underline{\zeta}_0$, the integration over the shed vortex surface is

$$\underline{q}_v = - \frac{1}{4\pi} \sum_{b=0}^{Z-1} \int_0^R \frac{d\Gamma}{dz_0} (z_0) \, dz_0 \int_{\theta_{TE}}^\infty \underline{I} \, d\gamma \qquad (5\text{-}24)$$

where $\underline{I}$ is given by Equation (B-10) in Appendix B; this is the form given previously in Section B of this Chapter. Thus this component of velocity is the same as that given by Pien,[39] Morgan and Wrench,[14] and others, except that this free-vorticity starts at the variable trailing edge and lies on the surface parallel to the undisturbed free-stream velocity.

The bound velocity on the blade is now needed. Since most of the previous investigators have derived equations appropriate for only constant pitch, we do also. This means that the zero-order normal from Equation (3-10) is

$$\underline{N}^+ = \underline{n} = \underline{e}_2$$

and

$$\underline{q}^+ - \underline{q}^- = \gamma \underline{e}_1 + \sigma \underline{e}_{\widetilde{\omega}} + \mu \underline{e}_2$$

where σ is unknown, and γ is given by Equation (3-24).

Hence the bound vorticity vector is

$$\underline{\Lambda} = \gamma \underline{e}_{\widetilde{\omega}} + \sigma \underline{e}_1 \qquad (5\text{-}25)$$

The explicit form of σ will be found presently but now the velocity induced by this bound-vorticity vector is desired:

$$\underline{q} = \frac{1}{4\pi} \sum_{b=0}^{Z-1} \int_0^R d\widetilde{\omega} \int_{c_2}^{c_1} \frac{(\sigma \underline{e}_1 + \gamma \underline{e}_{\widetilde{\omega}}) \times (\underline{r} - \underline{s}_0)}{|\underline{r} - \underline{s}_0|^3} \, d\xi_1$$

where $\underline{s}_0$ is given in Equation (3-9), which for constant pitch and with neither rake nor warp becomes

$$\underline{s}_0 = \xi_1 \sin \varphi_p \, \underline{i} + \widetilde{\omega} \underline{e}_{\widetilde{\omega}}$$

where

$$\underline{e}_{\widetilde{\omega}} = - \sin \left(\theta_b + \frac{\xi_1 \cos \varphi_p}{\widetilde{\omega}} \right) \underline{j} + \cos \left(\theta_b + \frac{\xi_1 \cos \varphi_p}{\widetilde{\omega}} \right) \underline{k}$$

Now for $\underline{r} = x\underline{i} + r\underline{e}_r(\phi)$,

$$\underline{e}_1 \times (\underline{r} - \underline{s}_0) = (\sin \varphi_p \, \underline{i} + \cos \varphi_p \, \underline{e}_\theta) \times \left\{ (x - \xi_1 \sin \varphi_p) \, \underline{i} + r\underline{e}_r - \widetilde{\omega}\underline{e}_{\widetilde{\omega}} \right\}$$

$$= \sin \varphi_p \, (r\underline{e}_\phi - \widetilde{\omega}\underline{e}_\theta) + \cos \varphi_p \left\{ (x - \xi_1 \sin \varphi_p) \, \underline{e}_{\widetilde{\omega}} \right.$$

$$\left. + (\widetilde{\omega} - r \cos (\theta - \phi)) \, \underline{i} \right\}$$

$$\underline{e}_{\widetilde{\omega}} \times (\underline{r} - \underline{s}_0) = \underline{e}_{\widetilde{\omega}} \times \left\{ (x - \xi_1 \sin \varphi_p) \, \underline{i} + r\underline{e}_r - \widetilde{\omega}\underline{e}_{\widetilde{\omega}} \right\}$$

$$= -(x - \xi_1 \sin \varphi_p) \, \underline{e}_\theta - r \sin \left(\theta_b + \frac{\xi_1 \sin \varphi_p}{\widetilde{\omega}} - \phi \right) \underline{i}$$

Hence:

$$\underline{q} \cdot \underline{i} = \frac{1}{4\pi} \sum_{b=0}^{Z-1} \int_0^R d\widetilde{\omega} \cdot \int_{c_2}^{c_1} \frac{\sigma \cos \varphi_p \, (\widetilde{\omega} - r \cos (\theta - \phi)) - \gamma \, r \sin (\theta - \phi)}{|\underline{r} - \underline{s}_0|^3} \, d\xi_1$$

$$\underline{q} \cdot \underline{e}_r = \frac{1}{4\pi} \sum_{b=0}^{Z-1} \int_0^R d\widetilde{\omega} \cdot \int_{c_2}^{c_1} \left\{ \frac{\sigma \left[\sin \varphi_p \sin (\theta - \phi) + \cos \varphi_p (x - \xi_1 \sin \varphi_p) \cos (\theta - \phi) \right]}{|\underline{r} - \underline{s}_0|^3} + \right.$$

$$(5\text{-}26)$$

$$+ \frac{\gamma \sin (\theta - \phi) (x - \xi_1 \sin \varphi_p)}{|\underline{r} - \underline{s}_0|^3} \Bigg\} d\xi_1$$

$$\underline{q} \cdot \underline{e}_\phi = \frac{1}{4\pi} \sum_{b=0}^{Z-1} \int_0^R d\widetilde{\omega} \cdot \int_{c_2}^{c_1} \Bigg\{ \frac{\sigma \left[\sin \varphi_p (r - \widetilde{\omega} \cos (\theta - \phi) + \cos \varphi_p (x - \xi_1 \sin \varphi_p) \sin (\theta - \phi) \right]}{|\underline{r} - \underline{s}_0|^3}$$

$$- \frac{\gamma (x - \xi_1 \sin \varphi_p) \cos (\theta - \phi)}{|\underline{r} - \underline{s}_0|^3} \Bigg\} d\xi_1 \qquad \begin{array}{l} \text{(5-26)} \\ \text{Cont'd} \end{array}$$

where

$$\theta = \theta_b + \frac{\xi_1 \cos \varphi_p}{\widetilde{\omega}}$$

$$|\underline{r} - \underline{s}_0|^3 = \left\{ (x - \xi_1 \sin \varphi_p)^2 + r^2 + \widetilde{\omega}^2 - 2 r \widetilde{\omega} \cos (\theta - \phi) \right\}^{3/2}$$

In the literature it is common to work with $\theta = \dfrac{\xi_1 \cos \varphi_p}{\widetilde{\omega}}$ rather than ξ_1. Since for $\widetilde{\omega} = constant$

$$d\,\theta = \frac{\cos \varphi_p}{\widetilde{\omega}} d\xi_1$$

the preceding velocity components become

$$\underline{q} \cdot \underline{i} = \frac{1}{4\pi} \sum_{b=0}^{Z-1} \int_0^R \frac{\widetilde{\omega} \, d \, \widetilde{\omega}}{\cos \varphi_p} \cdot \int_{\theta_{LE}(\widetilde{\omega})}^{\theta_{TE}(\widetilde{\omega})} \frac{a \cos \varphi_p (\widetilde{\omega} - r \cos (\theta_b + \theta - \phi)) - \gamma r \sin (\theta_b + \theta - \phi)}{|\underline{r} - \underline{s}_0|^3} d\theta$$

$$\text{(5-27)}$$

$$\underline{q} \cdot \underline{e}_r = \frac{1}{4\pi} \sum_{b=0}^{Z-1} \int_0^R \frac{\widetilde{\omega} \, d\widetilde{\omega}}{\cos \varphi_p}$$

$$\circ \int_{\theta_{LE}}^{\theta_{TE}} \left\{ \frac{\sigma \, (\sin \varphi_p \, \widetilde{\omega} \sin (\theta_b + \theta - \phi) + \cos \varphi_p \, (x - \widetilde{\omega} \tan \varphi_p \, \theta) \sin (\theta_b + \theta - \phi))}{|\underline{r} - \underline{s}_0|^3} \right.$$

$$\left. + \frac{\gamma \sin (\theta_b + \theta - \phi) \, (x - \widetilde{\omega} \tan \varphi_p \, \theta)}{|\underline{r} - \underline{s}_0|^3} \right\} d\theta$$

$$\underline{q} \cdot \underline{e}_\phi = \frac{1}{4\pi} \sum_{b=0}^{Z-1} \int_0^R \frac{\widetilde{\omega} \, d\widetilde{\omega}}{\cos \varphi_p}$$

$$\circ \int_{\theta_{LE}}^{\theta_{TE}} \left[\frac{\sigma \left\{ \sin \varphi_p \, (r - \widetilde{\omega} \cos (\theta_b + \theta - \phi)) + \cos \varphi_p \, (x - \widetilde{\omega} \tan \varphi_p \, \theta) \sin (\theta_b + \theta - \phi) \right\}}{|\underline{r} - \underline{s}_0|^3} \right.$$

$$\left. - \frac{\gamma \cos (\theta_b + \theta - \phi) \, (x - \widetilde{\omega} \tan \varphi_p \, \theta)}{|\underline{r} - \underline{s}_0|^3} \right] d\theta \qquad \text{(5-27)}$$
Cont'd

where

$$|\underline{r} - \underline{s}_0|^3 = \left\{ (x - \widetilde{\omega} \tan \varphi_p \, \theta)^2 + r^2 + \widetilde{\omega}^2 - 2 \, \widetilde{\omega} r \cos (\theta_b + \theta - \phi) \right\}^{3/2}$$

In the literature it is also common to break this surface integral up into two components

$$\underline{q} = \underline{q}_1 + \underline{q}_2 \qquad \text{(5-28)}$$

where

$$\underline{q}_1 = \frac{1}{4\pi} \sum_{b=0}^{Z-1} \iint_{S_{B_0^+}} \sigma \frac{\underline{e}_1 \times (\underline{r} - \underline{s}_0)}{|\underline{r} - \underline{s}_0|^3} \, ds \qquad \text{(5-29)}$$

$$q_2 = \frac{1}{4\pi} \sum_{b=0}^{Z-1} \iint_{S_{B_0^+}} \gamma \frac{e_{\widetilde{\omega}} X (r - s_0)}{|r - s_0|^3} \, ds \qquad (5\text{-}30)$$

and combine q_1 with the integral over the shed vortex sheet. When this is done it is customary to take the pitch angle of the shed vortex sheet and the blade-reference surface as the βi angle computed from lifting-line theory; this corresponds to the hydrodynamic pitch introduced in Equation (4-30).

When q_1 and q_v are combined, one has the form:

$$q_1 + q_v = \frac{1}{4\pi} \sum_{b=0}^{Z-1} \int_0^R d\widetilde{\omega} \int_{\theta_{LE}}^\infty \frac{\Delta X (r - s)}{|r - s|^3} \, h d\theta \qquad (5\text{-}31)$$

where

$$\left. \begin{array}{l} \Delta = \sigma \, e_1 \\[2mm] s = s_0 \\[2mm] h = \dfrac{\widetilde{\omega}}{\cos \varphi_p} \end{array} \right\} \quad \theta_{LE} \leqslant \theta \leqslant \theta_{TE}$$

$$\left. \begin{array}{l} \Delta = - \dfrac{\partial \Gamma}{\partial \widetilde{\omega}} \, (\sin \beta i + \cos \beta \, e_{\cdot \theta}) \\[3mm] s = s_0 \\[3mm] h = \dfrac{\widetilde{\omega}}{\cos \beta} \end{array} \right\} \quad \theta > \theta_{TE}$$

Because of the form of this equation it is also customary in the literature to speak of both q_1 and q_v as being induced by a trailing vortex system. In fact some authors derive their equations, postulating that the trailing vortex system starts on the blade.

Because of this confusion regarding the σ component of bound vorticity, it is not surprising that the literature contains several expressions for it. In order to determine σ, one uses the property that a distribution of vorticity must satisfy the equation

$$\nabla \cdot \Delta = 0$$

90

For a constant-pitch helical sheet, with the vorticity vector given by the component γ in the radial direction and the component σ directed in the surface perpendicular to the radial direction and tangent to a cylinder, one can determine the metric coefficients, Equation (5-21), and reciprocal unitary vectors[43] and thus find the equation for divergence on the blade

$$\nabla \cdot \underline{A} = \frac{1}{\sqrt{\left(\frac{P}{2\pi}\right)^2 + \widetilde{\omega}^2}} \left\{ \frac{\partial}{\partial \widetilde{\omega}} \left(\sqrt{\left(\frac{P}{2\pi}\right)^2 + \widetilde{\omega}^2}\ \gamma \right) + \frac{\partial \sigma}{\partial \theta} \right\} \qquad (5\text{-}32)$$

where $P/2\pi = \widetilde{\omega} \tan \varphi_p$

and on the shed vortex sheet

$$\nabla \cdot \underline{A} = \frac{\widetilde{\omega}}{\cos \beta} \frac{\partial}{\partial \theta} - \left(\frac{\partial \Gamma}{\partial \widetilde{\omega}} \right)$$

The expression in the wake is automatically satisfied since $\Gamma = \Gamma(\widetilde{\omega})$ only. Now one must find the form of σ on the blade.

From the first expression, one obtains

$$\sigma(\widetilde{\omega}, \theta) = - \int_{\theta_{LE}}^{\theta} \frac{\partial}{\partial \widetilde{\omega}} \left(\sqrt{\left(\frac{P}{2\pi}\right)^2 + \widetilde{\omega}^2}\ \gamma \right) d\phi + f(\widetilde{\omega})$$

where $f(\widetilde{\omega})$ is the integration "constant." The value of this constant of integration is obtained by requiring that the vorticity vector not run off the leading edge of the blade into the irrotational fluid. That is, if $\underline{t}$ is the tangent vector to the leading edge

$$\underline{t} \times \underline{A}\big|_{\theta = \theta_{LE}} = 0$$

Since

$$\underline{t} = \frac{d}{d\widetilde{\omega}} \left(\underline{\zeta}_{L.E.} \right)$$

$$= \left(\frac{P}{2\pi} \right) \frac{d\theta_{LE}}{d\widetilde{\omega}}\ \underline{i} + \underline{e}_{\widetilde{\omega}} + \widetilde{\omega} \underline{e}_{\theta} \frac{d\theta_{LE}}{d\widetilde{\omega}}$$

one finds that

$$f = \gamma(\theta_{LE}, \widetilde{\omega}) \frac{\widetilde{\omega}}{\cos \varphi_p} \frac{d\theta_{LE}}{d\widetilde{\omega}}$$

or that

$$\sigma = -\frac{\partial}{\partial \widetilde{\omega}} \int_{\theta_{LE}}^{\theta} \gamma \frac{\widetilde{\omega}}{\cos \varphi_p} \, d\phi \qquad (5\text{-}33)$$

$$= -\frac{\partial}{\partial \widetilde{\omega}} \Gamma_B(\widetilde{\omega}, \theta)$$

This is the expression obtained by Kerwin.[27]

Pien[30] and Murray[33] state that:

$$\sigma = -\frac{\partial}{\partial \widetilde{\omega}} \int_{\theta_{LE}}^{\theta} \Gamma_{\widetilde{\omega}} \, d\phi$$

where

$$\Gamma(\widetilde{\omega}) = \int_{\theta_{LE}}^{\theta_{TE}} \Gamma_{\widetilde{\omega}}(\widetilde{\omega}, \theta) \, d\theta$$

Thus the metric coefficient is absorbed in the definition of $\Gamma(\widetilde{\omega})$ which must be

$$\Gamma_{\widetilde{\omega}}(\widetilde{\omega}, \theta) = \frac{\widetilde{\omega}}{\cos \varphi_p} \gamma(\widetilde{\omega}, \theta)$$

where $\gamma(\widetilde{\omega}, \theta)$ is the radial component of vorticity.

Pien and Murray do calculate the velocities with an expression like that for $q_1 + q_v$ in Equation (5-31). Kerwin[27] first integrates the value of $\partial\sigma/\partial\widetilde{\omega}$ on the blade from θ to ∞, then integrates that value over the blade surface. In a later paper, Kerwin and Leopold,[29] change the formulas to the form of Equation (5-31).

D—EXAMINATION OF RADIAL COMPONENT IN BOUNDARY CONDITION

Although the formal development of the lifting-surface and lifting-line equations is important academically, it does not in itself contribute to improved propeller designs. However, the lifting-surface formulation does explicitly consider the radial velocity component in the boundary condition used to derive the camber distribution in Equation (3-27). Since this term might contribute significantly to the engineering aspects of propeller design, some idea of its effect on the computed camberline must be found. In order to examine the effect of this term, a rather crude approximation will be made for the radial

velocity. The only radial velocity components found in the literature are those calculated by Hough and Ordway.[57] Their results are for circumferentially averaged velocity components due to a lifting-line with a circulation distribution they call approximately optimum; for the radial component they do not actually compute values at the lifting line. Nevertheless, we use these values because no others are available.

Comparison will be made with the maximum camber ratios calculated by Cheng[58] from the formulation of Pien.[30] Comparisons of the averaged axial velocities for the optimum circulation distribution are reasonably close to those computed for the arbitrary circulation distribution actually used in the calculations by Cheng. If we assume the radial velocity component is approximately constant and approximately given by the values given by Hough and Ordway at the point closest to the lifting line, then the camber due to the new term is parabolic with amplitude for symmetrical blades

$$
\left.\frac{\Delta F_c}{2R}\right|_{max} = -\frac{1}{4} \frac{\left(\dfrac{C_1-C_2}{2R}\right)^2 \cdot R \left(\dfrac{sin\,2\,\varphi_p}{2\widetilde{\omega}} + \dfrac{d\varphi_p}{d\widetilde{\omega}}\right) \dfrac{w^*(\widetilde{\omega})}{U}}{\sqrt{1 + (\dfrac{\widetilde{\omega}\Omega}{U})^2}}
$$

(5-34)

$$
= \frac{-\dfrac{1}{4} \left(\dfrac{C_1-C_2}{2R}\right)^2 \cdot R \,\dfrac{dP}{d\widetilde{\omega}} \dfrac{cos^2\,\varphi_p}{2\pi\widetilde{\omega}} \dfrac{w^*(\widetilde{\omega})}{U}}{\left[1 + (\dfrac{\widetilde{\omega}\Omega}{U})^2\right]^{1/2}}
$$

In the calculation method proposed by Pien,[30] φ_p is β_i given in Equation (4-51). Cheng tabulates these values as well as the chord-to-diameter ratio. The following table lists the maximum camber computed by Cheng for his propeller 3916A and the increment computed by using the preceding equation, both for an 8-inch-diameter propeller

---

[57]Hough, G.R. and D.E. Ordway, "The Generalized Actuator Disk," Developments in Theoretical and Applied Mechanics, Pergamon Press, Inc., New York, Vol. II, pp. 317-336 (1965).

[58]Cheng, H.M., "Hydrodynamic Aspect of Propeller Design Based on Lifting-Surface Theory—Part I— Uniform Chordwise Load Distribution," NSRDC Report 1802 (1964).

$\dfrac{\widetilde{\omega}}{R}$	$E_c\vert_{max}$, Cheng,[58] Figs. 7 and 16	$\Delta E_c\vert_{max}$
0.3	0.088 in.	0.0002 in.
0.7	0.034 in.	−0.002 in.

The change in sign in $\Delta E_c\vert max$ reflects a change in sign of velocity component along the radius.

For this propeller, the change of camber is negligible for the $\widetilde{\omega}/R = 0.3$ radius. This is because of the small slope of the pitch curve in this region. For the 0.7 radius, the change in camber is about 6 percent of the contribution from the conventional calculations and would be significant for propellers of larger diameter.

Additional information about the importance of the radial component can be surmised by considering the effect of rake or warp. The effect of warp is especially important for improved cavitation performance and reduced alternating thrust when operating in a wake, Miller[59] and Boswell.[60] To date, investigations have been conducted with skewed propellers for which the blade-reference line lies in the helical surface which passes through a straight-line element in the $x = 0$ plane.[60] For such propellers the normal to the reference surface $\underline{N}_0$ would contribute a radial term approximately like that described for the camber effect; however, since ξ_1 is measured from $x = 0$, an angle-of-attack term would also occur. Such propellers have blades extending considerably downstream. This overhang requires that the propeller hub and the rudder be separated more than normal. If instead of skewed propellers, only warped propellers were utilized, this problem would not occur. Hence, the effect of warp on the design will be considered now.

Skew is usually given as a warp angle with the understanding that the blade-reference line lies in the helical reference surface through a θ_b line. The warp angles tabulated by Boswell[60] are approximately:

$$W(\widetilde{\omega}) = \theta_s \left(\frac{\widetilde{\omega}}{R} - \frac{\widetilde{\omega}_{HUB}}{R} \right) \bigg/ \left(1 - \frac{\widetilde{\omega}_{HUB}}{R} \right)$$

where θ_s is the designated amount of "skew."

[59]Miller, M.L., "Experimental Determination of Unsteady Propeller Forces," Seventh Symposium on Naval Hydrodynamics, Rome (1968).

[60]Boswell, R., "Design, Cavitation Performance, and Open-Water Performance of a Series of Research Skewed Propellers," NSRDC Report 3339 (1971).

That portion of the boundary condition of Equation (3-27) to be examined is

$$-\frac{\partial E_c}{\partial \xi_1} = \tilde{\omega}\frac{dW}{d\tilde{\omega}}\sin\varphi_p \frac{w(\xi_1,\,0,\,\tilde{\omega})}{\sqrt{U^2+\Omega^2\tilde{\omega}^2}} \tag{5-35}$$

If the preceding expression for warp is used, and if the radial component is again approximated by $w^*(\tilde{\omega})$, then warp contributes an angle of attack (or pitch correction) to the camberline shape. The tangent to this pitch angle is given by the preceding expression

$$-\tan(\Delta\alpha) = \tilde{\omega}\frac{dW}{d\tilde{\omega}}\sin\varphi_p \frac{w^*(\tilde{\omega})}{\sqrt{U^2+\tilde{\omega}^2\Omega^2}}$$

For $\theta_s = 2\pi/Z$.

$$-\tan(\Delta\alpha) = \frac{\tilde{\omega}}{R}\left(\frac{2\pi}{Z}\right)\sin\varphi_p \frac{w^*(\tilde{\omega})}{\sqrt{U^2+\Omega^2\tilde{\omega}^2}} \frac{1}{1-\dfrac{\tilde{\omega}_{HUB}}{R}}$$

For lack of other data, we approximate the φ_p values at the warped line by the β_i values for a straight blade-reference line.

By applying these approximations to the five-bladed propeller considered previously, the pitch-angle corrections would be

$\dfrac{\tilde{\omega}}{R}$	$\Delta\alpha$ in Degrees
0.3	− 0.2
0.7	0.5

These corrections are considered significant.

Because of the change in sign, the preceding corrections might tend to cancel in their effect on thrust. However, they could be important for cavitation performance which is one of the main reasons for designing a propeller rather than selecting one from a series.

E—DESIGN PROCEDURES (HYDRODYNAMIC)

In current design techniques by Morgan, Silovic, and Denny[61] and Kerwin and Leopold,[29] a combination of lifting-surface and lifting-line results is used. Briefly the mechanics of this procedure are to use the second-order, lifting-line equations for the outer flow to find the induced velocities at the blade-reference line, circulation distribution and thrust. The inner flow is ignored, and hence an integral equation must be solved. This is usually done by assuming either a $tan\ \beta_i$ or circulation distribution and scaling the chosen quantity to eventually give the required thrust (or power). The resulting circulation distribution is used to scale the chosen radial component of vorticity γ; see Equation (3-31). The lifting-line induced velocities are assumed to be approximately the average chordwise results from a lifting-surface calculation. They are used to approximate the velocities induced by the shed vortex wake and are used to give the reference surface $\varphi_p(\widetilde{\omega})$. Hence everything is known to compute the lifting-surface results, partially taking into account second-order effects. This procedure has worked remarkably well for the performance of conventional propellers, Cox.[37] On the other hand, it seems to be difficult to design a bad propeller since even the earlier, semi-empirical design procedures such as Hill's[62] produced propellers which developed the desired thrust. It is in other areas, especially cavitation inception, that the more refined analysis embodied in the lengthy lifting-surface calculations are expected to have a distinct advantage. Unfortunately, few experimental comparisons of the type necessary to judge the adequacy of the various hydrodynamic theories are found in the literature. However, when cavitation occurs first at the leading edge for the design condition, the design procedure has not been sufficient to produce the specified chordwise pressure distribution. Such is the case with a recent series of skewed propellers.[60] Some differences in the numerical results of various lifting-surface formulations are given by Johnson.[63]

Although the combination of lifting-line and lifting-surface results is quite practical, it is not entirely consistent. Specifically, the expansion for the circulation distribution in the lifting-line analysis can hardly be expected to apply for $\bar{\epsilon} \to 1$. However, for elliptic wings, Van Dyke[2,3] has shown that the lift computed from the integral equation is quite close to the exact value over the entire range of aspect ratios. Thus the lifting-line results might be adequate for parametric studies since calculations can be quickly done. For final design, though, the lifting-surface equations should be used since they will give a geometry better able to meet design conditions.

Another utilization of the lifting-line equations is to approximate $\varphi_p(\widetilde{\omega})$ and the position vector of the shed vortex sheet. The determination of the shed vortex sheet for the lifting-surface analysis by using

[61]Morgan, W.B. et al., "Propeller Lifting-Surface Corrections," Society of Naval Architects and Marine Engineers Transactions, Vol. 76, pp. 309-347 (1965).

[62]Hill, J.G., "The Design of Propellers," Society of Naval Architects and Marine Engineers Transactions, pp. 143-192 (1949).

[63]Johnson, C.A., "Comparison of Propeller Design Techniques," Fourth Symposium on Naval Hydrodynamics (1962).

the lifting-line induced velocities is probably not accurate near the lifting surface where it is most important; in any event, the current utilization is only an approximate second-order correction for a portion of the second-order terms. Other second-order terms should be calculated to determine their magnitude also.

To use the consistent first-order lifting surface calculations, the following procedure is recommended. In the first-order theory the approximate position of the shed vortex sheet is independent of the induced velocities and is known. The blade-section pitch angle φ_p is first approximated by the β angle. The magnitude of the circulation distribution needed to produce the thrust can be calculated from Equation (3-23). The propeller geometry can now be calculated. The angle of attack of the section can be used to define a new φ_p, and the calculations can be repeated. The second-order results could also be calculated if necessary. In particular the second-order thrust in Equation (3-29) could be calculated from the first-order data so that an adjustment in the circulation could be made to meet the given thrust or some other criteria used to iterate for the final solution.

Obviously, these alternative procedures would be more involved than the presently-used techniques but unless an entirely consistent approach to the design problem is taken one does not know the degree of approximation involved in the present calculations or what potential exists for design based on the lifting-surface formulation.

In the equations for design the chordwise component of velocity difference (or the spanwise component of vorticity) γ is assumed to be given as well as the total bound circulation curve $\Gamma(\widetilde{\omega})$. This is compatible with information which a designer should supply for a propeller designed from cavitation considerations: Two general criteria for the avoidance of cavitation are that no suction peaks occur on the blade and that the shed vorticity be distributed as uniformly as possible in the spanwise direction. The first conditions met by selecting the functiona form of γ; the second, by the functional form of $\Gamma(\widetilde{\omega})$, since the gradient of Γ gives the shed vorticity. The number of blades and the blade-area ratio are also part of these considerations since the average pressure times the blade area determines the load which must be sufficient to produce the required thrust.

F—RECOMMENDATIONS

Obviously the first recommendation is to include the radial velocity component in the boundary condition for propellers designed with variable geometric pitch, warp or rake. Although the inclusion of this term is not expected to have a significant effect on the thrust, it could lead to propellers with better cavitation performance. Since cavitation considerations are one of the main reasons for designing a propeller rather than selecting one from a series, and since a crude analysis shows the term to have a significant effect, detailed numerical calculations should be undertaken.

Since heavily-loaded propellers are becoming more common in practice, the second-order lifting-surface formulas should also be programmed for design calculations. One of the interesting aspects of such investigations would be determination of the position vector of the lines of constant circulation in the shed vortex sheet. Another interesting outcome of these calculations would be an evaluation of the magnitude of

the second-order terms. Presently, it is assumed that the shed vortex sheet needs to be described better than by ζ_0. Qualitatively this is saying that the infinite integral of $\zeta_1 = 0$ (ϵ) over the shed vortex sheet produces a zero-order contribution. The proposed calculations would evaluate this assumption.

The formal analysis described here should also be extended to include vorticity, i.e., an axisymmetric free-stream velocity, unsteady flow, and supercavitating propellers. Since unsteady flow with vorticity is the standard operating condition of propellers behind a ship, these two are important areas of research.

SUMMARY AND CONCLUSIONS

The mathematical development presented in the preceding chapters has been based on the equations of motion and certain mathematical relations which have permitted an exact formulation to be constructed. Application of formal perturbation procedures has yielded linearized solutions appropriate for numerical calculations. In Chapter 5, the velocities computed from the lifting-surface potential are shown to equal those computed by the Biot-Savart Law. These expressions are then shown to equal those found in the literature for the approximate geometrical conditions.

An examination of the literature did not reveal previous explicit consideration of the radial velocity component in the first-order lifting-surface perturbation problem, Equation (3-27). Of course, other investigators realized that such a term occurred for variable pitch propellers but did not examine the consequences of neglecting it for arbitrary pitch distribution. For the example considered, the contribution of this term was as much as 6 percent of the camber ratio determined by the conventional analysis.

In the lifting-line analysis, only propellers without rake and warp were considered. For these propellers, the two-dimensional sections were defined normal to the straight blade-reference line. However, to the order of the approximation considered, they could equally well have been considered as defined on cylinders as was done in the lifting-surface problem.

A method of design based only on the lifting-surface formulation has been discussed. This procedure makes no use of the lifting-line results and would involve greater computing effort since an iteration is appropriate.

Extension of the method utilized in this work to the problem of unsteady flow and shear flow is recommended. In addition, numerical results should be obtained. The numerical results could include wake trajectories for the shed vortex sheet.

APPENDIX A

POTENTIAL FOR LIFTING LINE DERIVED FROM THE BIOT-SAVART LAW

Traditional propeller lifting-line theory (Moriya,[11] Lerbs,[13] Morgan and Wrench,[14]) evaluates the velocity induced by the vortex system from the law of Biot-Savart. The vortex system considered is one for which an individual vortex is an element of circulation of strength $d\Gamma/d\tilde{\omega}$ shed at radius $\tilde{\omega}$; then by the conservation of vorticity this element remains bound in the line and leaves it at the axis of rotation. It is not clear from the literature how to interpret the vortex system when the lifting line extends from a finite radius off the axis to the propeller tip. (However, see Appendix B.)

Lifting-line theory for planar wings, Ashley and Landall,[47] uses a model which consists of an elemental horseshoe vortex of strength Γ. This is composed of two free vortices of equal but opposite strengh a distance Δz apart, joined together at the blade by a bound vortex element of the same strength. Such a system is shown in Figure 8 for a propeller lifting line.
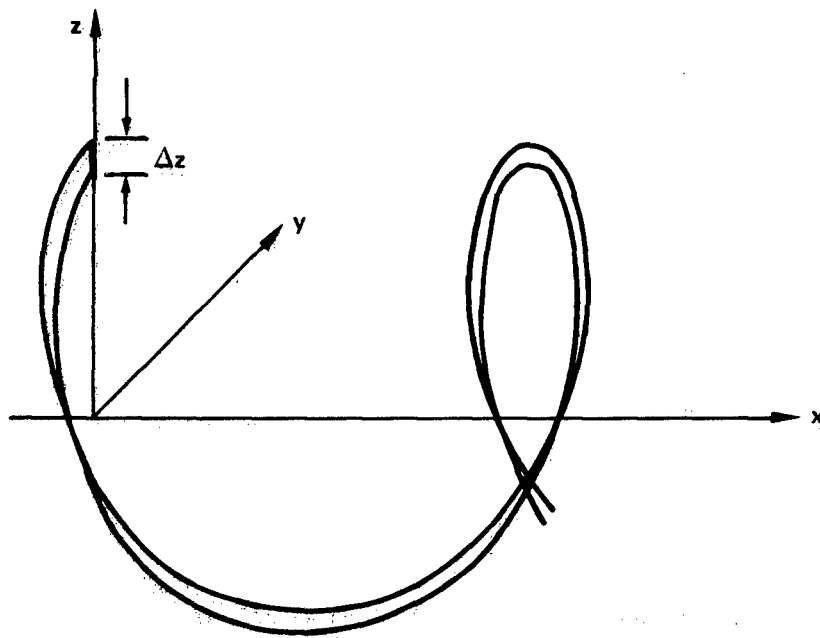
Figure 8 — Vortex Element

A sum of these elements distributed along the radius of the lifting line then approximates the vortex system. In Ashley and Landahl,[47] the potential for elements an infinitesimal distance apart is derived by integrating the potential of a doublet over the length of the element. Here it will be derived[*] from the Biot-Savart Law applied to the element. The path of integration is shown in Figure 9.
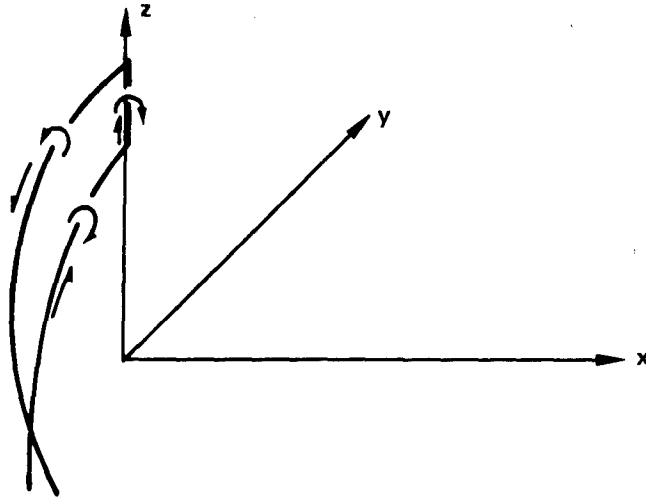
Figure 9 — Path of Integration

Let this path be L. The velocity induced by the element is

$$q = -\frac{\Gamma}{4\pi} \int_L d\underline{\ell} \times \nabla_{\underline{\ell}} \frac{1}{|\underline{r}-\underline{\ell}|} \tag{A1}$$

One of Stokes' theorems for vector integration is

$$\oint_C d\underline{\ell} \times \underline{u} = \iint_S (\underline{n} \times \nabla) \times \underline{u} \, ds \tag{A2}$$

---

[*]See also Lamb[64] and Kochin et al.[44]

[64]Lamb, H., "Hydrodynamics," Sixth Edition, Dover Publications, Inc., New York (1964).

where s is an area bounded by the curve c. Thus

$$\int_L d\underline{\ell} \times \frac{\underline{r}-\underline{\ell}}{|\underline{r}-\underline{\ell}|^3} = \iint_s (\underline{n} \times \nabla_s) \times \frac{\underline{r}-\underline{s}}{|\underline{r}-\underline{s}|^3} \, ds \qquad (A3)$$

where s is the area bounded by L. But

$$(\underline{n} \times \nabla_s) \times \frac{\underline{r}-\underline{s}}{|\underline{r}-\underline{s}|^3} = \left\{ \nabla_s \frac{\underline{r}-\underline{s}}{|\underline{r}-\underline{s}|^3} \right\} \cdot \underline{n} - \underline{n} \left(\nabla_s \frac{\underline{r}-\underline{s}}{|\underline{r}-\underline{s}|^3} \right) \qquad (A4)$$

Hence, since $\nabla \cdot (\underline{r}/r^3) = 0$, there remains

$$(\underline{n} \times \nabla_s) \times \frac{\underline{r}-\underline{s}}{|\underline{r}-\underline{s}|^3} = -\nabla_r \left(\frac{\underline{r}-\underline{s}}{|\underline{r}-\underline{s}|^3} \cdot \underline{n} \right) \qquad (A5)$$

since $\underline{n} = \underline{n}(\underline{s})$ only.

Thus the induced velocity is

$$\underline{q} = \frac{\Gamma}{4\pi} \iint_s -\nabla_r \left(\frac{\underline{r}-\underline{s}}{|\underline{r}-\underline{s}|^3} \cdot \underline{n} \right) ds$$

$$= -\frac{\Gamma}{4\pi} \nabla_r \iint_s \frac{\underline{r}-\underline{s}}{|\underline{r}-\underline{s}|^3} \cdot \underline{n} \, ds \qquad (A6)$$

Hence, by definition, the potential is

$$\phi = -\frac{\Gamma}{4\pi} \iint_s \frac{\underline{r}-\underline{s}}{|\underline{r}-\underline{s}|^3} \cdot \underline{n} \, ds \qquad (A7)$$

See Lamb[64] Equation 4, page 212.

The shed vortex sheet is envisioned as being composed of a radial distribution of these elements so that the distance between elements goes to zero and the width of an element goes to zero. In this limit the vector element of area becomes the negative of that in Equation (2-48):

$$\underline{n} \, ds = -\left(\frac{\partial \underline{\zeta}}{\partial \alpha} \times \frac{\partial \underline{\zeta}}{\partial z_0} \right) dz_0 \, d\alpha$$

and the potential for the total system becomes

$$\phi = \frac{1}{4\pi} \sum_{b=0}^{Z-1} \int_0^R \Gamma(z_0) \, dz_0 \int_{\theta_b}^\infty \frac{\underline{r} - \underline{\zeta}}{|\underline{r} - \underline{\zeta}|^3} \cdot \left(\frac{\partial \underline{\zeta}}{\partial \alpha} \times \frac{\partial \underline{\zeta}}{\partial z_0} \right) da \tag{A8}$$

When the zero-order position vector for the trailing vortex system is substituted into Equation (A8), Equation (4-5) is obtained.

As an application of Equation (A7), the potential of a circulation element for planar wings can be derived. For wings, the approximate location of the lines of constant circulation in the shed vortex sheet is on the x, y-plane at constant y values. Hence

$$\underline{n} \, ds = - \underline{k} \, dx \, \Delta y + 0(\Delta y^2)$$

and

$$\phi = \frac{\Gamma \Delta y}{4\pi} \int_0^\infty \frac{z \, dx_0}{\left[(x-x_0)^2 + (y-y_0)^2 + z^2 \right]^{3/2}} + 0(\Delta y^2)$$

$$= \frac{\Gamma \Delta y}{4\pi} \frac{z}{(y-y_0)^2 + z^2} \left[1 + \frac{x}{\sqrt{x^2 + (y-y_0)^2 + z^2}} \right] \tag{A9}$$

which is Equation (5-35) in Ashley and Landahl.[47] This can be rearranged to give

$$\phi = \frac{\Gamma \Delta y}{4\pi} \frac{z}{(x^2 + (y-y_0)^2 + z^2) - x^2} \frac{(x^2 + (y-y_0^2) + z^2)^{1/2} + x}{(x^2 + (y-y_0)^2 + z^2)^{1/2}}$$

$$+ 0(\Delta y^2)$$

$$= \frac{\Gamma \Delta y}{4\pi} \frac{z}{[x^2 + (y-y_0)^2 + z^2]^{1/2} - x} \frac{1}{[x^2 + (y-y_0)^2 + z^2]^{1/2}}$$

$$+ 0(\Delta y^2) \tag{A10}$$

102

which is the form derived by von Karman and Burgers (p. 128),[65] by Truckenbrodt,[66] and by Friedrichs (Equation 15.4).[1]

Returning to the propeller problem, one obtains Equation (4-5) by substituting the zero-order position vector of curves of constant circulation from Equation (4-3) into Equation (A8). Since only the kernel of Equation (4-5) is of interest, it can be considered alone:

$$G(\underline{r},z_0) = \sum_{b=0}^{Z-1} \int_0^\infty \frac{\underline{r}-\underline{\zeta}}{|\underline{r}-\underline{\zeta}|^3} \cdot \left(\frac{\partial\underline{\zeta}}{\partial a}\times\frac{\partial\underline{\zeta}}{\partial z_0}\right)da \tag{A11}$$

and the zero-order approximation to G is

$$G(\underline{r},z_0) = \sum_{b=0}^{Z-1} \int_0^\infty \left(-z_0\frac{\partial}{\partial x}+\frac{U}{\Omega z_0}\frac{\partial}{\partial\theta}\right)\frac{d\gamma}{r}$$

$$r = \sqrt{(x-\frac{U}{\Omega}\gamma)^2 + \varpi^2 + z_0^2 - 2z_0\,\varpi\cos(\theta-\gamma-\theta_b)} \tag{4-6}$$

A similar integral has been evaluated in the determination of induced velocities at a lifting line. For the induced velocities at the lifting line, Moriya[11] was able to integrate the expression analytically to obtain an infinite series of products of modified Bessel functions. Although the first impression is that replacing an infinite integral by an infinite series is not much of an improvement, Lerbs[13] showed that the series could be approximately summed and thus calculations could be quickly made. An excellent explanation of the integration process for the induced velocities at a lifting line and the numerical approximation to the series is given by Morgan and Wrench.[14] Included in that article is an improved approximation for the series summation which was developed by Wrench.

The rather circuitous method discovered by Moriya[11] will be applied to the integral in Equation (4-6). Unfortunately, the kernel cannot be evaluated at an arbitrary point; however, the form far downstream is found, and it is demonstrated that velocities from this expression are twice those at the lifting line as derived from the Biot-Savart Law, as would be expected.

The expression for $G(\underline{r},z_0)$ is given by Equation (4-6). From the Lipschitz integral, Watson, p.384,[67] one obtains

---

[65]von Karman, T. and J.M. Burgers, "General Aerodynamic Theory-Perfect Fluids," Vol. II of Aerodynamic Theory, edited by W.F. Durand, Springer; also reprinted by Dover Publications, Inc. (1963).

[66]Truckenbrodt, E., "Das Geschwindigkeitspotential der tragenden Fläche bei inkompressibler Strömung," Zeitschrift für angewandte Mathematik und Machanik, Berlin, Vol. 33, pp. 165-173 (1953).

[67]Watson, G.N., "Theory of Bessel Functions," Cambridge University, England (1944).

$$\frac{1}{r} = \int_0^\infty e^{-\left|x - \frac{U}{\Omega}\gamma\right|t} J_0\!\left(t\sqrt{\widetilde{\omega}^2 + z_0^2 - 2z_0\,\widetilde{\omega}\cos(\theta - \gamma - \theta_b)}\right) dt \qquad (A12)$$

From one of the addition theorems, Watson,[67] p. 128,

$$J_0\!\left(t\sqrt{\widetilde{\omega}^2 + z_0^2 - 2z_0\,\widetilde{\omega}\cos(\theta - \gamma - \theta_b)}\right)$$

$$= \sum_{m=0}^\infty k_m\, J_m(t\widetilde{\omega})\, J_m(tz_0)\cos(\theta - a) \qquad (A13)$$

where k_m is Neumann's factor, $(k_m = 0,\ m = 0;\ k_m = 2,\ m > 0)$. If one assumes uniform convergence for the integral, the order of integration can be switched and one obtains

$$G(\underline{r},\, z_0) = \sum_{m=0}^\infty \int_0^\infty k_m\, J_m(t\omega)\, J_m(tz_0)\,\mathscr{L}_m(\underline{r},z_0,t)\, dt \qquad (A14)$$

where

$$\mathscr{L}_m = \sum_{b=0}^{Z-1}\left(-z_0\frac{\partial}{\partial x} + \frac{U}{\Omega z_0}\frac{\partial}{\partial \theta}\right)\int_0^\infty e^{\pm\left(x - \frac{U}{\Omega}\gamma\right)t}\cos m(\theta - \theta_b - \gamma)\, d\gamma \qquad (A15)$$

Two cases occur, one for $x < 0$ and one for $x > 0$. For $x < 0$ the positive sign is used. For $x > 0$, two regions exist, one for $\gamma \leqslant \dfrac{\Omega x}{U}$ and one when it is greater. Only the case for $x > 0$ will be considered since it permits the form of the potential far downstream to be obtained. Thus for $x > 0$

$$\mathscr{L}_m(\underline{r},z_0,t) = \sum_{b=0}^{Z-1}\left(-z_0\frac{\partial}{\partial x} + \frac{U}{\Omega z_0}\frac{\partial}{\partial \theta}\right)\left\{ e^{-xt}\int_0^{\frac{\Omega x}{U}} e^{\frac{U\gamma t}{\Omega}}\cos m(\theta - \gamma - \theta_b)\, d\gamma \right.$$

$$\left. + e^{xt}\int_{\frac{\Omega x}{U}}^\infty e^{-\frac{U\gamma t}{\Omega}}\cos m(\theta - \gamma - \theta_b)\, d\gamma \right\} \qquad (A16)$$

The integrals appearing in Equation (A16) can be found by integrating by parts until the same expression occurs again and then by rearranging the equation. The resulting expression for $\mathscr{L}_m$ is

$$
\mathscr{L}_m (r, z_0, t) = \sum_{b=0}^{Z-1} \left\{ \frac{e^{-xt}\dfrac{Ut}{\Omega}}{\left(\dfrac{Ut}{\Omega}\right)^2 + m^2} \left[\left(\frac{m^2}{z_0 t} - z_0 t \right) \cos m\,(\theta - \theta_b) \right. \right.
$$

$$
\left. + \left(\frac{z_0 \Omega m}{U} + \frac{Um}{z_0 \Omega} \right) \sin m\,(\theta - \theta_b) \right] - 2 \left(\frac{z_0 \Omega}{U} + \frac{Um}{\Omega z_0} \right) \frac{\dfrac{Ut}{\Omega}}{\left(\dfrac{Ut}{\Omega}\right)^2 + m^2} \cdot
$$

$$
\left. \sin \left(\theta - \frac{\Omega x}{U} - \theta_b \right) \right\}
\tag{A17}
$$

Thus

$$
G(r, z_0) = \sum_{m=0}^{\infty} \sum_{b=0}^{Z-1} \int_0^{\infty} k_m \, J_m(t\widetilde{\omega}) \, J_m(tz_0) \frac{Ut/\Omega}{\left(\dfrac{Ut}{\Omega}\right)^2 + m^2} \left\{ e^{-xt} \left(\frac{m^2}{z_0 t} - z_0 t \right) \cdot \cos m\,(\theta - \theta_b) \right.
$$

$$
\left. + \left(\frac{z_0 \Omega m}{U} + \frac{Um}{\Omega z_0} \right) \left(e^{-xt} \sin (\theta - \theta_b) - 2 \sin m \left(\theta - \frac{\Omega x}{U} - \theta_b \right) \right) \right\} dt
\tag{A18}
$$

The portion of the integral involving the exponential disappears when the form far downstream is examined. The remaining portion of the integral can be integrated using a result on page 429 of Watson.[67] The resulting expression far downstream is

$$
G_\infty(r, z_0) \sim -\frac{2\Omega}{U} \sum_{b=0}^{Z-1} \sum_{m=0}^{\infty} m k_m \left(\frac{z_0 \Omega}{U} + \frac{U}{\Omega z_0} \right) \sin m \left(\theta - \frac{Ux}{\Omega} - \theta_b \right) A_m
\tag{A19}
$$

where A_m is a combination of modified Bessel Functions

$$A_m = \begin{cases} I_m \left(\dfrac{\Omega \widetilde{\omega} m}{U}\right) K_m \left(\dfrac{\Omega z_0 m}{U}\right) & z_0 > \widetilde{\omega} \\[2em] I_m \left(\dfrac{\Omega z_0 m}{U}\right) K_m \left(\dfrac{\Omega \widetilde{\omega} m}{U}\right) & z_0 < \widetilde{\omega} \end{cases} \tag{A20}$$

The expression for ϕ far downstream is

$$\phi \sim \frac{1}{4\pi} \int_0^R \Gamma(z_0) \, G_\infty(\underline{r}, z_0) \, dz_0 \tag{A21}$$

which can be integrated by parts to obtain

$$\phi \sim \frac{1}{4\pi} \int_0^R \frac{d\Gamma}{dz_0} \left(\int^{z_0} G(\underline{r}, \xi) \, d\xi \right) dz_0$$

After some manipulation, one finds

$$\phi \sim \frac{\Omega}{2\pi U} \int_0^R z_0 \frac{d\Gamma}{dz_0} \sum_{b=0}^{Z-1} \sum_{m=0}^{\infty} k_m \sin m \left(\theta - \frac{\Omega x}{U} - \theta_b \right) A'_m \, dz_0 \tag{A22}$$

where

$$A'_m = \begin{cases} I_m \left(\dfrac{\Omega \widetilde{\omega} m}{U}\right) k'_m \left(\dfrac{\Omega z_0 m}{U}\right) & z_0 > \widetilde{\omega} \\[2em] I'_m \left(\dfrac{\Omega z_0 m}{U}\right) k_m \left(\dfrac{\Omega \widetilde{\omega} m}{U}\right) & z_0 < \widetilde{\omega} \end{cases} \tag{A23}$$

The expression for the axial velocity, $\dfrac{\partial \phi}{\partial x}$, at $\theta \to 0$, $x \to 0$ can be easily obtained. After summing over b, the expression is

$$u_a(z) = -\frac{Z \, \Omega/U}{2\pi} \int_0^R \frac{d\Gamma}{dz_0} \, dz_0 \sum_{m=0}^{\infty} k_m \frac{mZ \, \Omega z_0}{U} A'_{mZ} \tag{A24}$$

This is twice the value of the axial velocity at the lifting line as determined from the Biot-Savart Law, as expected.

An expression for the portion of the potential involving the exponential integral can be obtained by expressing the Bessel Functions as infinite series. The integral then involves a triple infinite summation of terms with an integral now of the form

$$\int_0^\infty \frac{e^{-a\xi}}{\xi^2 + q^2} \, \xi^\beta \, d\xi$$

This expression can be integrated; see Gradshteyn and Ryzhik p. 313, 3.356(1) and (2)[68] in terms of sine and cosine integrals plus another finite summation. The resulting expression is quite cumbersome and is therefore not given. No use was made of it in the analysis.

[68]Gradshteyn, I.S. and I.M. Ryzhik, "Tables of Integrals Series and Products," (Translation of the Fourth Edition, Edited by A. Jeffrey), Academic Press, Inc., New York (1965).

APPENDIX B
INTERMEDIATE EXPANSION OF OUTER POTENTIAL

Equation (4-32) states the second-order potential for the outer flow. This expression is valid for a fixed point in the flow field as the parameter $\bar{\epsilon}$, equals chord-to-diameter ratio, goes to zero. Thus the outer flow consists of a singularity system distributed along the radial lines θ_b, $0 \leqslant \widetilde{\omega} \leqslant R$.

There are only two essential systems of singularities: one from the circulation distribution and one from the dipole distribution. The second-order contribution to the circulation will be included in the single integral involving the circulation. The two integrals will be ϕ_1 and ϕ_2, where ϕ_1 is given by Equation (4-5), and ϕ_2 is given by Equation (4-33). The ϕ_1 term will be considered first.

Since considerable difficulty was encountered in an attempt to expand the potential function for the lifting-line, the velocity expression was expanded and from it the expansion for the potential was constructed.

In Appendix A, the velocity from the Biot-Savart Law was shown to be derivable from a potential. Now it is convenient to return to the Biot-Savart Law in order to find the intermediate expansion. However, some rearrangement is in order before the appropriate form for expansion is obtained. The vortex system is envisioned as composed of a distribution of elements shown in Figure 8 along each of the lifting lines. The width between the free trailing portions of a vortex element is constant for all elements, and the elements are infinitesimally close together. The path $\mathscr{L}$ consists of the segment along the θ_b lines and the two free-trailing paths. Two adjacent trailing elements then have a common path of integration. Hence the total induced velocity for N of these elements is

$$\underline{q} = \sum_{b=0}^{Z-1} \left\{ -\sum_{n=1}^{N} \frac{\Gamma_n}{4\pi} \int_{z_n}^{z_{n+1}} \underline{e} \widetilde{\omega} (\theta_b) \mathsf{X} \frac{\underline{r} - z_0 \underline{e} \widetilde{\omega} (\theta_b)}{|\underline{r} - z_0 \underline{e} \widetilde{\omega} (\theta_b)|^3} d z_0 \right.$$
$$\left. - \sum_{n=0}^{N} \frac{\Gamma_n - \Gamma_{n+1}}{4\pi} \int_0^{\infty} d\underline{\ell} \mathsf{X} \frac{\underline{r} - \underline{\ell}_n}{|r - \underline{\ell}_n|^3} \right\} \tag{B1}$$

where $\Gamma_0 = \Gamma_{N+1} = 0$

$\underline{\ell}_n$ is the common path between the adjacent n and $n+1$ trailing vortices.

In the limit as $\Delta\widetilde{\omega} \rightarrow 0$, and the distribution of circulation becomes continuous with $\Gamma(0) = \Gamma(R) = 0$, the expression for the velocity becomes

$$q = \frac{1}{4\pi} \sum_{b=0}^{Z-1} \int_0^R \Gamma(z_0) \frac{r - z_0 \, \underline{e} \, \widetilde{\omega}(\theta_b)}{|r - z_0 \, \underline{e} \, \widetilde{\omega}(\theta_b)|^3} X \, \underline{e} \, \widetilde{\omega}(\theta_b) \, d z_0$$

(B2)

$$+ \frac{1}{4\pi} \sum_{b=0}^{Z-1} \int_0^R \frac{d \, \Gamma(z_0)}{d z_0} \, d z_0 \int_{P.P.}^{\infty} \frac{r - \underline{\zeta}}{|r - \underline{\zeta}|^3} X \, d \, \underline{\zeta}$$

Hence the first-order velocity distribution results when $\Gamma = \bar{\epsilon}\Gamma^{(1)}(z_0) + \cdots$ and $\underline{\zeta} = \underline{\zeta}_0 + \cdots$ are substituted into this equation. Since

$$\underline{\zeta}_0 = z_0 \, \underline{e} \, \widetilde{\omega}(\theta) + \frac{U}{\Omega}(\theta - \theta_b) \, \underline{i}$$

(B3)

one finds

$$d \, \underline{\zeta}_0 = z_0 \frac{d \, \underline{e} \, \widetilde{\omega}}{d\theta} \, d\theta + \frac{U}{\Omega} \, d\theta \, \underline{i}$$

$$= (z_0 \, \underline{e}_\theta + \frac{U}{\Omega} \, \underline{i}) \, d\theta$$

and since

$$|r - \underline{\zeta}_0| = \sqrt{\left\{ x - \frac{U}{\Omega}(\alpha - \theta_b) \right\}^2 + \widetilde{\omega}^2 + z_0^2 - 2 \widetilde{\omega} z_0 \cos(\theta - \alpha)}$$

one finds

$$(r - \underline{\zeta}_0) X \, d \, \underline{\zeta}_0 = \left[\left\{ -\frac{U}{\Omega}(y + z_0 \sin \alpha) - z_0 \cos \alpha \left(x - \frac{U}{\Omega}(\alpha - \theta_b) \right) \right\} \, \underline{k} \right.$$

$$+ \left\{ \frac{U}{\Omega}(z - z_0 \cos \alpha) + z_0 \sin \alpha \left(x - \frac{U}{\Omega}(\alpha - \theta_b) \right) \right\} \, \underline{j}$$

$$+ \left. \left\{ z_0 \, \widetilde{\omega} \cos(\theta - \alpha) - z_0^2 \right\} \, \underline{i} \right] d\alpha$$

(B3)

Hence

110

$$\underline{q} = \frac{\bar{\epsilon}}{4\pi} \sum_{b=0}^{Z-1} \int_0^R \Gamma \frac{-\tilde{\omega} \sin(\theta - \theta_b)\underline{i} - x \cos \theta_b \underline{j} - x \sin \theta_b \underline{k}}{[x^2 + (y + z_0 \sin \theta_b)^2 + (z - z_0 \cos \theta_b)^2]^{3/2}} d z_0$$

$$+ \frac{\bar{\epsilon}}{4\pi} \sum_{b=0}^{Z-1} \int_0^R d z_0 \frac{d\Gamma}{dz_0} \int_{\theta_b}^\infty \frac{(\underline{r} - \underline{\zeta}_0) \times \frac{\partial \underline{\zeta}_0}{\partial \alpha} d\alpha}{[(x - \frac{U}{\Omega}(\alpha - \theta_b))^2 + \tilde{\omega}^2 + z_0^2 - 2\tilde{\omega} z_0 \cos(\theta - \alpha)]^{3/2}}$$

(B4)

Consider first the expression from the bound vorticity. To find the intermediate expansion one substitutes the intermediate variables into the expression and rearranges it into an asymptotic sequence. By inspection of the denominator, one can see that a Taylor expansion is appropriate, except for the $b = 0$ lifting line. Thus

$$\underline{q}_B (g \bar{\bar{x}}, g \bar{\bar{y}}, z) = \frac{\bar{\epsilon}}{4\pi} \int_0^R \Gamma(z_0) - \frac{\bar{\bar{x}} g \underline{j} + g \bar{\bar{y}} \underline{i}}{[g^2(\bar{x}^2 + \bar{y}^2) + (z - z_0)^2]^{3/2}} d z_0$$

$$+ \frac{\bar{\epsilon}\underline{i}}{4\pi} \sum_{b=1}^{Z-1} \int_0^R \Gamma(z_0) \frac{z \sin \theta_b \, d z_0}{[(z_0 \sin \theta_b)^2 + (z - z_0 \cos \theta_b)^2]^{3/2}}$$

$$+ 0 (\bar{\epsilon}g)$$

(B5)

By symmetry the second term cancels, i.e., $\sin \theta_1 = - \sin \theta_{Z-1}$, etc. The first integral can be expanded by a binomial series in each region bordered by $(z - z_0)^2 = g^2 (\bar{x}^2 + \bar{y}^2)$. The result is given by Ogilvie, Equation (2-43)[54]

$$\underline{q}_B (g \bar{\bar{x}}, g \bar{\bar{y}}, z) = \frac{\bar{\epsilon}}{2\pi g} \Gamma(z) - \frac{\bar{\bar{x}} \underline{j} + \bar{\bar{y}} \underline{i}}{\bar{\bar{x}}^2 + \bar{\bar{y}}^2} + 0(\bar{\epsilon}g)$$

(B6)

Temporarily we convert to outer variables.

$$\underline{q}_B (x, y, z) = \frac{\bar{\epsilon}\Gamma(z)}{2\pi} \frac{y \underline{i} - x \underline{j}}{x^2 + y^2} + 0(\bar{\epsilon})$$

(B7)

and note that $\nabla \tan^{-1} \frac{y}{x} = \frac{y \underline{i} - x \underline{j}}{x^2 + y^2}$, hence

$$q_B \, (x, y, z) = - \frac{\bar{\epsilon}\Gamma(z)}{2\pi} \, \nabla \, tan^{-1}\frac{y}{x} + 0(\bar{\epsilon}) \qquad \text{(B8)}$$

From which one can conclude that, to within a function of z, the expansion of ϕ contains a term:

$$\phi_B \, (g\,\bar{\bar{x}}, \, g\,\bar{\bar{y}}, \, z) = - \frac{\bar{\epsilon}\Gamma}{2\pi} \, tan^{-1}\frac{\bar{\bar{y}}}{\bar{\bar{x}}} + 0(\bar{\epsilon}g^2) \qquad \text{(B9)}$$

due to the bound vortex.

Now the second part of the expression, the velocity due to the trailing vortices, must be determined. Letting $\gamma = a - \theta_b$, one finds

$$q_T \, (x, y, z) = \frac{\bar{\epsilon}}{4\pi} \sum_{b=0}^{Z-1} \int_0^R \frac{d\Gamma}{dz_0} \, d z_0 \int_0^\infty I \, d\gamma \qquad \text{(B10)}$$

$$I = \left\{ \frac{\begin{aligned} & (z_0 \, \widetilde{\omega} \cos{(\theta - \gamma - \theta_b)} - z_0^2) \, \underline{i} \\ & + \, [\frac{U}{\Omega}(z - z_0 \cos{(\gamma + \theta_b)} + z_0 \sin{(\gamma + \theta_b)} \, (x - \frac{U}{\Omega} \, \gamma)] \, \underline{j} \\ & - \, [\frac{U}{\Omega} \, (y + z_0 \sin{(\gamma + \theta_b)} + z_0 \cos{(\gamma + \theta_b)} \, (x - \frac{U}{\Omega} \, \gamma)] \, \underline{k} \end{aligned}}{[\left(x - \frac{U}{\Omega}\right)^2 + \left(y + z_0 \sin{(\gamma + \theta_b)}\right)^2 + (z - z_0 \cos{(\gamma + \theta_b)})^2]^{3/2}} \right.$$

Since the denominator is of positive definite form, it has a zero only for $x = \gamma = \theta_b = y = 0$, $z = z_0$. As shown by Moriya[11] and Morgan and Wrench,[14] the velocity vector, as $x = g\,\bar{\bar{x}}$ and $y = g\,\bar{\bar{y}}$ go to zero, is found to be

$$q_T \, (g\,\bar{\bar{x}}, \, g\,\bar{\bar{y}}, \, z) = \bar{\epsilon} u_a^{(1)} \, \underline{i} + \bar{\epsilon} u_t^{(1)} \, \underline{j} + \bar{\epsilon} u_z^{(1)} \, \underline{k} + H.O.T. \qquad \text{(B11)}$$

where

$$u_i^{(1)} \, (z) = \frac{1}{4\pi} \sum_{b=0}^{Z-1} \int_0^R \frac{d\Gamma}{dz_0} d z_0 \int_0^\infty \frac{H_i \, (z, z_0, \gamma) \, d\gamma}{[\left(\frac{U\gamma}{\Omega}\right)^2 + z^2 + z_0^2 - 2 z z_0 \cos{(\gamma + \theta_b)}]^{3/2}}$$

112

with

$$H_a (z, z_0, \gamma) = z z_0 \cos (\gamma + \theta_b) \quad z_0^2$$

$$H_t (z, z_0, \gamma) = \frac{U}{\Omega} [z - z_0 \cos (\gamma + \theta_b) - \gamma z_0 \sin (\gamma + \theta_b)]$$

$$H_z (z, z_0, \gamma) = - \frac{U z_0}{\Omega} [\sin (\gamma + \theta_b) - \gamma \cos (\gamma + \theta_b)] z_0$$

and where the bar through the integral means the singular point is excluded. Except for notation, these are identical with the expressions given in Equations (11) through (13) of Morgan and Wrench,[14] Equation (7) of Moriya[11] and the equations in Appendix 2 of Lerbs.[13] As shown by these authors, when U/Ω is constant, the infinite integral can be performed analytically for the axial and tangential component of velocity.

From the previously described form of the velocity vector in the intermediate region, one concludes that the expansion for the potential due to the trailing vortices has the terms

$$\phi_T (g \bar{\bar{x}}, g \bar{\bar{y}}, z) = \bar{\epsilon} g (\bar{\bar{x}} u_a^{(1)} + \bar{\bar{y}} u_t^{(1)}) + \bar{\epsilon} \int^z u_z^{(1)} \, dz \tag{B12}$$

Hence the expansion for the potential due to the vortex system has the following form

$$\bar{\epsilon} \phi_1 (g \bar{\bar{x}}, g \bar{\bar{y}}, z) = \phi_B + \phi_T$$

$$= F (z; \bar{\epsilon}) - \frac{\bar{\epsilon} \Gamma(z)}{2\pi} \tan^{-1} \frac{\bar{\bar{y}}}{\bar{\bar{x}}}$$

$$+ \bar{\epsilon} g (\bar{\bar{x}} u_a^{(1)} + \bar{\bar{y}} u_t^{(1)}) + H.O.T. \tag{B13}$$

The function $F(z;\bar{\epsilon})$ contains other unknown integration constants which are functions of z in addition to the integral of $u_z^{(1)}$. The construction of the potential expansion from the velocity components is not required since the matching could be done with the velocity components but it is simpler to work with the one potential expansion rather than the i and j velocity components.

The expression for ϕ_2 valid in the intermediate region is now to be found. For the expansion of this expression, it is not necessary to examine velocity components, since a direct expansion of the potential is possible. Substitution of intermediate variables in the expression for ϕ_2 gives

$$\phi_2 (g \bar{\bar{x}}, g \bar{\bar{y}}, z) = \frac{1}{4\pi} \sum_{b=0}^{Z-1} \int_0^R \frac{\left[g \bar{\bar{x}} \mu_1 (z_0) + (g \bar{\bar{y}} + z_0 \sin \theta_b) \mu_2 (z_0) \right] d z_0}{[(g \bar{\bar{x}})^2 + (g \bar{\bar{y}} + z_0 \sin \theta_b)^2 + (z - z_0 \cos \theta_b)^2]^{3/2}} \tag{B14}$$

113

For $b \neq 0$, the expansion is regular, and a Taylor expansion is possible. The term independent of g in the expansion is

$$\frac{1}{4\pi} \sum_{b=1}^{Z-1} \int_0^R \frac{z_0 \sin \theta_b \, \mu_2 (z_0) \quad d z_0}{[(z_0 \sin \theta_b)^2 + (z - z_0 \cos \theta_b)^2]^{3/2}}$$

Because of the symmetry of the lifting lines, the summation of this term is zero. The term corresponding to $b=0$ has the following expansion; see Ogilvie,[54] Equation (2.43)

$$\frac{1}{4\pi} \int_0^R \frac{\left[g \bar{\bar{x}} \mu_1 + g \bar{\bar{y}} \mu_2 \right] d z_0}{[(g \bar{\bar{x}})^2 + (g \bar{\bar{y}})^2 + (z - z_0)^2]^{3/2}} = \frac{1}{2\pi g} \frac{\bar{\bar{x}} \mu_1(z) + \bar{\bar{y}} \mu_2(z)}{\bar{\bar{x}}^2 + \bar{\bar{y}}^2}$$

$$+ H.O.T. \tag{B15}$$

Hence

$$\bar{\epsilon}^2 \phi_2 (g \bar{\bar{x}}, g \bar{\bar{y}}, z) = \frac{\bar{\epsilon}^2}{2\pi g} \frac{\bar{\bar{x}} \mu_1(z) + \bar{\bar{y}} \mu_2(z)}{\bar{\bar{x}}^2 + \bar{\bar{y}}^2} + H.O.T. \tag{B16}$$

Combining this with the expansion of the vortex terms, one finds that the expansion of the potential in the intermediate region has the form:

$$\phi (g \bar{\bar{x}}, g \bar{\bar{y}}, z) = F_0 (z; \bar{\epsilon}) - \bar{\epsilon} \frac{\Gamma(z)}{2\pi} \tan^{-1} \frac{\bar{\bar{y}}}{\bar{\bar{x}}} +$$

$$+ \bar{\epsilon} g (\bar{\bar{x}} u_a^{(1)} + \bar{\bar{y}} u_t^{(1)}) + \tag{4-34}$$

$$+ \frac{\bar{\epsilon}^2}{2\pi g} \frac{\bar{\bar{x}} \mu_1(z) + \bar{\bar{y}} \mu_2(z)}{\bar{\bar{x}}^2 + \bar{\bar{y}}^2} + H.O.T.$$

This is the expression stated in Equation (4-34).

114

REFERENCES

1. Friedrichs, K.O., "Special Topics in Fluid Dynamics," New York University (1953); also published by Gordon and Breach, New York (1966).

2. Van Dyke, M., "Lifting Line Theory as a Singular Perturbation Problem," Archiwum Mechaniki Stosowanej, Vol. 3, No. 16, pp. 601-614 (1964).

3. Van Dyke, M., "Perturbation Methods in Fluid Mechanics," Academic Press, Inc., New York (1964).

4. Kaplun, S., "Fluid Mechanics and Singular Perturbations," Edited by P.A. Lagerstrom, et al., Academic Press, Inc., New York (1967).

5. Cole, J.D., "Perturbation Methods in Applied Mathematics," Blaisdell (1968).

6. Prandtl, L., "Application of Modern Hydrodynamics to Aeronautics," National Advisory Committee for Aeronautics Report 116 (1921).

7. Thurber, J.K., "An Asymptotic Method for Determining the Lift Distribution of a Swept-Back Wing of Finite Span," Communications on Pure and Applied Mathematics, Vol. 18, pp. 733-756 (1965).

8. Rotta, N.R., "The Non-Planar, Moderate Aspect Ratio, Subsonic Wind," Ph.D. Thesis, New York University, University Microfilms 69-4576 (1968).

9. Hille, R., "Bestimmung der Dickenlinie von Propellerflügelprofilen bei vorgegebener Druckverteilung," Report 262 of the Institut für Schiffbau der Universität Hamburg, West Germany (1970).

10. Goldstein, S., "On the Vortex Theory of Screw Propellers," Procedure Royal Society of London, Series A, Vol. 123, pp. 440-465 (1929).

11. Moriya, T., "On the Integration of Biot-Savart's Law in Propeller Theory," (in Japanese), Journal of the Society for Aeronautical Science, Japan, Vol. 9, No. 89, of 1015-1020 (1942); English translation in Selected Scientific and Technical Papers by Tomijiro Moriya, Moriya Memorial Committee, University of Tokyo, Japan, pp. 74-80 (1959).

12. Kawada, S., "Induced Velocity by Helical Vortices," Journal of Aeronautical Sciences, Vol. 3, pp. 86-87 (1936).

13. Lerbs, H.W., "Moderately Loaded Propellers with a Finite Number of Blades and an Arbitrary Distribution of Circulation," Society of Naval Architects and Marine Engineers Transactions, Vol. 60, pp. 73-123 (1952).

14. Morgan, W.B. and J.W. Wrench, "Some Computational Aspects of Propeller Design," Methods of Computational Physicis, No. 4, pp. 301-331, Academic Press, Inc., New York (1965).

15. Ludwieg, H. and I. Ginzel, "Zur Theorie der Breitblattschraube," Aerodynamische Versuchsanstalt, Göttingen, Report 44/A/08 (1944); see Ginzel, G.I., "Theory of the Broad-Bladed Propeller," Aeronautical Research Council, Current Papers 208 (1955).

16. Strscheletzky, M., "Hydrodynamische Grundlagen zur Berechnung der Schiffsschrauben," Verlag G. Braun, Karlsruhe, West Germany (1950).

17. Strscheletzky, M., "Berechnungskurwen für dreiflugelige Schiffsschrauben," Verlag G. Braun, Karlsruhe, West Germany (1955).

18. Yamazaki, R., "A Study on Screw Propellers," Memoirs of the Faculty of Engineering, Kyushu University, Japan, Vol. 19, No. 1, pp. 1-75 (1960).

19. Yamazaki, R., "On the Theory of Screw Propellers," Fourth Symposium on Naval Hydrodynamics (1962).

20. Yamazaki, R., "On the Theory of Screw Propellers," Memoirs of the Faculty of Engineering, Kyushu University, Japan, Vol. 23, No. 2, pp. 97-112 (1963); corrected version of 1962 paper.

21. Yamazaki, R., "On the Theory of Screw Propellers in Non-Uniform Flows," Memoirs of the Faculty of Engineering, Kyushu University, Japan, Vol. 25, No. 2, pp. 107-174.

22. Yamazaki, R., "On the Propulsion Theory of Ships in Still Water (Introduction)," Memoirs of the Faculty of Engineering, Kyushu University, Japan, Vol. 27, No. 4, pp. 187-220 (1968).

23. Yamazaki, R., "Theory of Unsteady Propeller Forces," Seventh Symposium on Naval Hydrodynamics, Rome (1968).

24. Yamazaki, R., "On the Theory of Unsteady Propeller Forces," Memoirs of the Faculty of Engineering, Kyushu University, Japan, Vol. 28, Vol. 3, pp. 157-206 (1969).

25. Sparenberg, J.A., "Application of Lifting Surface Theory to Ship Screws," International Shipbuilding Progress, Vol. 7, No. 67, pp. 99-106 (1960).

26. Kerwin, J.E., "The Solution of Propeller Lifting Surface Problems by Vortex Lattice Methods," Massachusetts Institute of Technology, Naval Architecture Department Report (June 1961).

27. Kerwin, J.E., "Linearized Theory for Propellers in Steady Flow," Massachusetts Institute of Technology, Naval Architecture Department Report (1963).

28. Kerwin, J.E. and R. Leopold, "Propeller Incidence Correction Due to Blade Thickness," Journal of Ship Research, Vol. 7, No. 2, pp. 1-6 (1963).

29. Kerwin, J.E. and R. Leopold, "A Design Theory for Subcavitating Propellers," Society of Naval Architects and Marine Engineers Transactions, Vol. 72, pp. 294-335 (1964).

30. Pien, P.C., "The Calculation of Marine Propellers Based on Lifting Surface Theory," Journal of Ship Research, Vol. 5, No. 2, pp. 1-14 (1961).

31. Pien, P.C. and J. Strom-Tejsen, "A General Theory for Marine Propellers," Seventh Symposium on Naval Hydrodynamics, Rome (1968).

32. Hanaoka, T., "Hydrodynamics of an Oscillating Screw Propeller," Fourth Symposium on Naval Hydrodynamics (1962).

33. Murray, M.T., "Propeller Design and Analysis by Lifting Surface Theory," International Shipbuilding Progress, Vol. 14, No. 160, pp. 433-451 (1967).

34. Wu, T.Y., "Some Recent Developments in Propeller Theory," Schiffstechnik, Vol. 12, No. 60, pp. 1-11 (1965).

35. Isay, W.H., "Propellertheorie, Hydrodynamische Probleme," Springer-Verlag, Berlin (1964).

36. Isay, W.H., "Moderne Probleme der Propellertheorie, Springer-Verlag, Berlin (1970).

37. Cox, G.G., "State-of-the-Art for Subcavitating Propeller Design Methods," Appendix II of the Report of the Propeller Committee, 12th International Towing Tank Conference, Rome (1969).

38. Kerwin, J.E., "Machine Computation of Marine Propeller Characteristics," International Shipbuilding Progress, Vol. 6, No. 60, pp. 343-354 (1959).

39. Isay, W.H. and R. Armonat, "Zur Berechnung der Potentialtheoretischen Druckverteilung am Flügelblatt eines Propellers," Schiffstechnik, Vol. 13, No. 67, pp. 75-89 (1966).

40. Sugai, K., "Hydrodynamics of Screw Propellers Based on a New Lifting Surface Theory," Selected Papers from the Journal of the Society of Naval Architects of Japan, Vol. 4, Tokyo, pp. 96-106 (1970).

41. Tsakonas, S. and W.R. Jacobs, "Propeller Loading Distributions," Journal of Ship Research, Vol. 13, No. 4, pp. 237-257 (1969).

42. Armonat, R., "Untersuchung der Druckvertailung eines Propellers unter Berücksichtigung grenzschichthedingter Massstabseffekte," Schiffstechnik, Vol. 16, No. 81, pp. 41-54 (1969).

43. Wills, A.P., "Vector Analysis with an Introduction to Tensor Analysis," Dover Publications, Inc., New York (1958).

44. Kochin, N.E. et al., "Theoretical Hydromechanics," (Translation of Fifth Russian Edition), Interscience Publications, Inc., New York (1964).

45. Tychonov, A.N. and A.A. Samarski, "Partial Differential Equations of Mathematical Physics," Vol. 1, Holden-Day, Inc., San Francisco, Calif. (1964).

46. Mangler, K.W., "Improper Integrals in Theoretical Aerodynamics," Aeronautical Research Council, Current Papers 94 (1952).

47. Ashley, H. and M. Landahl, "Aerodynamics of Wings and Bodies," Addison-Wesley Publishing Co., Inc., Reading, Mass. (1965).

48. Milne-Thomson, L.M., "Theoretical Hydrodynamics," Fifth Edition, The Macmillan Company, New York (1968).

49. Ciolkowski, S.I., "The Swept-Back Wing," Ph.D. Thesis, New York University, University Microfilms 24,694 (1955).

50. Cummings, D., "Vortex Interactions in a Propeller Wake," Massachusetts Instutute of Technology, Naval Architecture Department Report 68-12 (Jun 1968).

51. Glauert, H., "Airplane Propellers," Division L, Aerodynamic Theory, Edited by W.F. Durand, J. Springer, 169-360 (1935); also published by Dover Publications, Inc., New York (1963).

52. Germain, P., "Recent Evolution in Problems and Methods in Aerodynamics," Journal of the Royal Aeronautical Society, Vol. 71, No. 682, pp. 673-691 (1967).

53. Thwaites, B., "Incompressible Aerodynamics," Oxford University Press, England (1962).

54. Ogilvie, T.F., "Singular Perturbation Problems in Ship Hydrodynamics," University of Michigan, Department of Naval Architecture, Report 096 (Oct 1970).

55. Erdélyi, A., "Asymptotic Expansions," Dover Publications, Inc., New York (1956).

56. Erickson, J.C. et al., "A Theory for VTOL Propeller Operation in a Static Condition," Curtiss-Wright Corporation, Caldwell, N.J. (Oct 1965).

57. Hough, G.R. and D.E. Ordway, "The Generalized Actuator Disk," Developments in Theoretical and Applied Mechanics, Pergamon Press, Inc., New York, Vol. II, pp. 317-336 (1965).

58. Cheng, H.M., "Hydrodynamic Aspect of Propeller Design Based on Lifting-Surface Theory— Part 1—Uniform Chordwise Load Distribution," NSRDC Report 1802 (1964).

59. Miller, M.L., "Experimental Determination of Unsteady Propeller Forces," Seventh Symposium on Naval Hydrodynamics, Rome (1968).

60. Boswell, R., "Design, Cavitation Performance, and Open-Water Performance of a Series of Research Skewed Propellers," NSRDC Report 3339 (1971).

61. Morgan, W.B. et al., "Propeller Lifting Surface Corrections," Society of Naval Architects and Marine Engineers Transactions, Vol. 76, pp. 309-347 (1968).

62. Hill, J.C., "The Design of Propellers," Society of Naval Architects and Marine Engineers Transactions, pp. 143-192 (1949).

63. Johnsson, C.A., "Comparison of Propeller Design Techniques," Fourth Symposium on Naval Hydrodynamics (1962).

64. Lamb, H., "Hydrodynamics," Sixth Edition, Dover Publications, Inc., New York (1964).

65. von Karman, T. and J.M. Burgers, "General Aerodynamic Theory-Perfect Fluids," Vol. II of Aerodynamic Theory, Edited by W.F. Durand, Springer; also reprinted by Dover Publications, Inc (1963).

66. Truckenbrodt, E., "Das Geschwindigkeitspotential der tragenden Flache bei inkompressibler Strömung," Zeitschrift für angewandte Mathematik und Mechanik, Berlin, Vol. 33, pp. 165-173 (1953).

67. Watson, G.N., "Theory of Bessel Functions," Cambridge, Mass. (1944).

68. Gradshteyn, I.S. and I.M. Ryzhik, "Tables of Integrals Series and Products," (Translation of Fourth Edition, Edited by A. Jeffrey), Academic Press, Inc., New York (1965).

INITIAL DISTRIBUTION

Copies		Copies	
2	CHONR	1	NAVSHIPYD Bremerton
	1 Fluid Dynamics (Code 438)	1	NAVSHIPYD Charleston
	1 Sys & Res Gp (Code 492)	1	NAVSHIPYD Long Beach
1	NRL	1	NAVSHIPYD Philadelphia
1	ONR Boston	1	NAVSHIPYD Portsmouth
1	ONR Chicago	8	NAVSEC
1	ONR Pasadena		1 SEC 6100
1	ONR San Francisco		2 SEC 6110
1	USNA		1 SEC 6140
1	USNPGSCOL, Monterey		2 SEC 6144
1	USNROTC		2 SEC 6148
1	NAVWARCOL	1	NAVSEC Norfolk (Code 6660)
20	NAVSHIPS	12	DDC
	1 SHIPS 033	1	Chief of R&D, OCS, Army
	2 SHIPS 03412B	1	Army Eng R&D, Ft. Belvoir
	1 SHIPS 037	1	Army Trans R&D, Ft. Eustis
	1 SHIPS 08	1	US MA
	3 SHIPS 2052	1	CMDT, USCOGARD
	1 SHIPS 2062	1	NASA College Park
	1 PMS 358		Attn: Sci & Tech Info, Acquisitions Br
	1 PMS 78		
	1 PMS 79	8	MARAD
	1 PMS 80		1 Ship Div
	1 PMS 81		1 Coord of Research
	1 PMS 82		1 Mr. F. Ebel
	1 PMS 83		1 Mr. R. Schubert
	1 PMS 84		1 Mr. R. Falls
	1 PMS 89		1 Mr. E.S. Dillon
	1 PMS 91		1 Mr. F. Dashnaw
	1 PMS 92		1 Mr. Hammar
1	NAVORD 05411	1	BUSTAND
1	NELC	1	Institute for Defense Analysis
1	NWC	1	Library of Congress
1	NURDC	1	Merchant Marine Academy
1	NCEL	1	National Science Foundation
1	NOL	4	Cal Inst of Tech
1	NWL		1 Dr. A.J. Acosta
1	NUSC		1 Dr. T.Y. Wu
1	NAVSHIPYD Boston		1 Dr. M.S. Plesset
			1 Library

122

DOCUMENT CONTROL DATA - R & D

Security classification of title, body of abstract and indexing annotation must be entered when the overall report is classified)

1. ORIGINATING ACTIVITY (Corporate author)	2a. REPORT SECURITY CLASSIFICATION
Naval Ship Research & Development Center	UNCLASSIFIED
Bethesda, Maryland 20034	2b. GROUP

3. REPORT TITLE

PROPELLER PERTURBATION PROBLEMS

4. DESCRIPTIVE NOTES (Type of report and inclusive dates)

5. AUTHOR(S) (First name, middle initial, last name)

Terry E. Brockett

6. REPORT DATE	7a. TOTAL NO. OF PAGES	7b. NO. OF REFS
October 1972	128	68

8a. CONTRACT OR GRANT NO	9a. ORIGINATOR'S REPORT NUMBER(S)
b. PROJECT NO.	3880
c. Subproject SR0Z30101, Task 00103	9b. OTHER REPORT NO(S) (Any other numbers that may be assigned this report)
d. Work Unit 1-1544-263	

10. DISTRIBUTION STATEMENT

APPROVED FOR PUBLIC RELEASE: DISTRIBUTION UNLIMITED.

11. SUPPLEMENTARY NOTES	12. SPONSORING MILITARY ACTIVITY
	NSRDC – GHR Program
	Bethesda, Md. 20034

13. ABSTRACT

For steady motion of a propeller operating in an inviscid fluid having an unbounded irrotational flow field, an expression for the velocity potential (in excess of the body motion) is derived in terms of the boundary values. From this expression perturbation solutions are determined—one for small thickness— or camber-to-chord ratio and one for small chord-to-diameter ratio.

The first problem (lifting-surface theory) is a regular-perturbation problem, and the second (lifting-line theory) is a singular-perturbation problem which requires construction of matched asymptotic expansions. Two terms of each series are found. Numerical techniques are not discussed. The outer solution for the lifting line is the same as that published in the literature. The formal lifting-surface differs from other developments in several ways. The most important of these is that for propellers with variable pitch, warp, and rake, the normal to the blade has a radial component which requires consideration of the radial velocity in determining the blade shape. For the case considered the sign of the contributions in the inner radii differ from the outer radii values; thus, this additional term might cause little effect on thrust but could be important for cavitation performance. A design procedure is discussed which involves only quantities appropriate for the lifting-surface analysis.

14 KEY WORDS	LINK A		LINK B		LINK C	
	ROLE	WT	ROLE	WT	ROLE	WT
Propellers						
Lifting-surface theory						
Lifting-line theory						
Regular-perturbation problem						
Singular-perturbation problem						
Subcavitating propeller						
Propeller design						
Fully wetted flow						